Elsevier Editorial System(tm) for BBA - Molecular and Cell Biology of Lipids
Manuscript Draft

Manuscript Number: BBALIP-16-66R2

Title: The Total and Mitochondrial Lipidome of Artemia franciscana Encysted Embryos

Article Type: Regular Paper

Keywords: extremophilia; cardiolipin; phosphatidylethanolamine; ceramide; phosphatidylglycerol; phosphatidylserine

Corresponding Author: Dr. Christos Chinopoulos, MD, PhD

Corresponding Author's Institution: Semmelweis University

First Author: Emily Chen

Order of Authors: Emily Chen; Michael A Kiebish; Justice McDaniel; Fei Gao; Niven R Narain; Rangaprasad Sarangarajan; Gergely Kacso; Dora Ravasz; Thomas N Seyfried; Vera Adam-Vizi; Christos Chinopoulos, MD, PhD

Abstract: Encysted embryos (cysts) of the crustacean Artemia franciscana exhibit enormous tolerance to adverse conditions encompassing high doses of radiation, years of anoxia, desiccation and extreme salinity. So far, several mechanisms have been proposed to contribute to this extremophilia, however, none were sought in the lipid profile of the cysts. Here in, we used high resolution shotgun lipidomics suited for detailed quantitation and analysis of lipids in uncharacterized biological membranes and samples and assembled the total, mitochondrial and mitoplastic lipidome of Artemia franciscana cysts. Overall, we identified and quantitated 1098 lipid species dispersed among 22 different classes and subclasses. Regarding the mitochondrial lipidome, most lipid classes exhibited little differences from those reported in other animals, however, Artemia mitochondria harboured much less phosphatidylethanolamine, plasmenylethanolamines and ceramides than mitochondria of other species, some of which by two orders of magnitude. Alternatively, Artemia mitochondria exhibited much higher levels of phosphatidylglycerols and phosphatidylserines. The identification and quantitation of the total and mitochondrial lipidome of the cysts may help in the elucidation of actionable extremophilia-affording proteins, such as the 'late embryogenesis abundant' proteins, which are known to interact with lipid membranes.

Response to Reviewers: We thank Reviewer #1 for the comments.

Reviewer #1: The results presented in paper demonstrated that the content of PS in mitochondria isolated from Artemia cysts is ~18% of total phospholipid. In addition, the content of PS in the inner mitochondrial membrane is ~27% of total phospholipid. The high quantities of PS that the authors were able to detect in mitochondria and IMM can be related with either unique features of Artemia cysts mitochondria or low purity of isolated mitochondria. Data on the purity of the mitochondria as well as IMM need to be presented. It is not accepted that mitochondria contain significant amount of PS. In many cases the content of PS in mitochondria is dependent on the purity of the samples. What is very well known and accepted is that in mammalian and plant mitochondria, PS is found in relatively small amounts compared to other phospholipids (~1.0 % of total phospholipid) (Daum and Vance 1997; Horvath and Daum, 2013 Mejia and Hatch, 2016). Slightly higher levels are found in the mitochondria of S. cerevisiae (~3 % of total mitochondrial phospholipid). However, higher levels of PS (~34 % of the total phospholipid) are found in its plasma membrane (Zinser et al. 1991).

Response: In the revised manuscript we show results of Western blots using antibodies raised against markers of certain membranes, for the various fractions during Artemia mitochondria and mitoplasts isolation; specifically, for the plasma membrane we used an antibody directed against the alpha 1 subunit of the Na+/K+ ATPase, for the outer mitochondrial membrane we used an antibody directed against VDAC, and for the inner mitochondrial membrane we used an antibody directed against COX subunit IV. Scanned images of these blots as well as the quantification of these bands (obtained from 4 different preparations) are now shown in figure 1. From the results shown in figure 1 of the revised manuscript we concluded that the purification of mitochondria by Percoll-gradient and the mitoplasts obtained from this fraction are essentially free (or contain very little amount) from plasma membrane components, and thus, plasma membrane lipids are unlikely to contribute to the high levels of PS observed in the mitochondrial and mitoplasts fractions. This finding is emphasized in the revised manuscript and discussed in view of the literature stressed by Reviewer #1. The reviewer is correct that PS content in artemia is high compared to the historic literature. The range of PS can indeed vary between 1% to up to 12% historically in mitochondria [with the average being around 3%) (Kiebish et al ASN Neuro 2009 1 (3); Kiebish et al J Neurochem 2008 106; Reitz et al Cancer Research 1977 (37); Schroeder et al Cancer Research 1984 (44); G Y Sun et al J Lipid Research 1974 (15); Ch E. Park et al Oncology 1970 (24); Morton et al Cancer Research 1976 (36); Ardail et al JBC 1990 (265); Paradies et al Biochimica et Biophysica Act 1992 (1103); Fleischer et al J Lipid Research 1967 (8); Hovius et al 1990 Biochimica et Biophysica Acta (1021); G Daum (Lipids of Mitochondria) Biochimica et Biophysica Acta 1985 (822); Getz et al 1968 Biochimica et Biophysica Acta (152); Lewin et al 1984 Mechanisms of Ageing and Development (24). Based on the EM images, Western blots of subcellular fractionations, and the fact that overall lipid content decreases (PC, PE, as well as others) with mitochondrial enrichment and CL increases, it is unlikely that PS is coming from other membrane fractions and the abundance is intrinsic to Artemia.

We thank Reviewer #2 for the comments.

1. The authors state that isotope correction wasn't performed as it is only required for low-resolution instruments to remove 13C signals. This however, is only half correct. Yes, one task of isotope correction is to de-isotope the spectra to remove isobaric interference but another important function is to correct for the increased proportion of isotopologues as lipids increase in size. If this is not performed then lipids larger than the internal standard will be underestimated and those smaller than the internal standard will be overestimated.

Response: To address these critiques we performed isotopic correction using the approach as previously described in Han and Gross 2001 Anal Biochem (295) 88-100 and Han and Gross 2005 Mass Spectrometry Reviews

(24) 367-412 to correct the MS/MSALL data. The reanalyzed data is reflected in the Figure 3 quantitative values as well as Supplemental Tables 1-17 using isotopic correction. We appreciate the Reviewer noting this critique.

2. More effort needs to be put into the statistics. A t test is not appropriate for comparing 3 variables. An ANOVA (if the data are normally distributed or have been transformed) or the like is more appropriate. There are also an enormous number of comparisons and therefore there also needs to be some form of correction for multiple comparisons.

Response: ANOVA was now performed on data comparisons followed by Tukey's, Fisher's LSD, or Dunnett's post-hoc analysis. This is reflected in Figure 1 and 4 and for Figure 2 and 3 corresponding statistical analysis is represented in Table 1 and 2 to make it easier for visualization of statistical differences.

Dear Editor,

We thank you for the Editorial efforts as well as the contributions made by the Reviewers. To our satisfaction, we have been able to address all remaining concerns of the Reviewers. We hope that in the present form, our manuscript is suitable for publication.

Sincerely,

Christos Chinopoulos MD, PhD

We thank Reviewer #1 for the comments.

Reviewer #1: The results presented in paper demonstrated that the content of PS in mitochondria isolated from Artemia cysts is ~18% of total phospholipid. In addition, the content of PS in the inner mitochondrial membrane is ~27% of total phospholipid. The high quantities of PS that the authors were able to detect in mitochondria and IMM can be related with either unique features of Artemia cysts mitochondria or low purity of isolated mitochondria. Data on the purity of the mitochondria as well as IMM need to be presented. It is not accepted that mitochondria contain significant amount of PS. In many cases the content of PS in mitochondria is dependent on the purity of the samples. What is very well known and accepted is that in mammalian and plant mitochondria, PS is found in relatively small amounts compared to other phospholipids (~1.0 % of total phospholipid) (Daum and Vance 1997; Horvath and Daum, 2013 Mejia and Hatch, 2016). Slightly higher levels are found in the mitochondria of S. cerevisiae (~3 % of total mitochondrial phospholipid). However, higher levels of PS (~34 % of the total phospholipid) are found in its plasma membrane (Zinser et al. 1991).

Response: In the revised manuscript we show results of Western blots using antibodies raised against markers of certain membranes, for the various fractions during Artemia mitochondria and mitoplasts isolation; specifically, for the plasma membrane we used an antibody directed against the alpha 1 subunit of the Na+/K+ ATPase, for the outer mitochondrial membrane we used an antibody directed against VDAC, and for the inner mitochondrial membrane we used an antibody directed against COX subunit IV. Scanned images of these blots as well as the quantification of these bands (obtained from 4 different preparations) are now shown in figure 1. From the results shown in figure 1 of the revised manuscript we concluded that the purification of mitochondria by Percoll-gradient and the mitoplasts obtained from this fraction are essentially free (or contain very little amount) from plasma membrane components, and thus, plasma membrane lipids are unlikely to contribute to the high levels of PS observed in the mitochondrial and mitoplasts fractions. This finding is emphasized in the revised manuscript and discussed in view of the literature stressed by Reviewer #1. The reviewer is correct that PS content in artemia is high compared to the historic literature. The range of PS can indeed vary between 1% to up to 12% historically in mitochondria [with the average being around 3%) (Kiebish et al ASN Neuro 2009 1 (3); Kiebish et al J Neurochem 2008 106; Reitz et al Cancer Research 1977 (37); Schroeder et al Cancer Research 1984 (44); G Y Sun et al J Lipid Research 1974 (15); Ch E. Park et al Oncology 1970 (24); Morton et al Cancer Research 1976 (36); Ardail et al JBC 1990 (265); Paradies et al Biochimica et Biophysica Act 1992 (1103); Fleischer et al J Lipid Research 1967 (8); Hovius et al 1990 Biochimica et Biophysica Acta (1021); G Daum (Lipids of Mitochondria) Biochimica et Biophysica Acta 1985 (822); Getz et al 1968 Biochimica et Biophysica Acta (152); Lewin et al 1984 Mechanisms of Ageing and Development (24). Based on the EM images, Western blots of subcellular fractionations, and the fact that overall lipid content decreases (PC, PE, as well as others) with mitochondrial enrichment and CL increases, it is unlikely that PS is coming from other membrane fractions and the abundance is intrinsic to Artemia.

We thank Reviewer #2 for the comments.

1. The authors state that isotope correction wasn't performed as it is only required for low-resolution instruments to remove 13C signals. This however, is only half correct. Yes, one task of

isotope correction is to de-isotope the spectra to remove isobaric interference but another important function is to correct for the increased proportion of isotopologues as lipids increase in size. If this is not performed then lipids larger than the internal standard will be underestimated and those smaller than the internal standard will be overestimated.

Response: To address these critiques we performed isotopic correction using the approach as previously described in Han and Gross 2001 Anal Biochem (295) 88-100 and Han and Gross 2005 Mass Spectrometry Reviews (24) 367-412 to correct the MS/MS^{ALL} data. The reanalyzed data is reflected in the Figure 3 quantitative values as well as Supplemental Tables 1-17 using isotopic correction. We appreciate the Reviewer noting this critique.

2. More effort needs to be put into the statistics. A t test is not appropriate for comparing 3 variables. An ANOVA (if the data are normally distributed or have been transformed) or the like is more appropriate. There are also an enormous number of comparisons and therefore there also needs to be some form of correction for multiple comparisons.

Response: ANOVA was now performed on data comparisons followed by Tukey's, Fisher's LSD, or Dunnett's post-hoc analysis. This is reflected in Figure 1 and 4 and for Figure 2 and 3 corresponding statistical analysis is represented in Table 1 and 2 to make it easier for visualization of statistical differences.

- The total and mitochondrial lipidome of Artemia cysts was identified
- Significant differences in lipid compositions were found from those of other species
- The identification of Artemia lipidome may help explain the action of LEA proteins

The Total and Mitochondrial Lipidome of *Artemia franciscana* Encysted Embryos

Emily Chen[1], Michael A. Kiebish[1], Justice McDaniel[1], Fei Gao[1], Niven R. Narain[1], Rangaprasad Sarangarajan[1], Gergely Kacso[2,3], Dora Ravasz[2,3], Thomas N. Seyfried[4], Vera Adam-Vizi[2,5] and Christos Chinopoulos[2,3]

[1]BERG LLC, Framingham, MA 01701, USA

[2]Department of Medical Biochemistry, Semmelweis University, Budapest, 1094, Hungary

[3]MTA-SE Lendület Neurobiochemistry Research Group, Budapest, 1094, Hungary

[4]Biology Department, Boston College, Chestnut Hill, Boston, MA, 02467, USA

[5]MTA-SE Laboratory for Neurobiochemistry, Budapest, 1094, Hungary

Address correspondence to: Dr. Christos Chinopoulos, Department of Medical Biochemistry, Semmelweis University, Budapest, Tuzolto street 37-47, 1094, Hungary. Tel: +361 4591500 ext. 60024, Fax: +361 2670031. E-mail: chinopoulos.christos@eok.sote.hu

Abstract

Encysted embryos (cysts) of the crustacean *Artemia franciscana* exhibit enormous tolerance to adverse conditions encompassing high doses of radiation, years of anoxia, desiccation and extreme salinity. So far, several mechanisms have been proposed to contribute to this extremophilia, however, none were sought in the lipid profile of the cysts. Here in, we used high resolution shotgun lipidomics suited for detailed quantitation and analysis of lipids in uncharacterized biological membranes and samples and assembled the total, mitochondrial and mitoplastic lipidome of *Artemia franciscana* cysts. Overall, we identified and quantitated 1098 lipid species dispersed among 22 different classes and subclasses. Regarding the mitochondrial lipidome, most lipid classes exhibited little differences from those reported in other animals, however, *Artemia* mitochondria harboured much less phosphatidylethanolamine, plasmenylethanolamines and ceramides than mitochondria of other species, some of which by two orders of magnitude. Alternatively, *Artemia* mitochondria exhibited much higher levels of phosphatidylglycerols and phosphatidylserines. The identification and quantitation of the total and mitochondrial lipidome of the cysts may help in the elucidation of actionable extremophilia-affording proteins, such as the 'late embryogenesis abundant' proteins, which are known to interact with lipid membranes.

Keywords: extremophilia; cardiolipin; phosphatidylethanolamine; ceramide; phosphatidylglycerol; phosphatidylserine

Abbreviations: Acylcarnitine; CE: cholesteryl esters; Cer: ceramide; CL: cardiolipin; CoQ: coenzyme Q; DAG: diacylglycerol; PA: phosphatidic acid; LPA: lysophosphatidic acid; PC: phosphatidylcholine; LPC: lysophosphatidylcholine; PE: phosphatidylethanolamine; LEA: 'late embryogenesis abundant; LPE: lysophosphatidylethanolamine; PG: phosphatidylglycerol; LPG: lysophosphatidylglycerol; PI: phosphatidylinositol; LPI: lysophosphatidylinositol; PS: phosphatidylserine; LPS: lysophosphatidylserine; SM: sphingomyelin; TAG: triacylglycerol.

1.1 Introduction

Encysted embryos (cysts) exiting females of the species *Artemia franciscana* may enter diapause [46], an extremophilic state during which metabolism is brought into a halt, accompanied by extreme augmentation of stress tolerance [23], [51], [55], [28]. Diapause has been documented in insects [25], rotifers [14], tardigrades [27], crustaceans [45], [13], killifish [57] and mammals [61], [8]. During this state, *Artemia franciscana* cysts tolerate high doses of UV and ionizing radiation, years of continuous anoxia while hydrated at physiological temperature, thermal extremes, desiccation-hydration cycles, and very high salinity [16], [53], [15], [62]. So far, the extremophilia of these cysts has been attributed to i) elaborate 'metabolic restructuring' [33], ii) high content of the non-reducing disaccharide trehalose [85], [19], [86] iii) a very large guanine nucleotide pool [80], iv) two heat shock proteins, p26 and artemin [81], [10], [17], [78], and v) expression of 'late embryogenesis abundant' (LEA) proteins [79], [34], [60]. Other mechanisms that have been reported in *C. elegans* larvae involving polyamine utilization, glyoxalase-dependent detoxification, lipid desaturation, and reactive oxygen species detoxification pathways may also be implicated in desiccation tolerance [24]. Furthermore, it has been discovered that mitochondria obtained from the cysts of *Artemia franciscana* lack the so -called 'permeability transition' [58], [50], a non-selective high-conductance channel which leads to cell death by allowing the flux of water and other molecules up to 1,500 Da across the inner mitochondrial membrane [3]. In addition, these mitochondria are refractory to bongkrekic acid (BKA), a dual inhibitor of the permeability transition and the adenine nucleotide translocase (ANT) [50]. However, if the *Artemia franciscana* ANT is heterologously expressed in yeasts, there it regains BKA sensitivity [83], a finding that has prompted the postulation that the lipid environment of the ANT may be crucial for the BKA response.

While trehalose is critical to desiccation tolerance in the cysts [19], [20], [18], [64] and it appears to work synergistically with p26 [77], [18] and LEA proteins [34], in experiments using liposomes the additive protection by LEA proteins plus trehalose was reported to be dependent on the lipid composition of the target membrane [60]. Accordingly, molecular modeling of the secondary structures of the cytosol-targeted AfrLEA2 and mitochondrially-targeted AfrLEA3m revealed bands of charged amino acids known to interact directly with lipid membranes [60]. Along this line, it has been shown that LEA proteins preferentially stabilize membranes of a particular lipid composition based on the protein's subcellular location [74], [75], [35].

The lipid compositions of mammalian membranes are well-defined [76], [38]. Among different cells and tissues the mitochondrial lipid composition is fairly similar [38], with the exceptions of those isolated from some organs which additionally contain phosphatidylcholine (PC) and phosphatidylethanolamine (PE) plasmalogens [59], [1]. Furthermore, the molecular species of cardiolipin, a polyglycerophospholipid found exclusively in the inner mitochondrial membrane [36] exhibit considerable diversity between tissues and among disease states [42], [12], [32], [31], [43], [11]. On the other hand, lipids from *Artemia franciscana* cysts have been scarcely investigated. So far, it is known that *Artemia franciscana* cysts are unique because they harbor complex fucosyl and neutral glycosphingolipids, not found in other animal species [49], [48], and also sphingomyelin (SM) [47], which has been found in species belonging to other invertebrate phyla but not Echinodermata and Lophotrochozoa [47]. Furthermore, it is known that the lipid content of *Artemia* varies considerably during enrichment and starvation periods, implying a dynamic character [63]; this dynamism in lipid profile is also supported by an intricate regiospecific distribution of fatty acids in triacylglycerols of *Artemia franciscana* nauplii enriched with fatty acid ethyl esters [2] or microalgae [9].

Mindful of i) the scarcity of information regarding the lipid profile of *Artemia franciscana* cysts, ii) the potential importance of lipid composition in affording extremophilia and the documented synergism of LEA proteins in doing so as a function of the lipid environment, we investigated the lipidome of the cysts. By using a MS/MS^{ALL} high resolution shotgun lipidomics workflow which is ideally suited for detailed quantitation and analysis of lipids in uncharacterized biological membranes and samples [30] we assembled the total and mitochondrial lipid profile of *Artemia franciscana* cysts. Comparisons of their lipidomes to those obtained from mammalian tissues revealed stark quantitative differences which may help to explain the extremophilia of the cysts, especially in relation to the functions of LEA proteins.

2.1 Materials and Methods

2.1. Hydration and dechorionation of Artemia franciscana cysts: No permits were required for the described study, which complied with all relevant regulations. Dehydrated, encysted gastrulae of *Artemia franciscana* were obtained from Salt Lake, Utah through Artemia International LLC (Fairview, Texas 75069, USA) and stored at 4°C until used. Embryos (15 gr) were hydrated in 0.25 M NaCl at room temperature for 16-18 h during constant aeration. After this developmental incubation, the embryos were dechorionated in modified antiformin solution (1% hypochlorite from bleach, 60 mM $NaCO_3$, and 0.4 M NaOH) for 30 min, followed by a rinse in 1% Na^+-thiosulfate (5 min) and multiple washings in ice-cold 0.25 M NaCl as previously described [52]. For further lipidomic analysis, dechorionated embryos were pelleted by centrifugation for 5 min at 300 g at 4°C, snap-frozen with liquid nitrogen and stored in -20 ^oC, until use.

2.1.2 Isolation of mitochondria and mitoplasts from Artemia franciscana: Mitochondria from embryos of *Artemia franciscana* were prepared as described elsewhere, with minor modifications [67]. Dechorionated embryos were filtered through filter paper, and ~10 gr were homogenized in ice-cold isolation buffer consisting of 0.5 M sucrose, 150 mM KCl, 1 mM EGTA, and 20 mM K^+-HEPES, pH 7.5, using a glass-Teflon homogenizer at 850 rpm for ten passages. The homogenate was centrifuged for 10 min at 3,000 g at 4°C, the upper fatty layer of the supernatant was aspirated and the remaining supernatant was centrifuged at 11,300 g for 10 min. The resulting pellet was gently resuspended in the same buffer, avoiding the green core. The green core was discarded, and the resuspended pellet was centrifuged again at 11,300 g for 10 min. The pellet was resuspended in 0.3 ml of ice-cold isolation buffer consisting of 15% Percoll, 0.5 M sucrose, 150 mM KCl, 1 mM EGTA, and 20 mM K^+-HEPES, pH 7.5 and layered on a preformed Percoll gradient (40 and 23%). After centrifugation at 30,000 g for 6 min, the fraction between the 15% and 23% Percoll gradient interface and the supernatant above the 15% Percoll layer were discarded, and the mitochondrial fraction located at the interface between the 23% and 40 % Percoll layer was removed, diluted with isolation buffer, and centrifuged at 16,600 g for 10 min. The resulting loose pellet was resuspended in isolation buffer and centrifuged at 6,700 g for 10 min. In pilot experiments where the resulting pellet was resuspended in a 15% Percoll and underwent a second round of a Percoll-gradient centrifugation, no more fractions between the 15% and 23% layers nor above the 15% layer formed, implying that no further purification could be achieved by this methodology. For further mitoplast isolation, the resulting pellet was resuspended in 40 ml of 10 mM K^+-HEPES pH 7.5, and kept under constant stirring at 4°C for 30 min. Subsequently, this fraction was centrifuged at 6,700 g for 10 min, the supernatant was discarded, and the pellet underwent one more round of centrifugation at 6,700 g for 10 min. The resulting pellet was snap-frozen with liquid nitrogen and stored in -20 ^oC, until use.

2.1.3 Western blot analysis: Artemia cysts (dechorionated) homogenates, Percoll-purified mitochondria and mitoplasts were solubilised in 10% sodium dodecyl sulphate, the insoluble pellets were discarded, and the supernatants were frozen at -20 ^oC for further analysis. These samples were thawed on ice, their protein concentration was determined using the bicinchoninic acid assay as detailed in section 2.14, loaded at a concentration of 20 μg per well on the gels and separated by sodium dodecyl sulphate – polyacrylamide gel electrophoresis (SDS-PAGE). Separated proteins were transferred to a methanol-activated polyvinylidene difluoride membrane. Immunoblotting was performed as recommended by the manufacturers of the antibodies. Rabbit polyclonal anti-alpha 1 subunit of Na^+/K^+ ATPase, mouse monoclonal anti-COX IV subunit, and rabbit monoclonal anti-VDAC1 (Abcam, Cambridge, UK), primary antibody were used at titers of 1:1,000. Immunoreactivity was detected using the appropriate peroxidase-linked secondary antibody (1:5,000, donkey anti-rabbit or donkey anti-mouse, Jackson Immunochemicals Europe Ltd, Cambridgeshire, UK) and enhanced chemiluminescence detection reagent (ECL system; Amersham Biosciences GE Healthcare Europe GmbH, Vienna, Austria). Densitometric analysis of the bands was performed in Fiji [69].

2.1.4 Protein determination: Protein concentration was determined using the bicinchoninic acid assay, and calibrated using bovine serum standards [73] using a Tecan Infinite® 200 PRO series plate reader (Tecan Deutschland GmbH, Crailsheim, Germany).

2.1.5 Transmission electron microscopy (TEM): Mitochondrial and mitoplasts fractions were pelleted by centrifugation and fixed overnight in 4% gluteraldehyde and 175 mM Na^+-cacodylate buffer, pH 7.5, at 4 ^oC. Subsequently, pellets were post-fixed with 1% osmium tetroxide for 100 min, followed by dehydration by alcohol and propylene oxide and embedded in Durcupan. Series of ultrathin sections (76 nm) were prepared by an ultramicrotome, mounted on single-slot copper grids, contrasted with 6 % uranyl acetate (20 min) and lead citrate (5 min), and observed with a JEOL 1200 EMX (Peabody, MA, USA) electron microscope.

2.1.6 Liquid/Liquid Extraction of Structural Lipids: Mitoplasts from Percoll-purified *Artemia franciscana* mitochondria, Percoll-purified *Artemia franciscana* mitochondria, and dechorionated hatched *Artemia franciscana* cysts were thawed and diluted with a ten-times diluted PBS solution. All samples were homogenized in Omni bead tubes with 2.8 mm ceramic beads in the Omni Bead Ruptor 24 with Cryo Cooling Unit (Omni International, Kennesaw, GA) at 4 ^oC for 2 minutes. Protein concentration was determined by the bicinchoninic acid assay. 1 mg proportion of protein from mitoplasts, Percoll-purified mitochondria, and dechorionated hatched cyst samples were aliquoted and a cocktail of deuterium-labeled and odd chain phospholipid standards from diverse lipid classes was added (supplemental table 18). Standards were chosen so that they represented each lipid class and were at designated concentrations chosen to provide the most accurate quantitation and dynamic range for each lipid species. 4 mL chloroform:methanol (1:1, by vol) was added to each sample and lipidomic extractions were performed as previously described [41]. Lipid extraction was automated using a customized sequence on a Hamilton Robotics STARlet system (Hamilton, Reno, NV). Lipid extracts were dried under nitrogen and reconstituted in chloroform:methanol (1:1, by vol). Samples were flushed with nitrogen and stored at -20°C.

2.1.7 Direct Infusion MS/MS^{ALL} Structural Lipidomics Platform: Samples were diluted 50 times in isopropanol:methanol:acetonitrile:water (3:3:3:1, by vol.) with 2 mM ammonium acetate in order to optimize ionization efficiency in positive and negative modes. Electrospray ionization-MS was performed on a TripleTOF® 5600^{+} (SCIEX, Framingham, MA), coupled to a customized direct injection loop on an Ekspert microLC200 system (SCIEX). 50 µL of sample was injected at a flow-rate of 6 µL/min. Lipids were analyzed using a customized data independent analysis strategy on the TripleTOF® 5600^{+} allowing for MS/MS^{ALL} high resolution and high mass accuracy analysis as previously described [72]. Quantification was performed using an in-house library on MultiQuant™ software (SCIEX) and isotopic correction was performed as described in [29] and reviewed in [30].

2.187 Standards and Chemicals

Cyst dechorionation and mitochondria/mitoplast preparation: Standard laboratory chemicals and alamethicin were from Sigma (St. Louis, MO, USA). Electron microscopy: Durcupan, gluteraldehyde, uranyl acetate and lead citrate were from Sigma. Lipidomics: All standards were purchased from Avanti Polar Lipids (Alabaster, AL), Nu-Chek Prep Inc. (Waterville, MN), or Cambridge Isotope Laboratories (Tewksbury, MA). All solvents were of HPLC or LC/MS grade and were acquired from Fisher Scientific (Waltham, MA) or VWR International (Radnor, PA).

2.1.9 Statistics

Data are presented as averages ± S.E.M.. Significant differences between three or more groups were evaluated by one-way analysis of variance followed by Tukey’s, Fisher’s LSD, or Dunnett's post-hoc analysis. $P < 0.05$ was considered statistically significant. If normality test failed, ANOVA on Ranks was performed. One-way ANOVA analysis was performed on MetaboAnalyst 3.0 as described in [84].

3.1 Results

3.1.1 Determination of the purity of mitochondria and mitoplasts isolated from Artemia franciscana cysts

One of the main objectives of this study was to assemble the mitochondrial lipidome from *Artemia franciscana* cysts therefore, it was necessary to evaluate the purity of our preparations. We isolated mitochondria from the cysts in two steps: i) a crude mitochondrial extract was prepared by standard differential centrifugation, followed by ii) purification of the extract by a Percoll gradient. Furthermore, from the Percoll-purified mitochondria, mitoplasts were prepared using a protocol that strips off the outer membrane of mitochondria without the use of detergents and yields a fraction exhibiting high purity of mitochondrial-derived lipids and proteins. The purity of intracellular organelle preparations is usually estimated by following the relative concentration of an organelle- or membrane-specific marker. Here, we tested the various fractions for the presence of a i) well-characterized plasma membrane marker, the alpha 1 subunit of Na/K ATPase (using ab211130 from Abcam), ii) VDAC as a marker of outer mitochondrial membrane, and iii) COX IV subunit as a marker of the inner mitochondrial membrane. We must note that we tested a number of different antibodies that either did not yield any bands in the samples obtained from the *Artemia*, or yielded bands that were far from the expected molecular weights, possibly due to insufficient homology between mammalian proteins (to which antibodies are usually raised) and those appearing in the *Artemia* cysts. The antibodies used hereby yielded bands at the expected molecular weight (the antibody used for the alpha 1 subunit of Na^{+}/K^{+} ATPase is marketed as suitable for *Danio rerio*, and there is a very high degree of homology of this protein between this organism and *Artemia franciscana*). VDAC and COX IV subunit are highly conserved proteins among many species. Scanned images of the Western blots are shown in figure 1. As shown in figure panel 1A, samples from four different preparations of each fraction (Artemia cysts, Percoll-purified mitochondria and mitoplasts) have been loaded in gels (20 micrograms each), and probed with the aforementioned antibodies. The quantification of the band densities are shown in figure panel 1B. It is evident that upon mitochondrial and mitoplasts purification, the presence of a plasma membrane component disappears, while mitochondrial components are enriched. The persistence of VDAC in mitoplasts is probably due to the fact that it is mostly localizes to 'contact sites', entities where the inner and the outer mitochondrial membranes meet, which cannot be removed by a hypotonic shock.

Furthermore, in order to assess the extent of contamination of the fractions by non-mitochondrial elements using a different approach, we performed an electron microscopic evaluation of each fraction and visually identify mitochondria and non-mitochondrial elements. Results are shown in supplemental figure 1.

From the results obtained from figure 1 and supplemental figure 1 we concluded that the mitochondrial and mitoplastic fractions are highly enriched in mitochondrial elements and essentially devoid of plasma membrane contaminants.

3.1.2 Determination of the total and mitochondrial lipidome of Artemia franciscana cysts

Artemia franciscana cysts, mitochondria and mitoplasts were subject to MS/MS^{ALL} high resolution shotgun lipidomics workflow. All samples were from 6 independent harvests, each measured two or four (for CL) times to receive optimal reproducible analytical measurements. The MS/MS^{ALL} acquisition technique, introduced by Simons et al [72], is one of information-independent tandem mass spectrometry. It implements a Q1 stepped mass isolation window through a set mass range in 1 Da increments, and then fragments and records all product ions and neutral losses. After the entire mass range was scanned in this fashion, all of the data collected was matched to an in-house database for lipid identification and quantitation (see Supplemental Figure 2). For lipid identification, we identified the different lipid classes and their molecular structures based on a variety of criteria, such as the polarity, the high mass-accuracy molecular weight and diagnostic MS/MS product ions (product ions or neutral losses, see supplemental table 17).

To assess the overall abundance and detection of molecular species across lipid classes, we plotted the number of species detected in cysts, mitochondria, and mitoplasts. There was a decrease in molecular complexity between cysts, mitochondria, and mitoplasts, respectively, based on the number of species detected specifically for negatively charged lipids such as phosphatidic acid, phosphatidylglycerol, phosphatidylinositol, and phosphatidylserine (Figure 2). This did not correspond to a decrease in the overall abundance of these lipids in mitoplasts (Figure 3). p values for comparisons among samples are given in Tables 1 and 2, for number of species per lipid class and total lipid concentrations, respectively. Only p values yielding a numerical return of <0.05 are given in the tables. Those that are left blank are not statistically significant.

In general, the mechanisms regulating lipidomic diversity, molecular sculpting, and biophysical adaption in the inner mitochondrial membrane compared to the rest of the cell are limited, allowing for homeostatic regulation that is more bioenergetically efficient within the mitochondrion. Further, acyl carnitines dramatically decreased in molecular diversity from cyst, mitochondria, and mitoplast, respectively as well as some triglyceride species (Figures 4 and 5). These changes are directly associated with the functional correlate of their metabolic regulation within mitochondria. Regarding mitochondrial and mitoplast enrichment, cardiolipin correspondingly increased, respectively, based on its abundance in the inner mitochondrial membrane. Interestingly, storage lipids, such as diacylglycerol and triacylglycerol, decreased by 80-90 percent in the mitoplast, indicative of the purity of the mitochondria and lack of association with these energy stores (Figure 3). Additionally, positively charged and neutral lipids such as phosphatidylcholine, sphingomyelin, and cholesterol esters decreased with enrichment of mitoplasts and negatively charged lipids such as PI, PG, and PA did not change except for the increase in cardiolipin. These characteristic changes are hallmark to mitochondrial and mitoplast lipid composition, since the proton gradient in mitochondria requires the enriched negative charge membrane to maintain the proton motive force as well as a corresponding decrease in positive, neutral or sterol lipid classes. Analysis of the molecular species characterization and fatty acid contributions to individual species revealed a predominance of palmitic, steric, oleic, and linoleic species as well as an abundance of linolenic fatty acid (18:3) (Supplemental Tables 1-15, using shorthand nomenclature as described in [54]), which surprisingly increased the proportion of 18:3 containing cardiolipin species (Supplemental Table 4). Additionally, the molecular species enrichment and diversity increased in mitoplasts compared to mitochondria and cysts (Figure 6). Thus, the global analysis of the *Artemia franciscana* cyst, mitochondrial, and mitoplast lipidome greatly enhanced the understanding of biophysical and structural diversity of lipids in theses cellular and subcellular compartments in these organisms.

4.1. Discussion

It is well established that lipids regulate the functions of membrane-embedded proteins, membrane fluidity and define compartmentalization. More specifically, mitochondrial membrane lipids regulate respiratory complex activities, protein import, adenine nucleotide exchange and ATP synthesis [26], [36], [66], [71], [39], [38], [6], [82], [37]. Furthermore, mitochondrial membrane fluidity regulated by lipid composition is known to be subject to endocrine regulation [4], [65], [40]. It is therefore prudent to consider that lipid composition affords an equal opportunity for diversification and adaptation as the other biological macromolecules, i.e. proteins and nucleic acids. Here, we assembled the total and mitochondrial lipidome of the extremophile cysts, *Artemia franciscana*. A comparison of the total lipidome of *Artemia franciscana* cysts to that of embryos from other organisms is perhaps less informative than the comparison of their mitochondrial lipidomes. The most striking findings in our work were that *Artemia* mitochondria harbour much less phosphatidylethanolamine, plasmenylethanolamines and ceramides than mitochondria of other species, some of which by two orders of magnitude, but on the other hand *Artemia* mitochondria exhibited much higher values of phosphatidylglycerols and phosphatidylserines [44], [43], [38]. The finding that *Artemia* mitochondria contain very high levels of phosphatidylserine is at odds to what is known and accepted for mammalian and plant mitochondria: in mammals and plants phosphatidylserine is found in abundance in plasma membranes (~34 % of the total phospholipid, [87]), as opposed to mitochondria that exhibit relatively small amounts compared to other phospholipids (~1.0 % of total phospholipid) [22], [38], [56]. These differences directly highlight the inherent biophysical and adaptive requirements of Artemia as well as their subcellular organelles to adapt to dynamic environmental changes. Decreases in zwitter ionic lipids and neutral lipids as well as corresponding increases in negatively charged lipids, such as phosphatidylglycerol and phosphatidylserine serve multiple roles in establishing metabolic adaption. Interestingly, it has been shown that increases in phosphatidylglycerol and phosphatidylserine to a lesser extent can serve as a compensatory mechanism to decreased cardiolipin content in non-mammalian systems [21]. In the present circumstances, there are no pathogenic changes in cardiolipin, thus demonstrating increases in endogenous PS and PG content serve as an evolutionary conserved mechanism compensating for ionic challenge and maintenance of the proton gradient [70]. The remaining lipid species exhibited quantitative variations, but they were within the same range. The large differences in the aforementioned lipid classes may well have an impact on the function of membrane-embedded proteins.

The composition of the mitochondrial lipidome is homeostatically regulated and tailored to its adaptive function for bioenergetic efficiency. Thus, the intricacy of cellular as well as mitochondrial lipidome demonstrate a systems level interpretation of biological function. In regard to the mitochondrial lipidome, the lipid composition and molecular species distributions is known to alter specific mitochondrial membrane-bound proteins, such as VDAC [68], [7] carnitine acyltransferase [21], complex I [43], and the ANT [6], [82], [5], [37]. By the same token, it is easy to envisage that LEA proteins afford a greater extent of extremophilia when embedded in lipid membranes the composition of which resemble that elucidated in the present study. Thus, characterization and enrichment of knowledge around the cellular, mitochondrial, and mitoplast lipidome in Artemia affords novel insight into the endogenous and evolutionary nature of the membrane in metabolically adaption in harsh environmental conditions.

Acknowledgements: We thank Ujvari Zsuzsa and Jakab Andrea for excellent technical assistance. The work described in the text was supported by the Országos Tudományos Kutatási Alapprogram (OTKA) grant 112230, the Hungarian Academy of Sciences grant 02001, the Hungarian Brain Research Program KTIA_13_NAP-A-III/6 to V.A.-V. and MTA-SE Lendület Neurobiochemistry Research Division 95003, OTKA NNF 78905, OTKA NNF2 85658 and OTKA K 100918 to C.C.

CONFLICT OF INTEREST STATEMENT: The authors declare no conflict of interests.

Reference List

1. C.J. Albert, D.S. Anbukumar, J.K. Monda, J.T. Eckelkamp, and D.A. Ford, Myocardial lipidomics. Developments in myocardial nuclear lipidomics, Front Biosci. 12 (2007) pp. 2750-2760.

2. Y. Ando, Y. Oomi, and K. Narukawa, Regiospecific distribution of fatty acids in triacylglycerols of Artemia franciscana nauplii enriched with fatty acid ethyl esters, Comp Biochem. Physiol B Biochem. Mol. Biol. 133 (2002) pp. 191-199.

3. L. Azzolin, von Stockum S., E. Basso, V. Petronilli, M.A. Forte, and P. Bernardi, The mitochondrial permeability transition from yeast to mammals, FEBS Lett. 584 (2010) pp. 2504-2509.

4. C.S. Bangur, J.L. Howland, and S.S. Katyare, Thyroid hormone treatment alters phospholipid composition and membrane fluidity of rat brain mitochondria, Biochem. J. 305 (Pt 1) (1995) pp. 29-32.

5. K. Beyer and M. Klingenberg, ADP/ATP carrier protein from beef heart mitochondria has high amounts of tightly bound cardiolipin, as revealed by 31P nuclear magnetic resonance, Biochemistry 24 (1985) pp. 3821-3826.

6. G. Brandolin, J. Doussiere, A. Gulik, T. Gulik-Krzywicki, G.J. Lauquin, and P.V. Vignais, Kinetic, binding and ultrastructural properties of the beef heart adenine nucleotide carrier protein after incorporation into phospholipid vesicles, Biochim. Biophys. Acta 592 (1980) pp. 592-614.

7. A.M. Campbell and S.H. Chan, Mitochondrial membrane cholesterol, the voltage dependent anion channel (VDAC), and the Warburg effect, J. Bioenerg. Biomembr. 40 (2008) pp. 193-197.

8. J. Cha, X. Sun, A. Bartos, J. Fenelon, P. Lefevre, T. Daikoku, G. Shaw, R. Maxson, B.D. Murphy, M.B. Renfree, and S.K. Dey, A new role for muscle segment homeobox genes in mammalian embryonic diapause, Open. Biol. 3 (2013) p. 130035.

9. R.D. Chakraborty, K. Chakraborty, and E.V. Radhakrishnan, Variation in fatty acid composition of Artemia salina nauplii enriched with microalgae and baker's yeast for use in larviculture, J. Agric. Food Chem 55 (2007) pp. 4043-4051.

10. T. Chen, R. Amons, J.S. Clegg, A.H. Warner, and T.H. MacRae, Molecular characterization of artemin and ferritin from Artemia franciscana, Eur. J. Biochem. 270 (2003) pp. 137-145.

11. H. Cheng, D.J. Mancuso, X. Jiang, S. Guan, J. Yang, K. Yang, G. Sun, R.W. Gross, and X. Han, Shotgun lipidomics reveals the temporally dependent, highly diversified cardiolipin profile in the mammalian brain: temporally coordinated postnatal diversification of cardiolipin molecular species with neuronal remodeling, Biochemistry 47 (2008) pp. 5869-5880.

12. A.J. Chicco and G.C. Sparagna, Role of cardiolipin alterations in mitochondrial dysfunction and disease, Am. J. Physiol Cell Physiol 292 (2007) p. C33-C44.

13. K.A. Clark, A.S. Brierley, D.W. Pond, and V.J. Smith, Changes in seasonal expression patterns of ecdysone receptor, retinoid X receptor and an A-type allatostatin in the copepod, Calanus finmarchicus, in a sea loch environment: an investigation of possible mediators of diapause, Gen. Comp Endocrinol. 189 (2013) pp. 66-73.

14. M.S. Clark, N.Y. Denekamp, M.A. Thorne, R. Reinhardt, M. Drungowski, M.W. Albrecht, S. Klages, A. Beck, M. Kube, and E. Lubzens, Long-term survival of hydrated resting eggs from Brachionus plicatilis, PLoS. ONE. 7 (2012) p. e29365.

15. J.S. Clegg, Cryptobiosis--a peculiar state of biological organization, Comp Biochem. Physiol B Biochem. Mol. Biol. 128 (2001) pp. 613-624.

16. J.S. Clegg, Desiccation tolerance in encysted embryos of the animal extremophile, artemia, Integr. Comp Biol. 45 (2005) pp. 715-724.

17. C.H. Collins and J.S. Clegg, A small heat-shock protein, p26, from the crustacean Artemia protects mammalian cells (Cos-1) against oxidative damage, Cell Biol. Int. 28 (2004) pp. 449-455.

18. J.H. Crowe, L.M. Crowe, W.F. Wolkers, A.E. Oliver, X. Ma, J.H. Auh, M. Tang, S. Zhu, J. Norris, and F. Tablin, Stabilization of dry Mammalian cells: lessons from nature, Integr. Comp Biol. 45 (2005) pp. 810-820.

19. J.H. Crowe, F.A. Hoekstra, and L.M. Crowe, Anhydrobiosis, Annu. Rev. Physiol 54 (1992) pp. 579-599.

20. J.H. Crowe, A.E. Oliver, and F. Tablin, Is there a single biochemical adaptation to anhydrobiosis?, Integr. Comp Biol. 42 (2002) pp. 497-503.

21. G. Daum, Lipids of mitochondria, Biochim. Biophys. Acta 822 (1985) pp. 1-42.

22. G. Daum and J.E. Vance, Import of lipids into mitochondria, Prog. Lipid Res. 36 (1997) pp. 103-130.

23. D.L. Denlinger, Regulation of diapause, Annu. Rev. Entomol. 47 (2002) pp. 93-122.

24. C. Erkut, A. Vasilj, S. Boland, B. Habermann, A. Shevchenko, and T.V. Kurzchalia, Molecular strategies of the Caenorhabditis elegans dauer larva to survive extreme desiccation, PLoS. ONE. 8 (2013) p. e82473.

25. L. Fan, J. Lin, Y. Zhong, and J. Liu, Shotgun proteomic analysis on the diapause and non-diapause eggs of domesticated silkworm Bombyx mori, PLoS. ONE. 8 (2013) p. e60386.

26. S. FLEISCHER, G. BRIERLEY, H. KLOUWEN, and D.B. SLAUTTERBACK, Studies of the electron transfer system. 47. The role of phospholipids in electron transfer, J. Biol. Chem 237 (1962) pp. 3264-3272.

27. R. Guidetti, T. Altiero, and L. Rebecchi, On dormancy strategies in tardigrades, J. Insect Physiol 57 (2011) pp. 567-576.

28. D.A. Hahn and D.L. Denlinger, Energetics of insect diapause, Annu. Rev. Entomol. 56 (2011) pp. 103-121.

29. X. Han and R.W. Gross, Quantitative analysis and molecular species fingerprinting of triacylglyceride molecular species directly from lipid extracts of biological samples by electrospray ionization tandem mass spectrometry, Anal. Biochem. 295 (2001) pp. 88-100.

30. X. Han and R.W. Gross, Shotgun lipidomics: electrospray ionization mass spectrometric analysis and quantitation of cellular lipidomes directly from crude extracts of biological samples, Mass Spectrom. Rev. 24 (2005) pp. 367-412.

31. X. Han, J. Yang, K. Yang, Z. Zhao, D.R. Abendschein, and R.W. Gross, Alterations in myocardial cardiolipin content and composition occur at the very earliest stages of diabetes: a shotgun lipidomics study, Biochemistry 46 (2007) pp. 6417-6428.

32. X. Han, K. Yang, J. Yang, H. Cheng, and R.W. Gross, Shotgun lipidomics of cardiolipin molecular species in lipid extracts of biological samples, J. Lipid Res. 47 (2006) pp. 864-879.

33. S.C. Hand, M.A. Menze, A. Borcar, Y. Patil, J.A. Covi, J.A. Reynolds, and M. Toner, Metabolic restructuring during energy-limited states: insights from Artemia franciscana embryos and other animals, J. Insect Physiol 57 (2011) pp. 584-594.

34. S.C. Hand, M.A. Menze, M. Toner, L. Boswell, and D. Moore, LEA proteins during water stress: not just for plants anymore, Annu. Rev. Physiol 73 (2011) pp. 115-134.

35. D.K. Hincha and A. Thalhammer, LEA proteins: IDPs with versatile functions in cellular dehydration tolerance, Biochem. Soc. Trans. 40 (2012) pp. 1000-1003.

36. F.L. Hoch, Cardiolipins and biomembrane function, Biochim. Biophys. Acta 1113 (1992) pp. 71-133.

37. B. Hoffmann, A. Stockl, M. Schlame, K. Beyer, and M. Klingenberg, The reconstituted ADP/ATP carrier activity has an absolute requirement for cardiolipin as shown in cysteine mutants, J. Biol. Chem. 269 (1994) pp. 1940-1944.

38. S.E. Horvath and G. Daum, Lipids of mitochondria, Prog. Lipid Res. 52 (2013) pp. 590-614.

39. F. Jiang, M.T. Ryan, M. Schlame, M. Zhao, Z. Gu, M. Klingenberg, N. Pfanner, and M.L. Greenberg, Absence of cardiolipin in the crd1 null mutant results in decreased mitochondrial membrane potential and reduced mitochondrial function, J. Biol. Chem 275 (2000) pp. 22387-22394.

40. S.S. Katyare, H.R. Modi, and M.A. Patel, Dehydroepiandrosterone treatment alters lipid/phospholipid profiles of rat brain and liver mitochondria, Curr. Neurovasc. Res. 3 (2006) pp. 273-279.

41. M.A. Kiebish, R. Bell, K. Yang, T. Phan, Z. Zhao, W. Ames, T.N. Seyfried, R.W. Gross, J.H. Chuang, and X. Han, Dynamic simulation of cardiolipin remodeling: greasing the wheels for an interpretative approach to lipidomics, J. Lipid Res. 51 (2010) pp. 2153-2170.

42. M.A. Kiebish, X. Han, H. Cheng, J.H. Chuang, and T.N. Seyfried, Cardiolipin and electron transport chain abnormalities in mouse brain tumor mitochondria: lipidomic evidence supporting the Warburg theory of cancer, J. Lipid Res. 49 (2008) pp. 2545-2556.

43. M.A. Kiebish, X. Han, H. Cheng, and T.N. Seyfried, In vitro growth environment produces lipidomic and electron transport chain abnormalities in mitochondria from non-tumorigenic astrocytes and brain tumours, ASN. Neuro. 1 (2009).

44. M.A. Kiebish, X. Han, and T.N. Seyfried, Examination of the brain mitochondrial lipidome using shotgun lipidomics, Methods Mol. Biol. 579 (2009) pp. 3-18.

45. A.M. King and T.H. MacRae, The small heat shock protein p26 aids development of encysting Artemia embryos, prevents spontaneous diapause termination and protects against stress, PLoS. ONE. 7 (2012) p. e43723.

46. A.M. King, J. Toxopeus, and T.H. MacRae, Artemin, a diapause-specific chaperone, contributes to the stress tolerance of Artemia franciscana cysts and influences their release from females, J. Exp. Biol. 217 (2014) pp. 1719-1724.

47. H. Kojima, T. Inoue, M. Sugita, S. Itonori, and M. Ito, Biochemical studies on sphingolipid of Artemia franciscana (I) isolation and characterization of sphingomyelin, Lipids 45 (2010) pp. 635-643.

48. H. Kojima, T. Shimizu, M. Sugita, S. Itonori, N. Fujita, and M. Ito, Biochemical studies on sphingolipids of Artemia franciscana: novel neutral glycosphingolipids, J. Lipid Res. 52 (2011) pp. 308-317.

49. H. Kojima, Y. Tohsato, K. Kabayama, S. Itonori, and M. Ito, Biochemical studies on sphingolipids of Artemia franciscana: complex neutral glycosphingolipids, Glycoconj. J. 30 (2013) pp. 257-268.

50. C. Konrad, G. Kiss, B. Torocsik, J.L. Labar, A.A. Gerencser, M. Mandi, V. Adam-Vizi, and C. Chinopoulos, A distinct sequence in the adenine nucleotide translocase from Artemia franciscana embryos is associated with insensitivity to bongkrekate and atypical effects of adenine nucleotides on Ca(2+) uptake and sequestration, FEBS J. 278 (2011) pp. 822-836.

51. V. Kostal, Eco-physiological phases of insect diapause, J. Insect Physiol 52 (2006) pp. 113-127.

52. K.E. Kwast and S.C. Hand, Regulatory features of protein synthesis in isolated mitochondria from Artemia embryos, Am. J. Physiol 265 (1993) p. R1238-R1246.

53. P. Liang and T.H. MacRae, The synthesis of a small heat shock/alpha-crystallin protein in Artemia and its relationship to stress tolerance during development, Dev. Biol. 207 (1999) pp. 445-456.

54. G. Liebisch, J.A. Vizcaino, H. Kofeler, M. Trotzmuller, W.J. Griffiths, G. Schmitz, F. Spener, and M.J. Wakelam, Shorthand notation for lipid structures derived from mass spectrometry, J. Lipid Res. 54 (2013) pp. 1523-1530.

55. T.H. MacRae, Gene expression, metabolic regulation and stress tolerance during diapause, Cell Mol. Life Sci. 67 (2010) pp. 2405-2424.

56. E.M. Mejia and G.M. Hatch, Mitochondrial phospholipids: role in mitochondrial function, J. Bioenerg. Biomembr. 48 (2016) pp. 99-112.

57. C.L. Meller, R. Meller, R.P. Simon, K.M. Culpepper, and J.E. Podrabsky, Cell cycle arrest associated with anoxia-induced quiescence, anoxic preconditioning, and embryonic diapause in embryos of the annual killifish Austrofundulus limnaeus, J. Comp Physiol B 182 (2012) pp. 909-920.

58. M.A. Menze, K. Hutchinson, S.M. Laborde, and S.C. Hand, Mitochondrial permeability transition in the crustacean Artemia franciscana: absence of a calcium-regulated pore in the face of profound calcium storage, Am. J. Physiol Regul. Integr. Comp Physiol 289 (2005) p. R68-R76.

59. T.W. Mitchell, R. Buffenstein, and A.J. Hulbert, Membrane phospholipid composition may contribute to exceptional longevity of the naked mole-rat (Heterocephalus glaber): a comparative study using shotgun lipidomics, Exp. Gerontol. 42 (2007) pp. 1053-1062.

60. D.S. Moore, R. Hansen, and S.C. Hand, Liposomes with diverse compositions are protected during desiccation by LEA proteins from Artemia franciscana and trehalose, Biochim. Biophys. Acta 1858 (2016) pp. 104-115.

61. B.D. Murphy, Embryonic diapause: advances in understanding the enigma of seasonal delayed implantation, Reprod. Domest. Anim 47 Suppl 6 (2012) pp. 121-124.

62. F. Nambu, S. Tanaka, and Z. Nambu, Inbred strains of brine shrimp derived from Artemia franciscana: lineage, RAPD analysis, life span, reproductive traits and mode, adaptation, and tolerance to salinity changes, Zoolog. Sci. 24 (2007) pp. 159-171.

63. M. Naz, The changes in the biochemical compositions and enzymatic activities of rotifer (Brachionus plicatilis, Muller) and Artemia during the enrichment and starvation periods, Fish. Physiol Biochem. 34 (2008) pp. 391-404.

64. A.E. Oliver, D.K. Hincha, and J.H. Crowe, Looking beyond sugars: the role of amphiphilic solutes in preventing adventitious reactions in anhydrobiotes at low water contents, Comp Biochem. Physiol A Mol. Integr. Physiol 131 (2002) pp. 515-525.

65. S.P. Patel and S.S. Katyare, Insulin status-dependent alterations in lipid/phospholipid composition of rat kidney microsomes and mitochondria, Lipids 41 (2006) pp. 819-825.

66. E. PETRUSHKA, J.H. Quastel, and P.G. SCHOLEFIELD, Role of phospholipids in oxidative phosphorylation and mitochondrial structure, Can. J. Biochem. Physiol 37 (1959) pp. 989-998.

67. J.A. Reynolds and S.C. Hand, Differences in isolated mitochondria are insufficient to account for respiratory depression during diapause in artemia franciscana embryos, Physiol Biochem. Zool. 77 (2004) pp. 366-377.

68. T.K. Rostovtseva and S.M. Bezrukov, VDAC regulation: role of cytosolic proteins and mitochondrial lipids, J. Bioenerg. Biomembr. 40 (2008) pp. 163-170.

69. J. Schindelin, I. Arganda-Carreras, E. Frise, V. Kaynig, M. Longair, T. Pietzsch, S. Preibisch, C. Rueden, S. Saalfeld, B. Schmid, J.Y. Tinevez, D.J. White, V. Hartenstein, K. Eliceiri, P. Tomancak, and A. Cardona, Fiji: an open-source platform for biological-image analysis, Nat. Methods 9 (2012) pp. 676-682.

70. I. Shibuya, C. Miyazaki, and A. Ohta, Alteration of phospholipid composition by combined defects in phosphatidylserine and cardiolipin synthases and physiological consequences in Escherichia coli, J. Bacteriol. 161 (1985) pp. 1086-1092.

71. K. Shinzawa-Itoh, H. Aoyama, K. Muramoto, H. Terada, T. Kurauchi, Y. Tadehara, A. Yamasaki, T. Sugimura, S. Kurono, K. Tsujimoto, T. Mizushima, E. Yamashita, T. Tsukihara, and S. Yoshikawa, Structures and physiological roles of 13 integral lipids of bovine heart cytochrome c oxidase, EMBO J. 26 (2007) pp. 1713-1725.

72. B. Simons, D. Kauhanen, T. Sylvanne, K. Tarasov, E. Duchoslav, and K. Ekroos, Shotgun Lipidomics by Sequential Precursor Ion Fragmentation on a Hybrid Quadrupole Time-of-Flight Mass Spectrometer, Metabolites. 2 (2012) pp. 195-213.

73. P.K. Smith, R.I. Krohn, G.T. Hermanson, A.K. Mallia, F.H. Gartner, M.D. Provenzano, E.K. Fujimoto, N.M. Goeke, B.J. Olson, and D.C. Klenk, Measurement of protein using bicinchoninic acid, Anal. Biochem. 150 (1985) pp. 76-85.

74. A. Thalhammer, M. Hundertmark, A.V. Popova, R. Seckler, and D.K. Hincha, Interaction of two intrinsically disordered plant stress proteins (COR15A and COR15B) with lipid membranes in the dry state, Biochim. Biophys. Acta 1798 (2010) pp. 1812-1820.

75. D. Tolleter, D.K. Hincha, and D. Macherel, A mitochondrial late embryogenesis abundant protein stabilizes model membranes in the dry state, Biochim. Biophys. Acta 1798 (2010) pp. 1926-1933.

76. van Meer G., D.R. Voelker, and G.W. Feigenson, Membrane lipids: where they are and how they behave, Nat. Rev. Mol. Cell Biol. 9 (2008) pp. 112-124.

77. R.I. Viner and J.S. Clegg, Influence of trehalose on the molecular chaperone activity of p26, a small heat shock/alpha-crystallin protein, Cell Stress. Chaperones. 6 (2001) pp. 126-135.

78. A.H. Warner, R.T. Brunet, T.H. MacRae, and J.S. Clegg, Artemin is an RNA-binding protein with high thermal stability and potential RNA chaperone activity, Arch. Biochem. Biophys. 424 (2004) pp. 189-200.

79. A.H. Warner, S. Chakrabortee, A. Tunnacliffe, and J.S. Clegg, Complexity of the heat-soluble LEA proteome in Artemia species, Comp Biochem. Physiol Part D. Genomics Proteomics. 7 (2012) pp. 260-267.

80. A.H. Warner and J.S. Clegg, Diguanosine nucleotide metabolism and the survival of artemia embryos during years of continuous anoxia, Eur. J. Biochem. 268 (2001) pp. 1568-1576.

81. J.K. Willsie and J.S. Clegg, Nuclear p26, a small heat shock/alpha-crystallin protein, and its relationship to stress resistance in Artemia franciscana embryos, J. Exp. Biol. 204 (2001) pp. 2339-2350.

82. G. Woldegiorgis and E. Shrago, Adenine nucleotide translocase activity and sensitivity to inhibitors in hepatomas. Comparison of the ADP/ATP carrier in mitochondria and in a purified reconstituted liposome system, J. Biol. Chem. 260 (1985) pp. 7585-7590.

83. M. Wysocka-Kapcinska, B. Torocsik, L. Turiak, G. Tsaprailis, C.L. David, A.M. Hunt, K. Vekey, V. Adam-Vizi, R. Kucharczyk, and C. Chinopoulos, The suppressor of AAC2 Lethality SAL1 modulates sensitivity of heterologously expressed artemia ADP/ATP carrier to bongkrekate in yeast, PLoS. ONE. 8 (2013) p. e74187.

84. J. Xia, I.V. Sinelnikov, B. Han, and D.S. Wishart, MetaboAnalyst 3.0--making metabolomics more meaningful, Nucleic Acids Res. 43 (2015) p. W251-W257.

85. G. Xie and S.N. Timasheff, The thermodynamic mechanism of protein stabilization by trehalose, Biophys. Chem 64 (1997) pp. 25-43.

86. P.H. Yancey, Organic osmolytes as compatible, metabolic and counteracting cytoprotectants in high osmolarity and other stresses, J. Exp. Biol. 208 (2005) pp. 2819-2830.

87. E. Zinser, C.D. Sperka-Gottlieb, E.V. Fasch, S.D. Kohlwein, F. Paltauf, and G. Daum, Phospholipid synthesis and lipid composition of subcellular membranes in the unicellular eukaryote Saccharomyces cerevisiae, J. Bacteriol. 173 (1991) pp. 2026-2034.

Legends to Figures

Figure 1: A: Scanned images of Western blotting of Artemia cysts, Percoll-purified mitochondria and mitoplasts for the alpha 1 subunit of the Na^+/K^+ ATPase, COX IV subunit and VDAC. **B**: Band density quantification of the scanned images shown in panel A. Data were arbitrarily normalized to the average density of the first four bands per blot. ***implies significance $p<0.001$.

Figure 2: Number of species identified in *Artemia* cysts, Percoll-purified mitochondria, and mitoplasts. AC: Acylcarnitine; CE: cholesteryl esters; Cer: ceramide; CL: cardiolipin; CoQ: coenzyme Q; DAG: diacylglycerol; PA: phosphatidic acid; LPA: lysophosphatidic acid; PC: phosphatidylcholine; LPC: lysophosphatidylcholine; PE: phosphatidylethanolamine; LPE: lysophosphatidylethanolamine; PG: phosphatidylglycerol; LPG: lysophosphatidylglycerol; PI: phosphatidylinositol; LPI: lysophosphatidylinositol; PS: phosphatidylserine; LPS: lysophosphatidylserine; SM: sphingomyelin; TAG: triacylglycerol. Data shown are Mean +/- S.E.M. (n=6).

Figure 3: Concentration of lipid classes in *Artemia* cysts, Percoll-purified mitochondria, and mitoplasts. Abbreviations are the same as in figure 2. Data shown are Mean +/- S.E.M. (n=6).

Figure 4: Concentrations of specific molecular lipid species in *Artemia* cysts, mitochondria and mitoplasts. Figures adapted from one-way ANOVA analysis performed on MetaboAnalyst 3.0. There is a significantly greater abundance of AC and TAG species in *Artemia* cysts (**A-D**), and an enrichment of MLCL (monolysocardiolipin) species in mitoplasts (**E**).

Figure 5: Hierarchical clustering performed by MetaboAnalyst 3.0 creating a heat map of the top 25 acylcarnitine molecular lipid species based on t-test/ANOVA.

Figure 6: The concentration (nmol/mg protein) of cardiolipin (CL) species listed by the brutto nomenclature (carbon:double bond) in (**A**) *Artemia* cysts, (**B**) mitochondria, and (**C**) mitoplasts with standard error shown. Monolysocardiolipin (MLCL) and dilysocardiolipin (DLCL) species are not included in the figure but species designation data can be seen in supplemental table 4. There is significant enrichment of cardiolipin species in the mitoplasts compared to the mitochondria and *Artemia* cysts, respectively.

Style Definition: Normal: Font:

The Total and Mitochondrial Lipidome of *Artemia franciscana* Encysted Embryos

Emily Chen[1], Michael A. Kiebish[1], Justice McDaniel[1], Fei Gao[1], Niven R. Narain[1], Rangaprasad Sarangarajan[1], Gergely Kacso[2,3], Dora Ravasz[2,3], Thomas N. Seyfried[4], Vera Adam-Vizi[2,5] and Christos Chinopoulos[2,3]

[1]BERG LLC, Framingham, MA 01701, USA
[2]Department of Medical Biochemistry, Semmelweis University, Budapest, 1094, Hungary
[3]MTA-SE Lendület Neurobiochemistry Research Group, Budapest, 1094, Hungary
[4]Biology Department, Boston College, Chestnut Hill, Boston, MA, 02467, USA
[5]MTA-SE Laboratory for Neurobiochemistry, Budapest, 1094, Hungary

Address correspondence to: Dr. Christos Chinopoulos, Department of Medical Biochemistry, Semmelweis University, Budapest, Tuzolto street 37-47, 1094, Hungary. Tel: +361 4591500 ext. 60024, Fax: +361 2670031. E-mail: chinopoulos.christos@eok.sote.hu

Abstract

Encysted embryos (cysts) of the crustacean *Artemia franciscana* exhibit enormous tolerance to adverse conditions encompassing high doses of radiation, years of anoxia, desiccation and extreme salinity. So far, several mechanisms have been proposed to contribute to this extremophilia, however, none were sought in the lipid profile of the cysts. Here in, ~~by using~~we used high resolution shotgun lipidomics suited for detailed quantitation and analysis of lipids in uncharacterized biological membranes and samples~~, we~~ and assembled the total, mitochondrial and mitoplastic lipidome of *Artemia franciscana* cysts. Overall, we identified and quantitated 1098 lipid species dispersed among 22 different classes and subclasses. Regarding the mitochondrial lipidome, most lipid classes exhibited little differences from those reported in other animals, however, *Artemia* mitochondria harboured much less phosphatidylethanolamine, plasmenylethanolamines and ceramides than mitochondria of other species, some of which by two orders of magnitude. Alternatively, *Artemia* mitochondria exhibited much higher levels of phosphatidylglycerols and phosphatidylserines. The identification and quantitation of the total and mitochondrial lipidome of the cysts may help in the elucidation of actionable extremophilia-affording proteins, such as the 'late embryogenesis abundant' proteins, which are known to interact with lipid membranes.

Keywords: extremophilia; cardiolipin; phosphatidylethanolamine; ceramide; phosphatidylglycerol; phosphatidylserine

Abbreviations: Acylcarnitine; CE: cholesteryl esters; Cer: ceramide; CL: cardiolipin; CoQ: coenzyme Q; DAG: diacylglycerol; PA: phosphatidic acid; LPA: lysophosphatidic acid; PC: phosphatidylcholine; LPC: lysophosphatidylcholine; PE: phosphatidylethanolamine; LEA: 'late embryogenesis abundant; LPE: lysophosphatidylethanolamine; PG: phosphatidylglycerol; LPG: lysophosphatidylglycerol; PI: phosphatidylinositol; LPI: lysophosphatidylinositol; PS: phosphatidylserine; LPS: lysophosphatidylserine; SM: sphingomyelin; TAG: triacylglycerol.

1.1 Introduction

Encysted embryos (cysts) exiting females of the species *Artemia franciscana* may enter diapause ~~(1)~~[46], an extremophilic state during which metabolism is brought into a halt, accompanied by extreme augmentation of stress tolerance ~~(2)~~[23], ~~(3)~~[51], ~~(4)~~[55], ~~(5)~~[28]. Diapause has been documented in insects ~~(6)~~[25], rotifers ~~(7)~~[14], tardigrades ~~(8)~~[27], crustaceans ~~(9)~~[45], ~~(10)~~[13], killifish ~~(11)~~[57] and mammals ~~(12)~~[61], ~~(13)~~[8]. During this state, *Artemia franciscana* cysts tolerate high doses of UV and ionizing radiation, years of continuous anoxia while hydrated at physiological temperature, thermal extremes, desiccation-hydration cycles, and very high salinity ~~(14)~~[16], ~~(15)~~[53], ~~(16)~~[15], ~~(17)~~[62]. So far, the extremophilia of these cysts has been attributed to i) elaborate 'metabolic restructuring' ~~(18)~~[33], ii) high content of the non-reducing disaccharide trehalose ~~(19)~~[85], ~~(20)~~[19], ~~(21)~~[86] iii) a very large guanine nucleotide pool ~~(22)~~[80], iv) two heat shock proteins, p26 and artemin ~~(23)~~[81], ~~(24)~~[10], ~~(25)~~[17], ~~(26)~~[78], and v) expression of 'late embryogenesis abundant' (LEA) proteins ~~(27)~~[79], ~~(28)~~[34], ~~(29)~~[60]. Other mechanisms that have been reported in *C. elegans* larvae involving polyamine utilization, glyoxalase-dependent detoxification, lipid desaturation, and reactive oxygen species detoxification pathways may also be implicated in desiccation tolerance ~~(30)~~[24]. Furthermore, it has been discovered that mitochondria obtained from the cysts of *Artemia franciscana* lack the so -called 'permeability transition' ~~(31)~~[58], ~~(32)~~[50], a non-selective high-conductance channel which leads to cell death by allowing the flux of water and other molecules up to 1,500 Da across the inner mitochondrial membrane ~~(33)~~[3]. In addition, these mitochondria are refractory to bongkrekic acid (BKA), a dual inhibitor of the permeability transition and the adenine nucleotide translocase (ANT) ~~(32)~~[50]. However, if the *Artemia franciscana* ANT is heterologously expressed in yeasts, there it regains BKA sensitivity ~~(34)~~[83], a finding that has prompted the postulation that the lipid environment of the ANT may be crucial for the BKA response.

While trehalose is critical to desiccation tolerance in the cysts ~~(20)~~[19], ~~(35)~~[20], ~~(36)~~[18], ~~(37)~~[64] and it appears to work synergistically with p26 ~~(38)~~[77], ~~(36)~~[18] and LEA proteins ~~(28)~~[34], in experiments using liposomes the additive protection by LEA proteins plus trehalose was reported to be dependent on the lipid composition of the target membrane ~~(29)~~[60]. Accordingly, molecular modeling of the secondary structures of the cytosol-targeted AfrLEA2 and mitochondrially-targeted AfrLEA3m revealed bands of charged amino acids known to interact directly with lipid membranes ~~(29)~~[60]. Along this line, it has been shown that LEA proteins preferentially stabilize membranes of a particular lipid composition based on the protein's subcellular location ~~(39)~~[74], ~~(40)~~[75], ~~(41)~~[35].

The lipid compositions of mammalian membranes are well-defined ~~(42)~~[76], ~~(43)~~[38]. Among different cells and tissues the mitochondrial lipid composition is fairly similar ~~(43)~~[38], with the exceptions of those isolated from some organs which additionally contain phosphatidylcholine (PC) and phosphatidylethanolamine (PE) plasmalogens ~~(44)~~[59], ~~(45)~~[1]. Furthermore, the molecular species of cardiolipin, a polyglycerophospholipid found exclusively in the inner mitochondrial membrane ~~(46)~~[36] exhibit considerable diversity between tissues and among disease states ~~(47)~~[42], ~~(48)~~[12], ~~(49)~~[32], ~~(50)~~[31], ~~(51)~~[43], ~~(52)~~[11]. On the other hand, lipids from *Artemia franciscana* cysts have been scarcely investigated. So far, it is known that *Artemia franciscana* cysts are unique because they harbor complex fucosyl and neutral glycosphingolipids, not found in other animal species ~~(53)~~[49], ~~(54)~~[48], and also sphingomyelin (SM) ~~(55)~~[47], which has been found in species belonging to other invertebrate phyla but not

Echinodermata and Lophotrochozoa ~~(55)~~[47]. Furthermore, it is known that the lipid content of *Artemia* varies considerably during enrichment and starvation periods, implying a dynamic character ~~(56)~~[63]; this dynamism in lipid profile is also supported by an intricate regiospecific distribution of fatty acids in triacylglycerols of *Artemia franciscana* nauplii enriched with fatty acid ethyl esters ~~(57)~~[2] or microalgae ~~(58)~~[9].

Mindful of i) the scarcity of information regarding the lipid profile of *Artemia franciscana* cysts, ii) the potential importance of lipid composition in affording extremophilia and the documented synergism of LEA proteins in doing so as a function of the lipid environment, we investigated the lipidome of the cysts. By using a MS/MS^{ALL} high resolution shotgun lipidomics workflow which is ideally suited for detailed quantitation and analysis of lipids in uncharacterized biological membranes and samples ~~(59)~~[30] we assembled the total and mitochondrial lipid profile of *Artemia franciscana* cysts. Comparisons of their lipidomes to those obtained from mammalian tissues revealed stark quantitative differences which may help to explain the extremophilia of the cysts, especially in relation to the functions of LEA proteins.

2.1 Materials and Methods

2.1. Hydration and dechorionation of Artemia franciscana cysts: No permits were required for the described study, which complied with all relevant regulations. Dehydrated, encysted gastrulae of *Artemia franciscana* were obtained from Salt Lake, Utah through Artemia International LLC (Fairview, Texas 75069, USA) and stored at 4°C until used. Embryos (15 gr) were hydrated in 0.25 M NaCl at room temperature for 16-18 h during constant aeration. After this developmental incubation, the embryos were dechorionated in modified antiformin solution (1% hypochlorite from bleach, 60 mM $NaCO_3$, and 0.4 M NaOH) for 30 min, followed by a rinse in 1% Na^+-thiosulfate (5 min) and multiple washings in ice-cold 0.25 M NaCl as previously described ~~(60)~~[52]. For further lipidomic analysis, dechorionated embryos were pelleted by centrifugation for 5 min at 300 g at 4°C, snap-frozen with liquid nitrogen and stored in -20 ^{o}C, until use.

2.1.2 Isolation of mitochondria and mitoplasts from Artemia franciscana: Mitochondria from embryos of *Artemia franciscana* were prepared as described elsewhere, with minor modifications ~~(61)~~[67]. Dechorionated embryos were filtered through filter paper, and ~10 gr were homogenized in ice-cold isolation buffer consisting of 0.5 M sucrose, 150 mM KCl, 1 mM EGTA, and 20 mM K^+-HEPES, pH 7.5, using a glass-Teflon homogenizer at 850 rpm for ten passages. The homogenate was centrifuged for 10 min at 3,000 g at 4°C, the upper fatty layer of the supernatant was aspirated and the remaining supernatant was centrifuged at 11,300 g for 10 min. The resulting pellet was gently resuspended in the same buffer, avoiding the green core. The green core was discarded, and the resuspended pellet was centrifuged again at 11,300 g for 10 min. The pellet was resuspended in 0.3 ml of ice-cold isolation buffer consisting of 15% ~~percoll~~Percoll, 0.5 M sucrose, 150 mM KCl, 1 mM EGTA, and 20 mM K^+-HEPES, pH 7.5 and layered on a preformed Percoll gradient (40 and 23%). After centrifugation at 30,000 g for 6 min, the fraction between the 15% and 23% Percoll gradient interface and the supernatant above the 15% Percoll layer were discarded, and the mitochondrial fraction located at the interface between the 23% and 40 % Percoll layer was removed, diluted with isolation buffer, and centrifuged at 16,600 g for 10 min. The resulting loose pellet was resuspended in isolation buffer and centrifuged at 6,700 g for 10 min. In pilot experiments where the resulting pellet was resuspended in a 15%

Percoll and underwent a second round of a Percoll-gradient centrifugation, no more fractions between the 15% and 23% layers nor above the 15% layer formed, implying that no further purification could be achieved by this methodology. For further mitoplast isolation, the resulting pellet was resuspended in 40 ml of 10 mM K^+-HEPES pH 7.5, and kept under constant stirring at 4°C for 30 min. Subsequently, this fraction was centrifuged at 6,700 g for 10 min, the supernatant was discarded, and the pellet underwent one more round of centrifugation at 6,700 g for 10 min. The resulting pellet was snap-frozen with liquid nitrogen and stored in -20 ^oC, until use.

~~*2.1.3 Protein determination*: Protein~~*2.1.3 Western blot analysis*: Artemia cysts (dechorionated) homogenates, Percoll-purified mitochondria and mitoplasts were solubilised in 10% sodium dodecyl sulphate, the insoluble pellets were discarded, and the supernatants were frozen at -20 ^oC for further analysis. These samples were thawed on ice, their protein concentration was determined using the bicinchoninic acid assay~~, and calibrated using bovine serum standards~~ as detailed in section 2.14, loaded at a concentration of 20 μg per well on the gels and separated by sodium dodecyl sulphate – polyacrylamide gel electrophoresis (SDS-PAGE). Separated proteins were transferred to a methanol-activated polyvinylidene difluoride membrane. Immunoblotting was performed as recommended by the manufacturers of the antibodies. Rabbit polyclonal anti-alpha 1 subunit of Na^+/K^+ ATPase, mouse monoclonal anti-COX IV subunit, and rabbit monoclonal anti-VDAC1 (Abcam, Cambridge, UK), primary antibody were used at titers of 1:1,000. Immunoreactivity was detected using the appropriate peroxidase-linked secondary antibody (1:5,000, donkey anti-rabbit or donkey anti-mouse, Jackson Immunochemicals Europe Ltd, Cambridgeshire, UK) and enhanced chemiluminescence detection reagent (ECL system; Amersham Biosciences GE Healthcare Europe GmbH, Vienna, Austria). Densitometric analysis of the bands was performed in Fiji ~~(62)~~[69].

Formatted: Font color: Custom Color(RGB(34,34,34))

Formatted: Font color: Custom Color(RGB(34,34,34))

Field Code Changed

2.1.4 Protein determination: Protein concentration was determined using the bicinchoninic acid assay, and calibrated using bovine serum standards [73] using a Tecan Infinite® 200 PRO series plate reader (Tecan Deutschland GmbH, Crailsheim, Germany).

2.1.~~4~~ 5 Transmission electron microscopy (TEM): Mitochondrial and mitoplasts fractions were pelleted by centrifugation and fixed overnight in 4% gluteraldehyde and 175 mM Na^+-cacodylate buffer, pH 7.5, at 4 ^oC. Subsequently, pellets were post-fixed with 1% osmium tetroxide for 100 min, followed by dehydration by alcohol and propylene oxide and embedded in Durcupan. Series of ultrathin sections (76 nm) were prepared by an ultramicrotome, mounted on single-slot copper grids, contrasted with 6 % uranyl acetate (20 min) and lead citrate (5 min), and observed with a JEOL 1200 EMX (Peabody, MA, USA) electron microscope.

2.1.~~5~~ 6 Liquid/Liquid Extraction of Structural Lipids: Mitoplasts from Percoll-purified *Artemia franciscana* mitochondria, Percoll-purified *Artemia franciscana* mitochondria, and dechorionated hatched *Artemia franciscana* cysts were thawed and diluted with a ten-times diluted PBS solution. All samples were homogenized in Omni bead tubes with 2.8 mm ceramic beads in the Omni Bead Ruptor 24 with Cryo Cooling Unit (Omni International, Kennesaw, GA) at 4 ^oC for 2 minutes. Protein concentration was determined by the bicinchoninic acid assay. 1 mg proportion of protein from mitoplasts, Percoll-purified mitochondria, and dechorionated hatched cyst samples were aliquoted and a cocktail of deuterium-labeled and odd chain phospholipid standards from diverse lipid classes was added (supplemental table 18). Standards were chosen so that they represented each lipid class and were at designated concentrations chosen to provide the most accurate quantitation and dynamic range for each lipid species. 4 mL chloroform:methanol (1:1, by vol) was added to each sample and lipidomic extractions were performed as previously described ~~(63)~~[41]. Lipid extraction was automated using a customized sequence on a Hamilton Robotics STARlet system (Hamilton, Reno, NV). Lipid extracts were dried under nitrogen and reconstituted in chloroform:methanol (1:1, by vol). Samples were flushed with nitrogen and stored at -20°C.

2.1.~~6~~ 7 Direct Infusion MS/MS^{ALL} Structural Lipidomics Platform: Samples were diluted 50 times in isopropanol:methanol:acetonitrile:water (3:3:3:1, by vol.) with 2 mM ammonium acetate in order to optimize ionization efficiency in positive and negative modes. Electrospray ionization-MS was performed on a TripleTOF® 5600^{+} (SCIEX, Framingham, MA), coupled to a customized direct injection loop on an Ekspert microLC200 system (SCIEX). 50 μL of sample was injected at a flow-rate of 6 μL/min. Lipids were analyzed using a customized data independent analysis strategy on the TripleTOF® 5600^{+} allowing for MS/MS^{ALL} high resolution and high mass accuracy analysis as previously described ~~(64)~~[72]. Quantification was performed using an in-house library on MultiQuant™ software (SCIEX~~).~~

) and isotopic correction was performed as described in [29] and reviewed in [30].

2.1.~~.~~87 Standards and Chemicals

Cyst dechorionation and mitochondria/mitoplast preparation: Standard laboratory chemicals and alamethicin were from Sigma (St. Louis, MO, USA). Electron microscopy: Durcupan, gluteraldehyde, uranyl acetate and lead citrate were from Sigma. Lipidomics: All standards were purchased from Avanti Polar Lipids (Alabaster, AL), Nu-Chek Prep Inc. (Waterville, MN), or Cambridge Isotope Laboratories (Tewksbury, MA). All solvents were of HPLC or LC/MS grade and were acquired from Fisher Scientific (Waltham, MA) or VWR International (Radnor, PA).

2.1.~~8~~9 Statistics

Data are presented as averages ± S.E.M.. Significant differences between three or more groups were evaluated by one-way analysis of variance followed by Tukey's, Fisher's LSD, or Dunnett's post-hoc analysis. $P < 0.05$ was considered statistically significant. If normality test failed, ANOVA on Ranks was performed. One-way ANOVA analysis was performed on MetaboAnalyst 3.0 as described in ~~(65)~~[84].

3.1 Results

3.1.1 Determination of the purity of mitochondria and mitoplasts isolated from Artemia franciscana cysts

One of the main objectives of this study was to assemble the mitochondrial lipidome from *Artemia franciscana* cysts therefore, it was necessary to evaluate the purity of our preparations. We isolated mitochondria from the cysts in two steps: i) a crude mitochondrial extract was prepared by standard differential centrifugation, followed by ii) purification of the extract by a Percoll gradient. Furthermore, from the Percoll-purified mitochondria, mitoplasts were prepared using a protocol that strips off the outer membrane of mitochondria without the use of detergents and yields a fraction exhibiting high purity of mitochondrial-derived lipids and proteins. The purity of intracellular organelle preparations is usually estimated by following the relative concentration of an organelle- or membrane-specific marker~~, and/or a marker not found in the particular organelles, during the purification protocol. However, such approaches are at the mercy of the sensitivity of probing for these markers; furthermore, we were interested in quantifying the amount of lipid classes which are distributed among most biological membranes. In~~. Here, we tested the various fractions for the presence of a i) well-characterized plasma membrane marker, the alpha 1 subunit of Na/K ATPase (using ab211130 from Abcam), ii) VDAC as a marker of outer mitochondrial membrane, and iii) COX IV subunit as a marker of the inner mitochondrial membrane. We must note that we tested a number of different antibodies that either did not yield any bands in the samples obtained from the *Artemia*, or yielded bands that were far from the expected molecular weights, possibly due to insufficient homology between mammalian proteins (to which antibodies are usually raised) and those appearing in the *Artemia* cysts. The antibodies used hereby yielded bands at the expected molecular weight (the antibody used for the alpha 1 subunit of Na^+/K^+ ATPase is marketed as suitable for *Danio rerio*, and there is a very high degree of homology of this protein between this organism and *Artemia franciscana*). VDAC and COX IV subunit are highly conserved proteins among many species. Scanned images of the Western blots are shown in figure 1. As shown in figure panel 1A, samples from four different preparations of each fraction (Artemia cysts, Percoll-purified mitochondria and mitoplasts) have been loaded in gels (20 micrograms each), and probed with the aforementioned antibodies. The quantification of the band densities are shown in figure panel 1B. It is evident that upon mitochondrial and mitoplasts purification, the presence of a plasma membrane component disappears, while mitochondrial components are enriched. The persistence of VDAC in mitoplasts is probably due to the fact that it is mostly localizes to ‘contact sites’, entities where the inner and the outer mitochondrial membranes meet, which cannot be removed by a hypotonic shock.

Furthermore, in order to assess the extent of contamination of the fractions by non-mitochondrial elements using a different approach, we performed an electron microscopic evaluation of each fraction and visually identify mitochondria and non-mitochondrial elements. Results are shown in supplemental figure 1.

From the results obtained from figure 1 and supplemental figure 1 we concluded that the mitochondrial and mitoplastic fractions are highly enriched in mitochondrial elements and essentially devoid of plasma membrane contaminants.

Formatted: Indent: First line: 0 cm

3.1.2 Determination of the total and mitochondrial lipidome of Artemia franciscana cysts

Artemia franciscana cysts, mitochondria and mitoplasts were subject to MS/MS^{ALL} high resolution shotgun lipidomics workflow. All samples were from 6 independent harvests, each measured two or four (for CL) times to receive optimal reproducible analytical measurements. The MS/MS^{ALL} acquisition technique, introduced by Simons et al ~~(64)~~[72], is one of information-independent tandem mass spectrometry. It implements a Q1 stepped mass isolation window through a set mass range in 1 Da increments, and then fragments and records all product ions and neutral losses. After the entire mass range was scanned in this fashion, all of the data collected was matched to an in-house database for lipid identification and quantitation (see Supplemental Figure 2). For lipid identification, we identified the different lipid classes and their molecular structures based on a variety of criteria, such as the polarity, the high mass-accuracy molecular weight and diagnostic MS/MS product ions (product ions or neutral losses, see supplemental table 17).

To assess the overall abundance and detection of molecular species across lipid classes, we plotted the number of species detected in cysts, mitochondria, and mitoplasts. There was a decrease in molecular complexity between cysts, mitochondria, and mitoplasts, respectively, based on the number of species detected specifically for negatively charged lipids such as phosphatidic acid, phosphatidylglycerol, phosphatidylinositol, and phosphatidylserine (Figure ~~1~~2). This did not correspond to a decrease in the overall abundance of these lipids in mitoplasts (Figure ~~2~~3). p values for comparisons among samples are given in Tables 1 and 2, for number of species per lipid class and total lipid concentrations, respectively. Only p values yielding a numerical return of <0.05 are given in the tables. Those that are left blank are not statistically significant.

In general, the mechanisms regulating lipidomic diversity, molecular sculpting, and biophysical adaption in the inner mitochondrial membrane compared to the rest of the cell are limited, allowing for homeostatic regulation that is more bioenergetically efficient within the mitochondrion. Further, acyl carnitines dramatically decreased in molecular diversity from cyst, mitochondria, and mitoplast, respectively as well as some triglyceride species (Figures ~~3~~4 and ~~4~~5). These changes are directly associated with the functional correlate of their metabolic regulation within mitochondria. Regarding mitochondrial and mitoplast enrichment, cardiolipin correspondingly increased, respectively, based on its abundance in the inner mitochondrial membrane. Interestingly, storage lipids, such as diacylglycerol and triacylglycerol, decreased by 80-90 percent in the mitoplast, indicative of the purity of the mitochondria and lack of association with these energy stores (Figure ~~2~~3). Additionally, positively charged and neutral lipids such as phosphatidylcholine, sphingomyelin, and cholesterol esters decreased with enrichment of mitoplasts and negatively charged lipids such as PI, ~~PS,~~ PG, and PA did not change except for the increase in cardiolipin. These characteristic changes are hallmark to mitochondrial and mitoplast lipid composition, since the proton gradient in mitochondria requires the enriched negative charge membrane to maintain the proton motive force as well as a corresponding decrease in positive, neutral or sterol lipid classes. Analysis of the molecular species characterization and fatty acid contributions to individual species revealed a predominance of palmitic, steric, oleic, and linoleic species as well as an abundance of linolenic fatty acid (18:3) (Supplemental Tables 1-15, using shorthand nomenclature as described in ~~(66)~~[54]), which surprisingly increased the proportion of 18:3 containing cardiolipin species (Supplemental Table 4). Additionally, the molecular species enrichment and diversity increased in mitoplasts compared to mitochondria and cysts (Figure ~~5~~6). Thus, the global analysis of the *Artemia franciscana* cyst, mitochondrial, and mitoplast lipidome greatly enhanced the understanding of biophysical and structural diversity of lipids in theses cellular and subcellular compartments in these organisms.

Formatted: Tab stops: 6.03 cm, Left

4.1. Discussion

It is well established that lipids regulate the functions of membrane-embedded proteins, membrane fluidity and define compartmentalization. More specifically, mitochondrial membrane lipids regulate respiratory complex activities, protein import, adenine nucleotide exchange and ATP synthesis ~~(67)~~[26], ~~(46)~~[36], ~~(68)~~[66], ~~(69)~~[71], ~~(70)~~[39], ~~(43)~~[38], ~~(71)~~[6], ~~(72)~~[82], ~~(73)~~[37]. Furthermore, mitochondrial membrane fluidity regulated by lipid composition is known to be subject to endocrine regulation ~~(74)~~[4], ~~(75)~~[65], ~~(76)~~[40]. It is therefore prudent to

Field Code Changed

Field Code Changed

Field Code Changed

Field Code Changed

consider that lipid composition affords an equal opportunity for diversification and adaptation as the other biological macromolecules, i.e. proteins and nucleic acids.

Here, we assembled the total and mitochondrial lipidome of the extremophile cysts, *Artemia franciscana*. A comparison of the total lipidome of *Artemia franciscana* cysts to that of embryos from other organisms is perhaps less informative than the comparison of their mitochondrial lipidomes. The most striking findings in our work were that *Artemia* mitochondria harbour much less phosphatidylethanolamine, plasmenylethanolamines and ceramides than mitochondria of other species, some of which by two orders of magnitude, but on the other hand *Artemia* mitochondria exhibited much higher values of phosphatidylglycerols and phosphatidylserines ~~(77)~~[44], ~~(51)~~[43], ~~(43)~~[38]. The finding that *Artemia* mitochondria contain very high levels of phosphatidylserine is at odds to what is known and accepted for mammalian and plant mitochondria: in mammals and plants phosphatidylserine is found in abundance in plasma membranes (~34 % of the total phospholipid, [87]), as opposed to mitochondria that exhibit relatively small amounts compared to other phospholipids (~1.0 % of total phospholipid) [22], [38], [56]. These differences directly highlight the inherent biophysical and adaptive requirements of Artemia as well as their subcellular organelles to adapt to dynamic environmental changes. Decreases in zwitter ionic lipids and neutral lipids as well as corresponding increases in negatively charged lipids, such as phosphatidylglycerol and phosphatidylserine serve multiple roles in establishing metabolic adaption. Interestingly, it has been shown that increases in phosphatidylglycerol and phosphatidylserine to a lesser extent can serve as a compensatory mechanism to decreased cardiolipin content in non-mammalian systems ~~(78)~~[21]. In the present circumstances, there are no pathogenic changes in cardiolipin, thus demonstrating increases in endogenous PS and PG content serve as an evolutionary conserved mechanism compensating for ionic challenge and maintenance of the proton gradient ~~(79)~~[70]. The remaining lipid species exhibited quantitative variations, but they were within the same range. The large differences in the aforementioned lipid classes may well have an impact on the function of membrane-embedded proteins.

Formatted: Indent: First line: 1.27 cm

The composition of the mitochondrial lipidome is homeostatically regulated and tailored to its adaptive function for bioenergetic efficiency. Thus, the intricacy of cellular as well as mitochondrial lipidome demonstrate a systems level interpretation of biological function. In regard to the mitochondrial lipidome, the lipid composition and molecular species distributions is known to alter specific mitochondrial membrane-bound proteins, such as VDAC ~~(80)~~[68], ~~(81)~~[7] carnitine acyltransferase ~~(78)~~[21], complex I ~~(51)~~[43], and the ANT ~~(71)~~[6], ~~(72)~~[82], ~~(82)~~[5], ~~(73)~~[37]. By the same token, it is easy to envisage that LEA proteins afford a greater extent of extremophilia when embedded in lipid membranes the composition of which resemble that elucidated in the present study. Thus, characterization and enrichment of knowledge around the cellular, mitochondrial, and mitoplast lipidome in Artemia affords novel insight into the endogenous and evolutionary nature of the membrane in metabolically adaption in harsh environmental conditions.

Acknowledgements: We thank Ujvari Zsuzsa and Jakab Andrea for excellent technical assistance. The work described in the text was supported by the Országos Tudományos Kutatási Alapprogram (OTKA) grant 112230, the Hungarian Academy of Sciences grant 02001, the Hungarian Brain Research Program KTIA_13_NAP-A-III/6 to V.A.-V. and MTA-SE Lendület Neurobiochemistry Research Division 95003, OTKA NNF 78905, OTKA NNF2 85658 and OTKA K 100918 to C.C.

CONFLICT OF INTEREST STATEMENT: The authors declare no conflict of interests.

Reference List

1. ~~King, A. M., Toxopeus, J., and MacRae, T. H. (2014)Artemin, a diapause-specific chaperone, contributes to the stress tolerance of Artemia franciscana cysts and influences their release from females *J. Exp. Biol.* **217,** 1719-1724~~

~~2. Denlinger, D. L. (2002)Regulation of diapause *Annu. Rev. Entomol.* **47,** 93-122~~

~~3. Kostal, V. (2006)Eco-physiological phases of insect diapause *J. Insect Physiol* **52,** 113-127~~

~~4. MacRae, T. H. (2010)Gene expression, metabolic regulation and stress tolerance during diapause *Cell Mol. Life Sci.* **67,** 2405-2424~~

~~5. Hahn, D. A. and Denlinger, D. L. (2011)Energetics of insect diapause *Annu. Rev. Entomol.* **56,** 103-121~~

~~6. Fan, L., Lin, J., Zhong, Y., and Liu, J. (2013)Shotgun proteomic analysis on the diapause and non-diapause eggs of domesticated silkworm Bombyx mori *PLoS. ONE.* **8,** e60386~~

~~7. Clark, M. S., Denekamp, N. Y., Thorne, M. A., Reinhardt, R., Drungowski, M., Albrecht, M. W., Klages, S., Beck, A., Kube, M., and Lubzens, E. (2012)Long-term survival of hydrated resting eggs from Brachionus plicatilis *PLoS. ONE.* **7,** e29365~~

~~8. Guidetti, R., Altiero, T., and Rebecchi, L. (2011)On dormancy strategies in tardigrades *J. Insect Physiol* **57,** 567-576~~

~~9. King, A. M. and MacRae, T. H. (2012)The small heat shock protein p26 aids development of encysting Artemia embryos, prevents spontaneous diapause termination and protects against stress *PLoS. ONE.* **7,** e43723~~

~~10. Clark, K. A., Brierley, A. S., Pond, D. W., and Smith, V. J. (2013)Changes in seasonal expression patterns of ecdysone receptor, retinoid X receptor and an A-type allatostatin in the copepod, Calanus finmarchicus, in a sea loch environment: an investigation of possible mediators of diapause *Gen. Comp Endocrinol.* **189,** 66-73~~

~~11. Meller,~~ C. ~~L., Meller, R., Simon, R. P., Culpepper, K. M., and Podrabsky,~~ J. ~~E. (2012)Cell cycle arrest associated with anoxia-induced quiescence, anoxic preconditioning, and embryonic diapause in embryos of the annual killifish Austrofundulus limnaeus *J. Comp Physiol B* **182,** 909-920~~

~~12. Murphy, B. D. (2012)Embryonic diapause: advances in understanding the enigma of seasonal delayed implantation *Reprod. Domest. Anim* **47 Suppl 6,** 121-124~~

13. ~~Cha, J., Sun, X., Bartos, A., Fenelon, J., Lefevre, P., Daikoku, T., Shaw, G., Maxson, R., Murphy, B. D., Renfree, M. B., and Dey, S. K. (2013)A new role for muscle segment homeobox genes in mammalian embryonic diapause *Open. Biol.* **3,** 130035~~

14. ~~Clegg, J. S. (2005)Desiccation tolerance in encysted embryos of the animal extremophile, artemia *Integr. Comp Biol.* **45,** 715-724~~

15. ~~Liang, P. and MacRae, T. H. (1999)The synthesis of a small heat shock/alpha-crystallin protein in Artemia and its relationship to stress tolerance during development *Dev. Biol.* **207,** 445-456~~

16. ~~Clegg, J. S. (2001)Cryptobiosis--a peculiar state of biological organization *Comp Biochem. Physiol B Biochem. Mol. Biol.* **128,** 613-624~~

17. ~~Nambu, F., Tanaka, S., and Nambu, Z. (2007)Inbred strains of brine shrimp derived from Artemia franciscana: lineage, RAPD analysis, life span, reproductive traits and mode, adaptation, and tolerance to salinity changes *Zoolog. Sci.* **24,** 159-171~~

18. ~~Hand, S. C., Menze, M. A., Borcar, A., Patil, Y., Covi, J. A., Reynolds, J. A., and Toner, M. (2011)Metabolic restructuring during energy-limited states: insights from Artemia franciscana embryos and other animals *J. Insect Physiol* **57,** 584-594~~

19. ~~Xie, G. and Timasheff, S. N. (1997)The thermodynamic mechanism of protein stabilization by trehalose *Biophys. Chem* **64,** 25-43~~

20. ~~Crowe, J. H., Hoekstra, F. A., and Crowe, L. M. (1992)Anhydrobiosis *Annu. Rev. Physiol* **54,** 579-599~~

21. ~~Yancey, P. H. (2005)Organic osmolytes as compatible, metabolic and counteracting cytoprotectants in high osmolarity and other stresses *J. Exp. Biol.* **208,** 2819-2830~~

22. ~~Warner, A. H. and Clegg, J. S. (2001)Diguanosine nucleotide metabolism and the survival of artemia embryos during years of continuous anoxia *Eur. J. Biochem.* **268,** 1568-1576~~

23. ~~Willsie, J. K. and Clegg, J. S. (2001)Nuclear p26, a small heat shock/alpha-crystallin protein, and its relationship to stress resistance in Artemia franciscana embryos *J. Exp. Biol.* **204,** 2339-2350~~

24. ~~Chen, T., Amons, R., Clegg, J. S., Warner, A. H., and MacRae, T. H. (2003)Molecular characterization of artemin and ferritin from Artemia franciscana *Eur. J. Biochem.* **270,** 137-145~~

25. ~~Collins, C. H. and Clegg, J. S. (2004)A small heat-shock protein, p26, from the crustacean Artemia protects mammalian cells (Cos-1) against oxidative damage *Cell Biol. Int.* **28,** 449-455~~

26. ~~Warner, A. H., Brunet, R. T., MacRae, T. H., and Clegg, J. S. (2004)Artemin is an RNA-binding protein with high thermal stability and potential RNA chaperone activity *Arch. Biochem. Biophys.* **424,** 189-200~~

27. ~~Warner, A. H., Chakrabortee, S., Tunnacliffe, A., and Clegg, J. S. (2012)Complexity of the heat-soluble LEA proteome in Artemia species *Comp Biochem. Physiol Part D. Genomics Proteomics.* **7,** 260-267~~

28. ~~Hand, S. C., Menze, M. A., Toner, M., Boswell, L., and Moore, D. (2011)LEA proteins during water stress: not just for plants anymore *Annu. Rev. Physiol* **73,** 115-134~~

29. ~~Moore, D. S., Hansen, R., and Hand, S. C. (2016)Liposomes with diverse compositions are protected during desiccation by LEA proteins from Artemia franciscana and trehalose *Biochim. Biophys. Acta* **1858,** 104-115~~

30. ~~Erkut, C., Vasilj, A., Boland, S., Habermann, B., Shevchenko, A., and Kurzchalia, T. V. (2013)Molecular strategies of the Caenorhabditis elegans dauer larva to survive extreme desiccation *PLoS. ONE.* **8,** e82473~~

31. ~~Menze, M. A., Hutchinson, K., Laborde, S. M., and Hand, S. C. (2005)Mitochondrial permeability transition in the crustacean Artemia franciscana: absence of a calcium-regulated pore in the face of profound calcium storage *Am. J. Physiol Regul. Integr. Comp Physiol* **289,** R68-R76~~

~~32. Konrad, C., Kiss, G., Torocsik, B., Labar, J. L., Gerencser, A. A., Mandi, M., Adam-Vizi, V., and Chinopoulos, C. (2011)A distinct sequence in the adenine nucleotide translocase from Artemia franciscana embryos is associated with insensitivity to bongkrekate and atypical effects of adenine nucleotides on Ca(2+) uptake and sequestration *FEBS J.* **278,** 822-836~~

~~33. Azzolin, L., von Stockum S., Basso, E., Petronilli, V., Forte, M. A., and Bernardi, P. (2010)The mitochondrial permeability transition from yeast to mammals *FEBS Lett.* **584,** 2504-2509~~

~~34. Wysocka-Kapcinska, M., Torocsik, B., Turiak, L., Tsaprailis, G., David, C. L., Hunt, A. M., Vekey, K., Adam-Vizi, V., Kucharczyk, R., and Chinopoulos, C. (2013)The suppressor of AAC2 Lethality SAL1 modulates sensitivity of heterologously expressed artemia ADP/ATP carrier to bongkrekate in yeast *PLoS. ONE.* **8,** e74187~~

~~35. Crowe, J. H., Oliver, A. E., and Tablin, F. (2002)Is there a single biochemical adaptation to anhydrobiosis? *Integr. Comp Biol.* **42,** 497-503~~

~~36. Crowe, J. H., Crowe, L. M., Wolkers, W. F., Oliver, A. E., Ma, X., Auh, J. H., Tang, M., Zhu, S., Norris, J., and Tablin, F. (2005)Stabilization of dry Mammalian cells: lessons from nature *Integr. Comp Biol.* **45,** 810-820~~

~~37. Oliver, A. E., Hincha, D. K., and Crowe, J. H. (2002)Looking beyond sugars: the role of amphiphilic solutes in preventing adventitious reactions in anhydrobiotes at low water contents *Comp Biochem. Physiol A Mol. Integr. Physiol* **131,** 515-525~~

~~38. Viner, R. I. and Clegg, J. S. (2001)Influence of trehalose on the molecular chaperone activity of p26, a small heat shock/alpha-crystallin protein *Cell Stress. Chaperones.* **6,** 126-135~~

~~39. Thalhammer, A., Hundertmark, M., Popova, A. V., Seckler, R., and Hincha, D. K. (2010)Interaction of two intrinsically disordered plant stress proteins (COR15A and COR15B) with lipid membranes in the dry state *Biochim. Biophys. Acta* **1798,** 1812-1820~~

~~40. Tolleter, D., Hincha, D. K., and Macherel, D. (2010)A mitochondrial late embryogenesis abundant protein stabilizes model membranes in the dry state *Biochim. Biophys. Acta* **1798,** 1926-1933~~

~~41. Hincha, D. K. and Thalhammer, A. (2012)LEA proteins: IDPs with versatile functions in cellular dehydration tolerance *Biochem. Soc. Trans.* **40,** 1000-1003~~

~~42. van Meer G., Voelker, D. R., and Feigenson, G. W. (2008)Membrane lipids: where they are and how they behave *Nat. Rev. Mol. Cell Biol.* **9,** 112-124~~

~~43. Horvath, S. E. and Daum, G. (2013)Lipids of mitochondria *Prog. Lipid Res.* **52,** 590-614~~

~~44. Mitchell, T. W., Buffenstein, R., and Hulbert, A. J. (2007)Membrane phospholipid composition may contribute to exceptional longevity of the naked mole-rat (Heterocephalus glaber): a comparative study using shotgun lipidomics *Exp. Gerontol.* **42,** 1053-1062~~

~~45.~~ Albert, ~~C. J.,~~D.S. Anbukumar, ~~D. S.,~~ J.K. Monda, J.~~K.,~~ T. Eckelkamp, ~~J. T.,~~ and D.A. Ford, ~~D. A. (2007)~~Myocardial lipidomics. Developments in myocardial nuclear lipidomics, Front Biosci. 12~~,~~ (2007) pp. 2750-2760.

46. ~~Hoch, F. L. (1992)Cardiolipins and biomembrane function *Biochim. Biophys. Acta* **1113,** 71-133~~

~~47. Kiebish, M. A., Han, X., Cheng, H., Chuang, J. H., and Seyfried, T. N. (2008)Cardiolipin and electron transport chain abnormalities in mouse brain tumor mitochondria: lipidomic evidence supporting the Warburg theory of cancer *J. Lipid Res.* **49,** 2545-2556~~

~~48. Chicco, A. J. and Sparagna, G. C. (2007)Role of cardiolipin alterations in mitochondrial dysfunction and disease *Am. J. Physiol Cell Physiol* **292,** C33-C44~~

Formatted: Indent: Left: 0 cm, Hanging: 2.54 cm

Formatted: Font: Not Italic

Formatted: Font: Not Bold

~~49. Han, X., Yang, K., Yang, J., Cheng, H., and Gross, R. W. (2006)Shotgun lipidomics of cardiolipin molecular species in lipid extracts of biological samples *J. Lipid Res.* **47,** 864-879~~

~~50. Han, X., Yang, J., Yang, K., Zhao, Z., Abendschein, D. R., and Gross, R. W. (2007)Alterations in myocardial cardiolipin content and composition occur at the very earliest stages of diabetes: a shotgun lipidomics study *Biochemistry* **46,** 6417-6428~~

~~51. Kiebish, M. A., Han, X., Cheng, H., and Seyfried, T. N. (2009)In vitro growth environment produces lipidomic and electron transport chain abnormalities in mitochondria from non-tumorigenic astrocytes and brain tumours *ASN. Neuro.* **1,**~~

~~52. Cheng, H., Mancuso, D. J., Jiang, X., Guan, S., Yang, J., Yang, K., Sun, G., Gross, R. W., and Han, X. (2008)Shotgun lipidomics reveals the temporally dependent, highly diversified cardiolipin profile in the mammalian brain: temporally coordinated postnatal diversification of cardiolipin molecular species with neuronal remodeling *Biochemistry* **47,** 5869-5880~~

~~53. Kojima, H., Tohsato,~~ 2. Y.~~, Kabayama, K., Itonori, S., and Ito, M. (2013)Biochemical studies on sphingolipids of Artemia franciscana: complex neutral glycosphingolipids *Glycoconj. J.* **30,** 257-268~~

~~54. Kojima, H., Shimizu, T., Sugita, M., Itonori, S., Fujita, N., and Ito, M. (2011)Biochemical studies on sphingolipids of Artemia franciscana: novel neutral glycosphingolipids *J. Lipid Res.* **52,** 308-317~~

~~55. Kojima, H., Inoue, T., Sugita, M., Itonori, S., and Ito, M. (2010)Biochemical studies on sphingolipid of Artemia franciscana (I) isolation and characterization of sphingomyelin *Lipids* **45,** 635-643~~

~~56. Naz, M. (2008)The changes in the biochemical compositions and enzymatic activities of rotifer (Brachionus plicatilis, Muller) and Artemia during the enrichment and starvation periods *Fish. Physiol Biochem.* **34,** 391-404~~

~~57.~~ Ando, Y.~~,~~ Oomi, ~~Y.,~~ and K. Narukawa, ~~K. (2002)~~Regiospecific distribution of fatty acids in triacylglycerols of Artemia franciscana nauplii enriched with fatty acid ethyl esters, Comp Biochem. Physiol B Biochem. Mol. Biol. 133~~,~~ (2002) pp. 191-199.

~~58. Chakraborty, R. D., Chakraborty, K., and Radhakrishnan,~~3. L. Azzolin, von Stockum S., E. ~~V. (2007)Variation in fatty acid composition of Artemia salina nauplii enriched with microalgae and baker's yeast for use in larviculture *J. Agric. Food Chem* **55,** 4043-4051~~Basso, V. Petronilli, M.A. Forte, and P. Bernardi, The mitochondrial permeability transition from yeast to mammals, FEBS Lett. 584 (2010) pp. 2504-2509.

~~59. Han, X. and Gross, R. W. (2005)Shotgun lipidomics: electrospray ionization mass spectrometric analysis and quantitation of cellular lipidomes directly from crude extracts of biological samples *Mass Spectrom. Rev.* **24,** 367-412~~

~~60. Kwast, K. E. and Hand,~~ 4. C.S. ~~C. (1993)Regulatory features of protein synthesis in isolated mitochondria from Artemia embryos *Am. J. Physiol* **265,** R1238-R1246~~

~~61. Reynolds, J. A. and Hand, S. C. (2004)Differences in isolated mitochondria are insufficient to account for respiratory depression during diapause in artemia franciscana embryos *Physiol Biochem. Zool.* **77,** 366-377~~

~~62. Smith, P. K., Krohn, R. I., Hermanson, G. T., Mallia, A. K., Gartner, F. H., Provenzano, M. D., Fujimoto, E. K., Goeke, N. M., Olson, B. J., and Klenk, D. C. (1985)Measurement of protein using bicinchoninic acid *Anal. Biochem.* **150,** 76-85~~

~~63. Kiebish, M. A., Bell, R., Yang, K., Phan, T., Zhao, Z., Ames, W., Seyfried, T. N., Gross, R. W., Chuang, J. H., and Han, X. (2010)Dynamic simulation of cardiolipin remodeling: greasing the wheels for an interpretative approach to lipidomics *J. Lipid Res.* **51,** 2153-2170~~

Formatted: Indent: Left: 0 cm, Hanging: 2.54 cm

Formatted: Font: Not Italic

Formatted: Font: Not Bold

~~64. Simons, B., Kauhanen, D., Sylvanne, T., Tarasov, K., Duchoslav, E., and Ekroos, K. (2012)Shotgun Lipidomics by Sequential Precursor Ion Fragmentation on a Hybrid Quadrupole Time-of-Flight Mass Spectrometer *Metabolites.* **2,** 195-213~~

~~65. Xia, J., Sinelnikov, I. V., Han, B., and Wishart, D. S. (2015)MetaboAnalyst 3.0--making metabolomics more meaningful *Nucleic Acids Res.* **43,** W251-W257~~

~~66. Liebisch, G., Vizcaino, J. A., Kofeler, H., Trotzmuller, M., Griffiths, W. J., Schmitz, G., Spener, F., and Wakelam, M. J. (2013)Shorthand notation for lipid structures derived from mass spectrometry *J. Lipid Res.* **54,** 1523-1530~~

~~67. FLEISCHER, S., BRIERLEY, G., KLOUWEN, H., and SLAUTTERBACK, D. B. (1962)Studies of the electron transfer system. 47. The role of phospholipids in electron transfer *J. Biol. Chem* **237,** 3264-3272~~

~~68. PETRUSHKA, E., Quastel, J. H., and SCHOLEFIELD, P. G. (1959)Role of phospholipids in oxidative phosphorylation and mitochondrial structure *Can. J. Biochem. Physiol* **37,** 989-998~~

~~69. Shinzawa-Itoh, K., Aoyama, H., Muramoto, K., Terada, H., Kurauchi, T., Tadehara, Y., Yamasaki, A., Sugimura, T., Kurono, S., Tsujimoto, K., Mizushima, T., Yamashita, E., Tsukihara, T., and Yoshikawa, S. (2007)Structures and physiological roles of 13 integral lipids of bovine heart cytochrome c oxidase *EMBO J.* **26,** 1713-1725~~

~~70. Jiang, F., Ryan, M. T., Schlame, M., Zhao, M., Gu, Z., Klingenberg, M., Pfanner, N., and Greenberg, M. L. (2000)Absence of cardiolipin in the crd1 null mutant results in decreased mitochondrial membrane potential and reduced mitochondrial function *J. Biol. Chem* **275,** 22387-22394~~

~~71. Brandolin, G., Doussiere, J., Gulik, A., Gulik-Krzywicki, T., Lauquin, G. J., and Vignais, P. V. (1980)Kinetic, binding and ultrastructural properties of the beef heart adenine nucleotide carrier protein after incorporation into phospholipid vesicles *Biochim. Biophys. Acta* **592,** 592-614~~

~~72. Woldegiorgis, G. and Shrago, E. (1985)Adenine nucleotide translocase activity and sensitivity to inhibitors in hepatomas. Comparison of the ADP/ATP carrier in mitochondria and in a purified reconstituted liposome system *J. Biol. Chem.* **260,** 7585-7590~~

~~73. Hoffmann, B., Stockl, A., Schlame, M., Beyer, K., and Klingenberg, M. (1994)The reconstituted ADP/ATP carrier activity has an absolute requirement for cardiolipin as shown in cysteine mutants *J. Biol. Chem.* **269,** 1940-1944~~

~~74.~~ Bangur, ~~C. S.,~~ J.L. Howland, ~~J. L.,~~ and S.S. Katyare, ~~S. S. (1995)~~Thyroid hormone treatment alters phospholipid composition and membrane fluidity of rat brain mitochondria. Biochem. J. 305 (Pt 1~~),~~) (1995) pp. 29-32.

~~75. Patel, S. P. and Katyare, S. S. (2006)Insulin status-dependent alterations in lipid/phospholipid composition of rat kidney microsomes and mitochondria *Lipids* **41,** 819-825~~

~~76. Katyare, S. S., Modi, H. R., and Patel, M. A. (2006)Dehydroepiandrosterone treatment alters lipid/phospholipid profiles of rat brain and liver mitochondria *Curr. Neurovasc. Res.* **3,** 273-279~~

~~77. Kiebish, M. A., Han, X., and Seyfried, T. N. (2009)Examination of the brain mitochondrial lipidome using shotgun lipidomics *Methods Mol. Biol.* **579,** 3-18~~

~~78. Daum, G. (1985)Lipids of mitochondria *Biochim. Biophys. Acta* **822,** 1-42~~

~~79. Shibuya, I., Miyazaki, C., and Ohta, A. (1985)Alteration of phospholipid composition by combined defects in phosphatidylserine and cardiolipin synthases and physiological consequences in Escherichia coli *J. Bacteriol.* **161,** 1086-1092~~

~~80. Rostovtseva, T.~~ 5. K. ~~and Bezrukov, S. M. (2008)VDAC regulation: role of cytosolic proteins and mitochondrial lipids *J. Bioenerg. Biomembr.* **40,** 163-170~~

Formatted: Indent: Left: 0 cm, Hanging: 2.54 cm

Formatted: Font: Not Italic

Formatted: Font: Not Bold

~~81. Campbell, A. M. and Chan, S. H. (2008)Mitochondrial membrane cholesterol, the voltage dependent anion channel (VDAC), and the Warburg effect *J. Bioenerg. Biomembr.* **40,** 193-197~~

~~82.~~ Beyer~~, K. and~~ and M. Klingenberg, ~~M. (1985)~~ADP/ATP carrier protein from beef heart mitochondria has high amounts of tightly bound cardiolipin, as revealed by 31P nuclear magnetic resonance, Biochemistry 24~~,~~ (1985) pp. 3821-3826.

6. G. Brandolin, J. Doussiere, A. Gulik, T. Gulik-Krzywicki, G.J. Lauquin, and P.V. Vignais, Kinetic, binding and ultrastructural properties of the beef heart adenine nucleotide carrier protein after incorporation into phospholipid vesicles, Biochim. Biophys. Acta 592 (1980) pp. 592-614.

7. A.M. Campbell and S.H. Chan, Mitochondrial membrane cholesterol, the voltage dependent anion channel (VDAC), and the Warburg effect, J. Bioenerg. Biomembr. 40 (2008) pp. 193-197.

8. J. Cha, X. Sun, A. Bartos, J. Fenelon, P. Lefevre, T. Daikoku, G. Shaw, R. Maxson, B.D. Murphy, M.B. Renfree, and S.K. Dey, A new role for muscle segment homeobox genes in mammalian embryonic diapause, Open. Biol. 3 (2013) p. 130035.

9. R.D. Chakraborty, K. Chakraborty, and E.V. Radhakrishnan, Variation in fatty acid composition of Artemia salina nauplii enriched with microalgae and baker's yeast for use in larviculture, J. Agric. Food Chem 55 (2007) pp. 4043-4051.

10. T. Chen, R. Amons, J.S. Clegg, A.H. Warner, and T.H. MacRae, Molecular characterization of artemin and ferritin from Artemia franciscana, Eur. J. Biochem. 270 (2003) pp. 137-145.

11. H. Cheng, D.J. Mancuso, X. Jiang, S. Guan, J. Yang, K. Yang, G. Sun, R.W. Gross, and X. Han, Shotgun lipidomics reveals the temporally dependent, highly diversified cardiolipin profile in the mammalian brain: temporally coordinated postnatal diversification of cardiolipin molecular species with neuronal remodeling, Biochemistry 47 (2008) pp. 5869-5880.

12. A.J. Chicco and G.C. Sparagna, Role of cardiolipin alterations in mitochondrial dysfunction and disease, Am. J. Physiol Cell Physiol 292 (2007) p. C33-C44.

13. K.A. Clark, A.S. Brierley, D.W. Pond, and V.J. Smith, Changes in seasonal expression patterns of ecdysone receptor, retinoid X receptor and an A-type allatostatin in the copepod, Calanus finmarchicus, in a sea loch environment: an investigation of possible mediators of diapause, Gen. Comp Endocrinol. 189 (2013) pp. 66-73.

14. M.S. Clark, N.Y. Denekamp, M.A. Thorne, R. Reinhardt, M. Drungowski, M.W. Albrecht, S. Klages, A. Beck, M. Kube, and E. Lubzens, Long-term survival of hydrated resting eggs from Brachionus plicatilis, PLoS. ONE. 7 (2012) p. e29365.

15. J.S. Clegg, Cryptobiosis--a peculiar state of biological organization, Comp Biochem. Physiol B Biochem. Mol. Biol. 128 (2001) pp. 613-624.

16. J.S. Clegg, Desiccation tolerance in encysted embryos of the animal extremophile, artemia, Integr. Comp Biol. 45 (2005) pp. 715-724.

17. C.H. Collins and J.S. Clegg, A small heat-shock protein, p26, from the crustacean Artemia protects mammalian cells (Cos-1) against oxidative damage, Cell Biol. Int. 28 (2004) pp. 449-455.

18. J.H. Crowe, L.M. Crowe, W.F. Wolkers, A.E. Oliver, X. Ma, J.H. Auh, M. Tang, S. Zhu, J. Norris, and F. Tablin, Stabilization of dry Mammalian cells: lessons from nature, Integr. Comp Biol. 45 (2005) pp. 810-820.

19. J.H. Crowe, F.A. Hoekstra, and L.M. Crowe, Anhydrobiosis, Annu. Rev. Physiol 54 (1992) pp. 579-599.

20. J.H. Crowe, A.E. Oliver, and F. Tablin, Is there a single biochemical adaptation to anhydrobiosis?, Integr. Comp Biol. 42 (2002) pp. 497-503.

Formatted: Indent: Left: 0 cm, Hanging: 2.54 cm, Space After: 12 pt

Formatted: Font: Not Italic

Formatted: Font: Not Bold

21. G. Daum, Lipids of mitochondria, Biochim. Biophys. Acta 822 (1985) pp. 1-42.

22. G. Daum and J.E. Vance, Import of lipids into mitochondria, Prog. Lipid Res. 36 (1997) pp. 103-130.

23. D.L. Denlinger, Regulation of diapause, Annu. Rev. Entomol. 47 (2002) pp. 93-122.

24. C. Erkut, A. Vasilj, S. Boland, B. Habermann, A. Shevchenko, and T.V. Kurzchalia, Molecular strategies of the Caenorhabditis elegans dauer larva to survive extreme desiccation, PLoS. ONE. 8 (2013) p. e82473.

25. L. Fan, J. Lin, Y. Zhong, and J. Liu, Shotgun proteomic analysis on the diapause and non-diapause eggs of domesticated silkworm Bombyx mori, PLoS. ONE. 8 (2013) p. e60386.

26. S. FLEISCHER, G. BRIERLEY, H. KLOUWEN, and D.B. SLAUTTERBACK, Studies of the electron transfer system. 47. The role of phospholipids in electron transfer, J. Biol. Chem 237 (1962) pp. 3264-3272.

27. R. Guidetti, T. Altiero, and L. Rebecchi, On dormancy strategies in tardigrades, J. Insect Physiol 57 (2011) pp. 567-576.

28. D.A. Hahn and D.L. Denlinger, Energetics of insect diapause, Annu. Rev. Entomol. 56 (2011) pp. 103-121.

29. X. Han and R.W. Gross, Quantitative analysis and molecular species fingerprinting of triacylglyceride molecular species directly from lipid extracts of biological samples by electrospray ionization tandem mass spectrometry, Anal. Biochem. 295 (2001) pp. 88-100.

30. X. Han and R.W. Gross, Shotgun lipidomics: electrospray ionization mass spectrometric analysis and quantitation of cellular lipidomes directly from crude extracts of biological samples, Mass Spectrom. Rev. 24 (2005) pp. 367-412.

31. X. Han, J. Yang, K. Yang, Z. Zhao, D.R. Abendschein, and R.W. Gross, Alterations in myocardial cardiolipin content and composition occur at the very earliest stages of diabetes: a shotgun lipidomics study, Biochemistry 46 (2007) pp. 6417-6428.

32. X. Han, K. Yang, J. Yang, H. Cheng, and R.W. Gross, Shotgun lipidomics of cardiolipin molecular species in lipid extracts of biological samples, J. Lipid Res. 47 (2006) pp. 864-879.

33. S.C. Hand, M.A. Menze, A. Borcar, Y. Patil, J.A. Covi, J.A. Reynolds, and M. Toner, Metabolic restructuring during energy-limited states: insights from Artemia franciscana embryos and other animals, J. Insect Physiol 57 (2011) pp. 584-594.

34. S.C. Hand, M.A. Menze, M. Toner, L. Boswell, and D. Moore, LEA proteins during water stress: not just for plants anymore, Annu. Rev. Physiol 73 (2011) pp. 115-134.

35. D.K. Hincha and A. Thalhammer, LEA proteins: IDPs with versatile functions in cellular dehydration tolerance, Biochem. Soc. Trans. 40 (2012) pp. 1000-1003.

36. F.L. Hoch, Cardiolipins and biomembrane function, Biochim. Biophys. Acta 1113 (1992) pp. 71-133.

37. B. Hoffmann, A. Stockl, M. Schlame, K. Beyer, and M. Klingenberg, The reconstituted ADP/ATP carrier activity has an absolute requirement for cardiolipin as shown in cysteine mutants, J. Biol. Chem. 269 (1994) pp. 1940-1944.

38. S.E. Horvath and G. Daum, Lipids of mitochondria, Prog. Lipid Res. 52 (2013) pp. 590-614.

39. F. Jiang, M.T. Ryan, M. Schlame, M. Zhao, Z. Gu, M. Klingenberg, N. Pfanner, and M.L. Greenberg, Absence of cardiolipin in the crd1 null mutant results in decreased mitochondrial membrane potential and reduced mitochondrial function, J. Biol. Chem 275 (2000) pp. 22387-22394.

40. S.S. Katyare, H.R. Modi, and M.A. Patel, Dehydroepiandrosterone treatment alters lipid/phospholipid profiles of rat brain and liver mitochondria, Curr. Neurovasc. Res. 3 (2006) pp. 273-279.

41. M.A. Kiebish, R. Bell, K. Yang, T. Phan, Z. Zhao, W. Ames, T.N. Seyfried, R.W. Gross, J.H. Chuang, and X. Han, Dynamic simulation of cardiolipin remodeling: greasing the wheels for an interpretative approach to lipidomics, J. Lipid Res. 51 (2010) pp. 2153-2170.

42. M.A. Kiebish, X. Han, H. Cheng, J.H. Chuang, and T.N. Seyfried, Cardiolipin and electron transport chain abnormalities in mouse brain tumor mitochondria: lipidomic evidence supporting the Warburg theory of cancer, J. Lipid Res. 49 (2008) pp. 2545-2556.

43. M.A. Kiebish, X. Han, H. Cheng, and T.N. Seyfried, In vitro growth environment produces lipidomic and electron transport chain abnormalities in mitochondria from non-tumorigenic astrocytes and brain tumours, ASN. Neuro. 1 (2009).

44. M.A. Kiebish, X. Han, and T.N. Seyfried, Examination of the brain mitochondrial lipidome using shotgun lipidomics, Methods Mol. Biol. 579 (2009) pp. 3-18.

45. A.M. King and T.H. MacRae, The small heat shock protein p26 aids development of encysting Artemia embryos, prevents spontaneous diapause termination and protects against stress, PLoS. ONE. 7 (2012) p. e43723.

46. A.M. King, J. Toxopeus, and T.H. MacRae, Artemin, a diapause-specific chaperone, contributes to the stress tolerance of Artemia franciscana cysts and influences their release from females, J. Exp. Biol. 217 (2014) pp. 1719-1724.

47. H. Kojima, T. Inoue, M. Sugita, S. Itonori, and M. Ito, Biochemical studies on sphingolipid of Artemia franciscana (I) isolation and characterization of sphingomyelin, Lipids 45 (2010) pp. 635-643.

48. H. Kojima, T. Shimizu, M. Sugita, S. Itonori, N. Fujita, and M. Ito, Biochemical studies on sphingolipids of Artemia franciscana: novel neutral glycosphingolipids, J. Lipid Res. 52 (2011) pp. 308-317.

49. H. Kojima, Y. Tohsato, K. Kabayama, S. Itonori, and M. Ito, Biochemical studies on sphingolipids of Artemia franciscana: complex neutral glycosphingolipids, Glycoconj. J. 30 (2013) pp. 257-268.

50. C. Konrad, G. Kiss, B. Torocsik, J.L. Labar, A.A. Gerencser, M. Mandi, V. Adam-Vizi, and C. Chinopoulos, A distinct sequence in the adenine nucleotide translocase from Artemia franciscana embryos is associated with insensitivity to bongkrekate and atypical effects of adenine nucleotides on Ca(2+) uptake and sequestration, FEBS J. 278 (2011) pp. 822-836.

51. V. Kostal, Eco-physiological phases of insect diapause, J. Insect Physiol 52 (2006) pp. 113-127.

52. K.E. Kwast and S.C. Hand, Regulatory features of protein synthesis in isolated mitochondria from Artemia embryos, Am. J. Physiol 265 (1993) p. R1238-R1246.

53. P. Liang and T.H. MacRae, The synthesis of a small heat shock/alpha-crystallin protein in Artemia and its relationship to stress tolerance during development, Dev. Biol. 207 (1999) pp. 445-456.

54. G. Liebisch, J.A. Vizcaino, H. Kofeler, M. Trotzmuller, W.J. Griffiths, G. Schmitz, F. Spener, and M.J. Wakelam, Shorthand notation for lipid structures derived from mass spectrometry, J. Lipid Res. 54 (2013) pp. 1523-1530.

55. T.H. MacRae, Gene expression, metabolic regulation and stress tolerance during diapause, Cell Mol. Life Sci. 67 (2010) pp. 2405-2424.

56. E.M. Mejia and G.M. Hatch, Mitochondrial phospholipids: role in mitochondrial function, J. Bioenerg. Biomembr. 48 (2016) pp. 99-112.

57. C.L. Meller, R. Meller, R.P. Simon, K.M. Culpepper, and J.E. Podrabsky, Cell cycle arrest associated with anoxia-induced quiescence, anoxic preconditioning, and embryonic diapause in embryos of the annual killifish Austrofundulus limnaeus, J. Comp Physiol B 182 (2012) pp. 909-920.

58. M.A. Menze, K. Hutchinson, S.M. Laborde, and S.C. Hand, Mitochondrial permeability transition in the crustacean Artemia franciscana: absence of a calcium-regulated pore in the face of profound calcium storage, Am. J. Physiol Regul. Integr. Comp Physiol 289 (2005) p. R68-R76.

59. T.W. Mitchell, R. Buffenstein, and A.J. Hulbert, Membrane phospholipid composition may contribute to exceptional longevity of the naked mole-rat (Heterocephalus glaber): a comparative study using shotgun lipidomics, Exp. Gerontol. 42 (2007) pp. 1053-1062.

60. D.S. Moore, R. Hansen, and S.C. Hand, Liposomes with diverse compositions are protected during desiccation by LEA proteins from Artemia franciscana and trehalose, Biochim. Biophys. Acta 1858 (2016) pp. 104-115.

61. B.D. Murphy, Embryonic diapause: advances in understanding the enigma of seasonal delayed implantation, Reprod. Domest. Anim 47 Suppl 6 (2012) pp. 121-124.

62. F. Nambu, S. Tanaka, and Z. Nambu, Inbred strains of brine shrimp derived from Artemia franciscana: lineage, RAPD analysis, life span, reproductive traits and mode, adaptation, and tolerance to salinity changes, Zoolog. Sci. 24 (2007) pp. 159-171.

63. M. Naz, The changes in the biochemical compositions and enzymatic activities of rotifer (Brachionus plicatilis, Muller) and Artemia during the enrichment and starvation periods, Fish. Physiol Biochem. 34 (2008) pp. 391-404.

64. A.E. Oliver, D.K. Hincha, and J.H. Crowe, Looking beyond sugars: the role of amphiphilic solutes in preventing adventitious reactions in anhydrobiotes at low water contents, Comp Biochem. Physiol A Mol. Integr. Physiol 131 (2002) pp. 515-525.

65. S.P. Patel and S.S. Katyare, Insulin status-dependent alterations in lipid/phospholipid composition of rat kidney microsomes and mitochondria, Lipids 41 (2006) pp. 819-825.

66. E. PETRUSHKA, J.H. Quastel, and P.G. SCHOLEFIELD, Role of phospholipids in oxidative phosphorylation and mitochondrial structure, Can. J. Biochem. Physiol 37 (1959) pp. 989-998.

67. J.A. Reynolds and S.C. Hand, Differences in isolated mitochondria are insufficient to account for respiratory depression during diapause in artemia franciscana embryos, Physiol Biochem. Zool. 77 (2004) pp. 366-377.

68. T.K. Rostovtseva and S.M. Bezrukov, VDAC regulation: role of cytosolic proteins and mitochondrial lipids, J. Bioenerg. Biomembr. 40 (2008) pp. 163-170.

69. J. Schindelin, I. Arganda-Carreras, E. Frise, V. Kaynig, M. Longair, T. Pietzsch, S. Preibisch, C. Rueden, S. Saalfeld, B. Schmid, J.Y. Tinevez, D.J. White, V. Hartenstein, K. Eliceiri, P. Tomancak, and A. Cardona, Fiji: an open-source platform for biological-image analysis, Nat. Methods 9 (2012) pp. 676-682.

70. I. Shibuya, C. Miyazaki, and A. Ohta, Alteration of phospholipid composition by combined defects in phosphatidylserine and cardiolipin synthases and physiological consequences in Escherichia coli, J. Bacteriol. 161 (1985) pp. 1086-1092.

71. K. Shinzawa-Itoh, H. Aoyama, K. Muramoto, H. Terada, T. Kurauchi, Y. Tadehara, A. Yamasaki, T. Sugimura, S. Kurono, K. Tsujimoto, T. Mizushima, E. Yamashita, T. Tsukihara, and S. Yoshikawa, Structures and physiological roles of 13 integral lipids of bovine heart cytochrome c oxidase, EMBO J. 26 (2007) pp. 1713-1725.

72. B. Simons, D. Kauhanen, T. Sylvanne, K. Tarasov, E. Duchoslav, and K. Ekroos, Shotgun Lipidomics by Sequential Precursor Ion Fragmentation on a Hybrid Quadrupole Time-of-Flight Mass Spectrometer, Metabolites. 2 (2012) pp. 195-213.

73. P.K. Smith, R.I. Krohn, G.T. Hermanson, A.K. Mallia, F.H. Gartner, M.D. Provenzano, E.K. Fujimoto, N.M. Goeke, B.J. Olson, and D.C. Klenk, Measurement of protein using bicinchoninic acid, Anal. Biochem. 150 (1985) pp. 76-85.

74. A. Thalhammer, M. Hundertmark, A.V. Popova, R. Seckler, and D.K. Hincha, Interaction of two intrinsically disordered plant stress proteins (COR15A and COR15B) with lipid membranes in the dry state, Biochim. Biophys. Acta 1798 (2010) pp. 1812-1820.

75. D. Tolleter, D.K. Hincha, and D. Macherel, A mitochondrial late embryogenesis abundant protein stabilizes model membranes in the dry state, Biochim. Biophys. Acta 1798 (2010) pp. 1926-1933.

76. van Meer G., D.R. Voelker, and G.W. Feigenson, Membrane lipids: where they are and how they behave, Nat. Rev. Mol. Cell Biol. 9 (2008) pp. 112-124.

77. R.I. Viner and J.S. Clegg, Influence of trehalose on the molecular chaperone activity of p26, a small heat shock/alpha-crystallin protein, Cell Stress. Chaperones. 6 (2001) pp. 126-135.

78. A.H. Warner, R.T. Brunet, T.H. MacRae, and J.S. Clegg, Artemin is an RNA-binding protein with high thermal stability and potential RNA chaperone activity, Arch. Biochem. Biophys. 424 (2004) pp. 189-200.

79. A.H. Warner, S. Chakrabortee, A. Tunnacliffe, and J.S. Clegg, Complexity of the heat-soluble LEA proteome in Artemia species, Comp Biochem. Physiol Part D. Genomics Proteomics. 7 (2012) pp. 260-267.

80. A.H. Warner and J.S. Clegg, Diguanosine nucleotide metabolism and the survival of artemia embryos during years of continuous anoxia, Eur. J. Biochem. 268 (2001) pp. 1568-1576.

81. J.K. Willsie and J.S. Clegg, Nuclear p26, a small heat shock/alpha-crystallin protein, and its relationship to stress resistance in Artemia franciscana embryos, J. Exp. Biol. 204 (2001) pp. 2339-2350.

82. G. Woldegiorgis and E. Shrago, Adenine nucleotide translocase activity and sensitivity to inhibitors in hepatomas. Comparison of the ADP/ATP carrier in mitochondria and in a purified reconstituted liposome system, J. Biol. Chem. 260 (1985) pp. 7585-7590.

83. M. Wysocka-Kapcinska, B. Torocsik, L. Turiak, G. Tsaprailis, C.L. David, A.M. Hunt, K. Vekey, V. Adam-Vizi, R. Kucharczyk, and C. Chinopoulos, The suppressor of AAC2 Lethality SAL1 modulates sensitivity of heterologously expressed artemia ADP/ATP carrier to bongkrekate in yeast, PLoS. ONE. 8 (2013) p. e74187.

84. J. Xia, I.V. Sinelnikov, B. Han, and D.S. Wishart, MetaboAnalyst 3.0--making metabolomics more meaningful, Nucleic Acids Res. 43 (2015) p. W251-W257.

85. G. Xie and S.N. Timasheff, The thermodynamic mechanism of protein stabilization by trehalose, Biophys. Chem 64 (1997) pp. 25-43.

86. P.H. Yancey, Organic osmolytes as compatible, metabolic and counteracting cytoprotectants in high osmolarity and other stresses, J. Exp. Biol. 208 (2005) pp. 2819-2830.

87. E. Zinser, C.D. Sperka-Gottlieb, E.V. Fasch, S.D. Kohlwein, F. Paltauf, and G. Daum, Phospholipid synthesis and lipid composition of subcellular membranes in the unicellular eukaryote Saccharomyces cerevisiae, J. Bacteriol. 173 (1991) pp. 2026-2034.

Formatted: Indent: Left: 0 cm, Hanging: 2.54 cm

Legends to Figures

Figure 1: **A**: Scanned images of Western blotting of Artemia cysts, Percoll-purified mitochondria and mitoplasts for the alpha 1 subunit of the Na^+/K^+ ATPase, COX IV subunit and VDAC. **B**: Band density quantification of the scanned images shown in panel A. Data were arbitrarily normalized to the average density of the first four bands per blot. ***implies significance $p<0.001$.

Formatted: Justified

Formatted: Font: Bold

Formatted: Font: Bold

Figure 2: Number of species identified in *Artemia* cysts, Percoll-purified mitochondria, and mitoplasts. AC: Acylcarnitine; CE: cholesteryl esters; Cer: ceramide; CL: cardiolipin; CoQ: coenzyme Q; DAG: diacylglycerol; PA: phosphatidic acid; LPA: lysophosphatidic acid; PC: phosphatidylcholine; LPC: lysophosphatidylcholine; PE: phosphatidylethanolamine; LPE: lysophosphatidylethanolamine; PG: phosphatidylglycerol; LPG: lysophosphatidylglycerol; PI: phosphatidylinositol; LPI: lysophosphatidylinositol; PS: phosphatidylserine; LPS: lysophosphatidylserine; SM: sphingomyelin; TAG: triacylglycerol. Data shown are Mean +/- S.E.M. (n=6).

Formatted: Justified

Figure ~~2~~3: Concentration of lipid classes in *Artemia* cysts, Percoll-purified mitochondria, and mitoplasts. Abbreviations are the same as in figure 2. Data shown are Mean +/- S.E.M. (n=6).

Figure ~~3~~4: Concentrations of specific molecular lipid species in *Artemia* cysts, mitochondria and mitoplasts. Figures adapted from one-way ANOVA analysis performed on MetaboAnalyst 3.0. There is a significantly greater abundance of AC and TAG species in *Artemia* cysts (**A-D**), and an enrichment of MLCL (monolysocardiolipin) species in mitoplasts (**E**).

Figure ~~4~~5: Hierarchical clustering performed by MetaboAnalyst 3.0 creating a heat map of the top 25 acylcarnitine molecular lipid species based on t-test/ANOVA.

Figure ~~5~~6: The concentration (nmol/mg protein) of cardiolipin (CL) species listed by the brutto nomenclature (carbon:double bond) in (**A**) *Artemia* cysts, (**B**) mitochondria, and (**C**) mitoplasts with standard error shown. Monolysocardiolipin (MLCL) and dilysocardiolipin (DLCL) species are not included in the figure but species designation data can be seen in supplemental table 4. There is significant enrichment of cardiolipin species in the mitoplasts compared to the mitochondria and *Artemia* cysts, respectively.

Formatted: Justified

Table 1

Table 1: Differences in the Number of Lipid Species per Lipid Class

	f.value	p.value	-LOG10(p)	FDR	Fisher's LSD*
AC	157.87	8.41E-11	10.075	1.98E-09	1 - 2; 1 - 3; 2 - 3
CE	20.111	5.69E-05	4.2451	0.000535	1 - 2; 1 - 3
CoQ10	4.0909	0.038201	1.4179	0.081612	2 - 3
DAG	7.1306	0.00666	2.1765	0.024079	1 - 2; 1 - 3
SM	4.5258	0.02898	1.5379	0.065698	1 - 3; 2 - 3
TAG	5.4263	0.016861	1.7731	0.047214	1 - 3
LPC	4.738	0.025418	1.5949	0.062875	1 - 3; 2 - 3
LPG	4.9167	0.022799	1.6421	0.059532	1 - 2; 1 - 3
PA	7.4803	0.005579	2.2534	0.021851	1 - 3; 2 - 3
PE	5.4044	0.017077	1.7676	0.047214	1 - 3
PI	8.1797	0.003962	2.4021	0.016929	1 - 3; 2 - 3
PS	9.2527	0.002412	2.6177	0.011335	1 - 3; 2 - 3

*Here, 1 = *Artemia* cysts, 2 = *Artemia* mitochondria, 3 = *Artemia* mitoplasts

Table 2

Table 2: Differences in the Concentration of Lipid Species per Lipid Class

	f.value	p.value	-LOG10(p)	FDR	Fisher's LSD*
AC	138.4	2.15E-10	9.6675	3.37E-09	1 - 2; 1 - 3
CE	17.227	0.00013	3.8858	0.001019	1 - 2; 1 - 3
CL	9.6508	0.002022	2.6942	0.011335	3 - 1; 3 - 2
DAG	24.189	2.02E-05	4.6939	0.000238	1 - 2; 1 - 3
SM	6.7948	0.007927	2.1009	0.026613	1 - 3
TAG	567.21	7.36E-15	14.133	3.46E-13	1 - 2; 1 - 3
LPC	9.2808	0.002382	2.6231	0.011335	1 - 3; 2 - 3
PC	13.129	0.000506	3.2956	0.003399	1 - 2; 1 - 3
PG	4.5052	0.029355	1.5323	0.065698	2 - 1; 2 - 3
PI	5.746	0.014039	1.8527	0.043989	1 - 3; 2 - 3

*Here, 1 = *Artemia* cysts, 2 = *Artemia* mitochondria, 3 = *Artemia* mitoplasts

Figure 1
Click here to download high resolution image

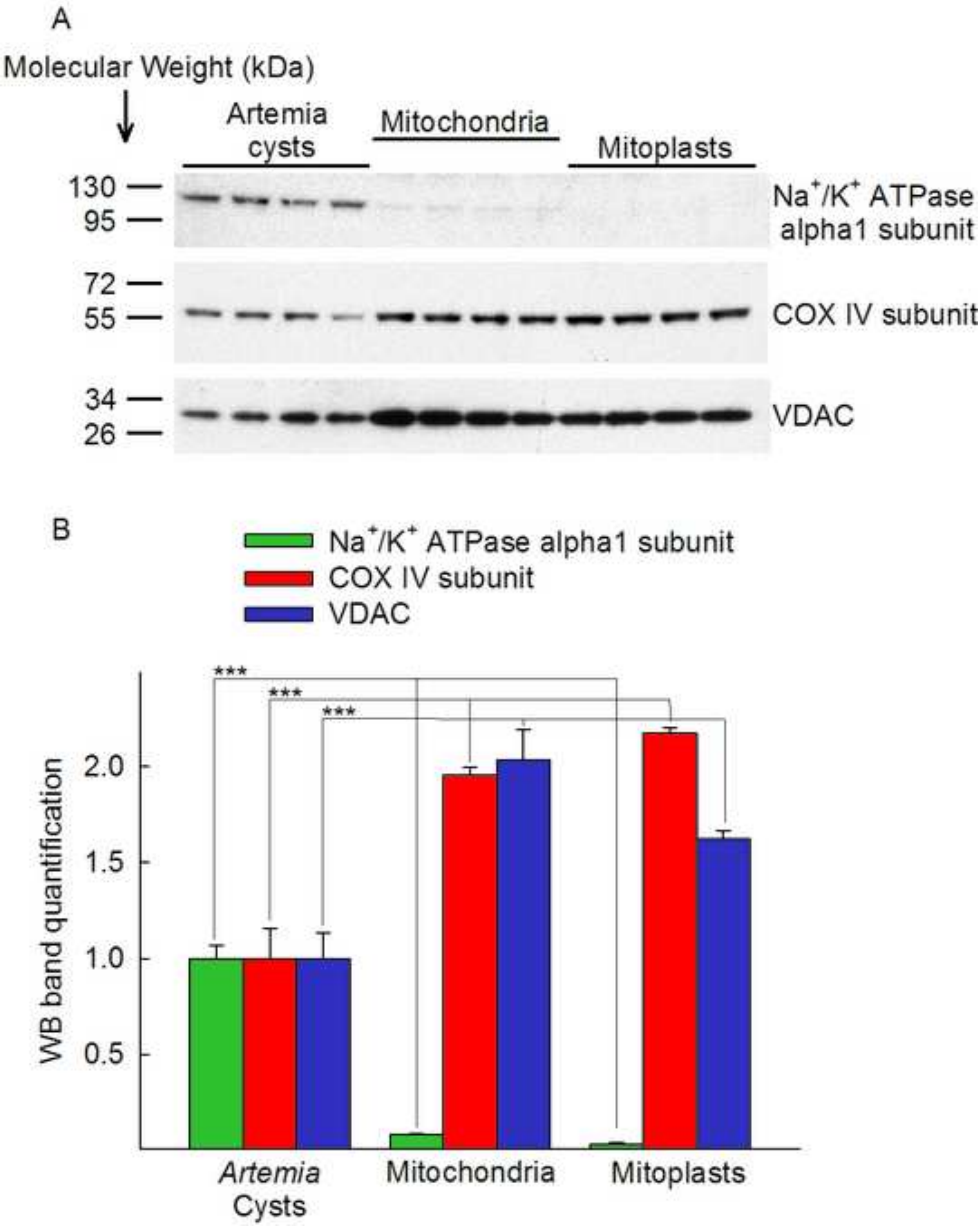

Figure 2
Click here to download high resolution image

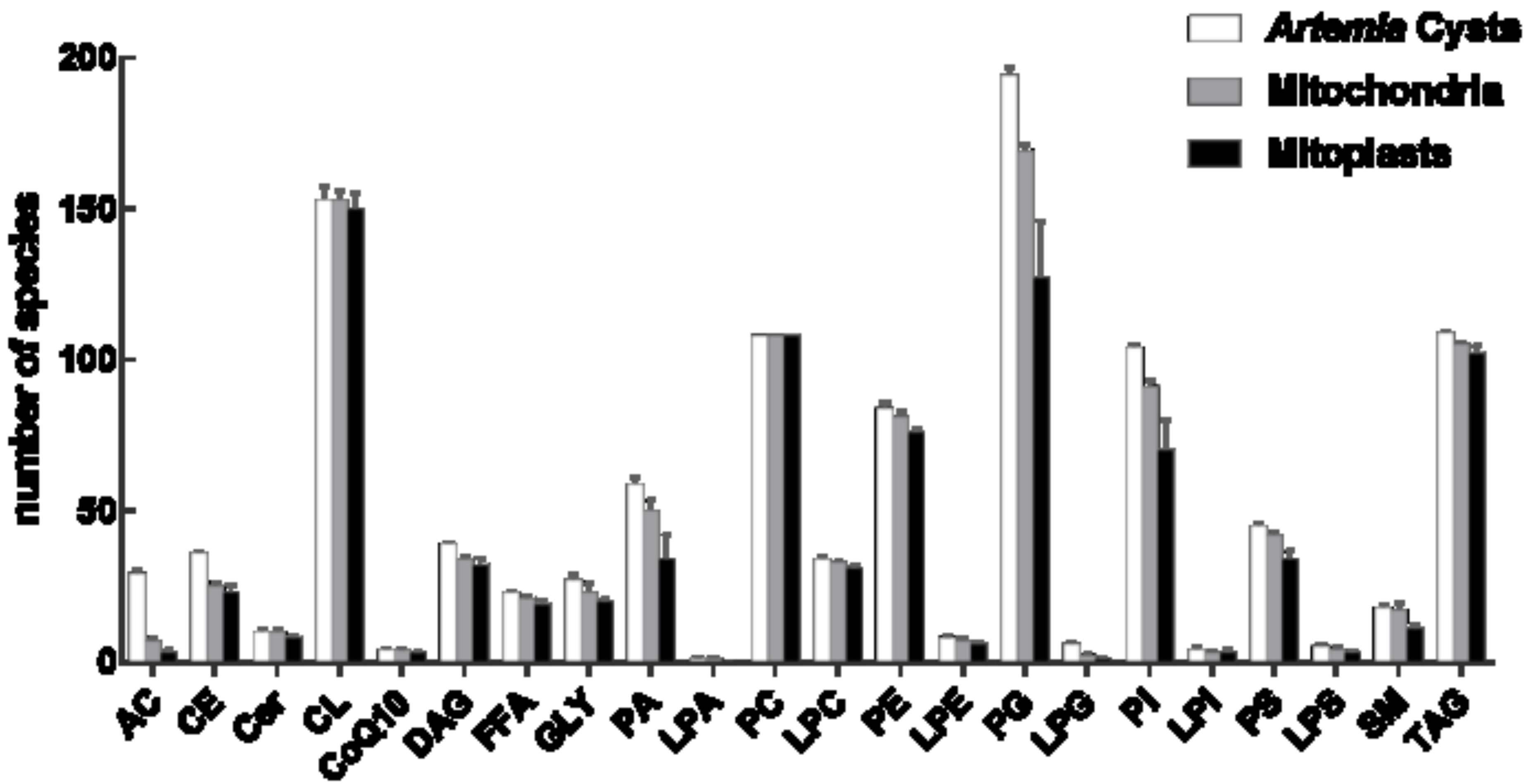

Figure 3
Click here to download high resolution image

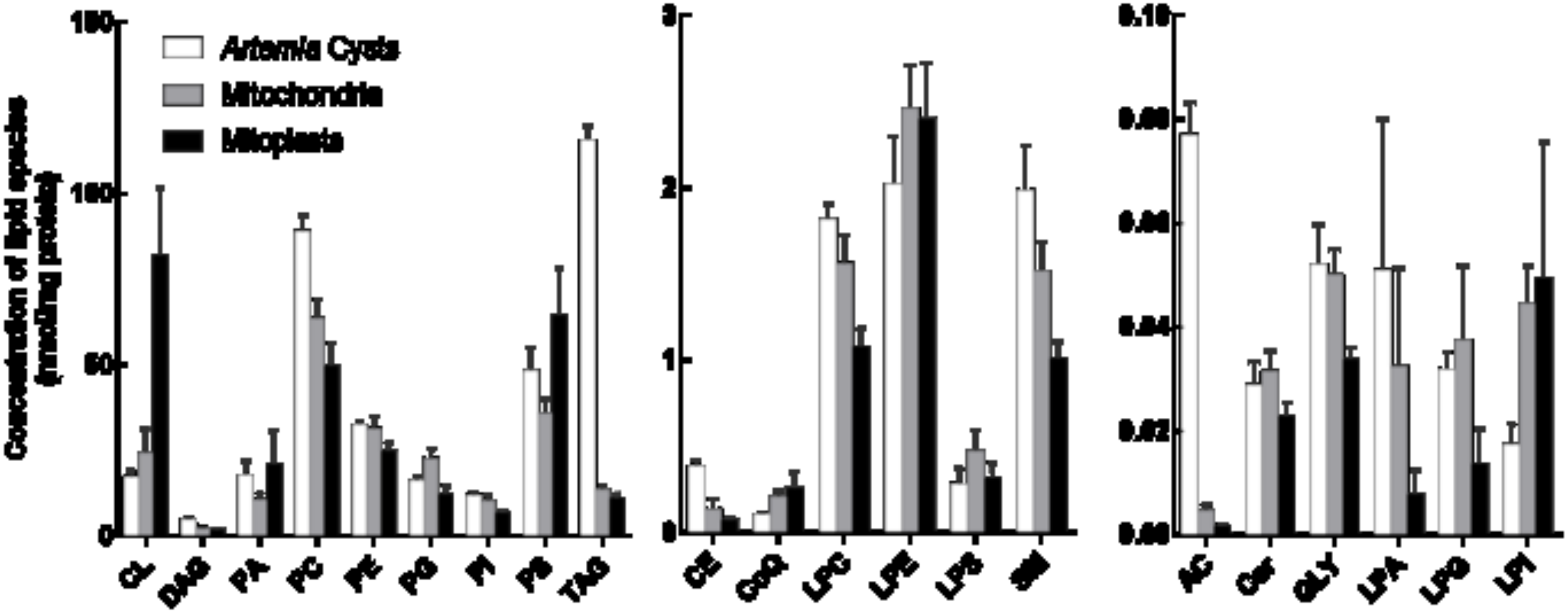

Figure 4

Click here to download high resolution image

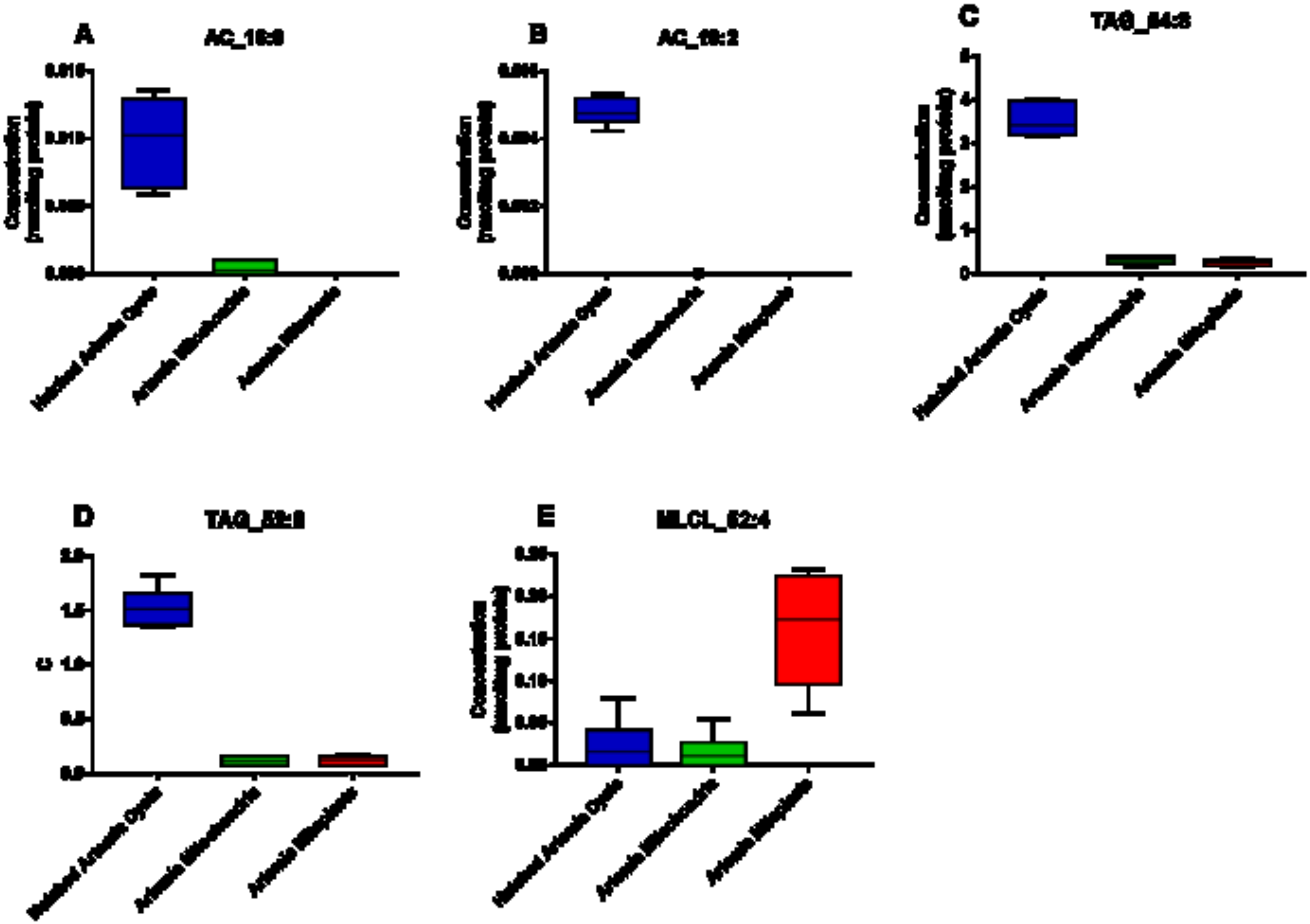

Figure 5

Click here to download high resolution image

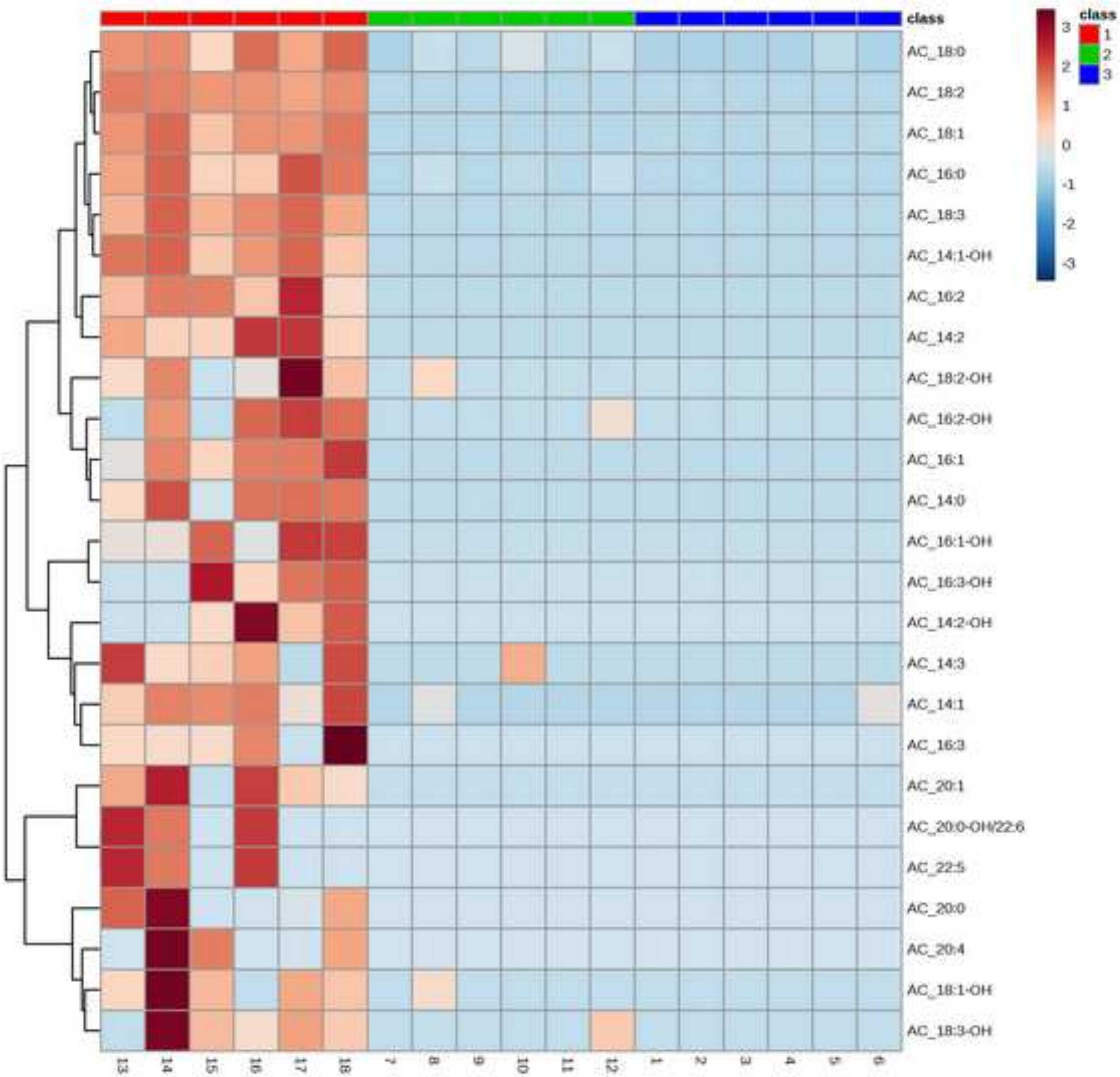

Figure 6
Click here to download high resolution image

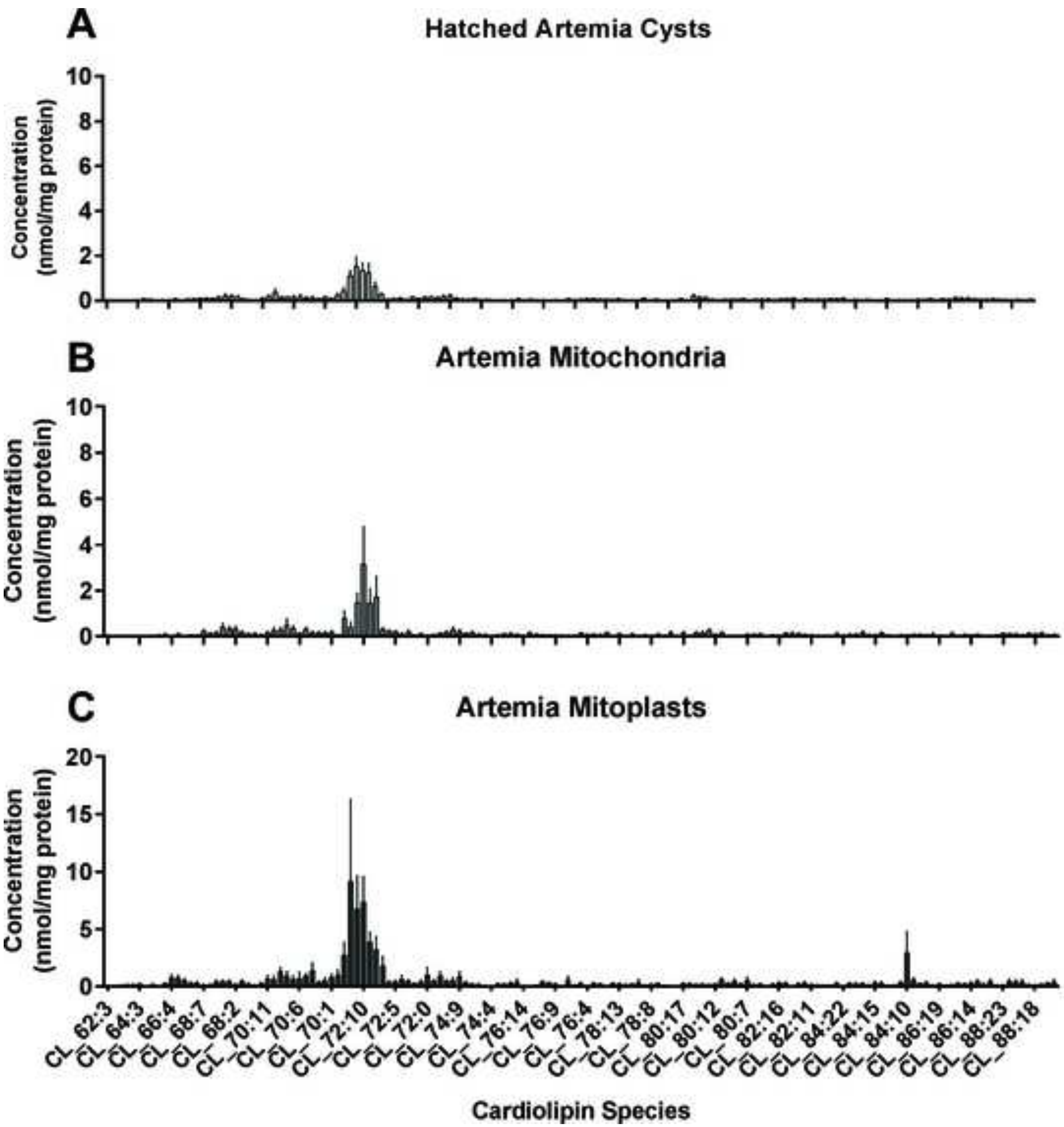

SUPPLEMENTAL MATERIAL

The Total and Mitochondrial Lipidome of *Artemia franciscana* Encysted Embryos

Emily Chen[1], Michael A. Kiebish[1], Justice McDaniel[1], Fei Gao[1], Niven R. Narain[1], Rangaprasad Sarangarajan[1], Gergely Kacso[2,3], Dora Ravasz[2,3], Thomas N. Seyfried[4], Vera Adam-Vizi[2,5] and Christos Chinopoulos[2,3]

[1]BERG LLC, Framingham, MA 01701, USA
[2]Department of Medical Biochemistry, Semmelweis University, Budapest, 1094, Hungary
[3]MTA-SE Lendület Neurobiochemistry Research Group, Budapest, 1094, Hungary
[4]Biology Department, Boston College, Chestnut Hill, Boston, MA, 02467, USA
[5]MTA-SE Laboratory for Neurobiochemistry, Budapest, 1094, Hungary

Address correspondence to: Dr. Christos Chinopoulos, Department of Medical Biochemistry, Semmelweis University, Budapest, Tuzolto street 37-47, 1094, Hungary. Tel: +361 4591500 ext. 60024, Fax: +361 2670031. E-mail: chinopoulos.christos@eok.sote.hu

As shown in supplemental figure 1, in the crude mitochondrial fraction (panel A) there is a considerable number of identifiable mitochondria (red asterisks), but also a substantial amount of non-mitochondrial elements. In panel B an electron-microscopy micrograph of the Percoll-purified mitochondria is shown, and it is apparent that the vast majority of identifiable structures are mitochondria. By subjecting the Percoll-purified mitochondria to hypotonic conditions (see under "Materials and Methods"), we obtained a mitoplast fraction, shown in panel C. There, a large number of mitoplasts are shown exhibiting intact matrix and inner mitochondrial membranes. However, in the mitoplasts fraction, a substantial amount of outer mitochondrial membranes are also evident. In order to confirm that hypotonic treatment of mitochondria yielded genuine mitoplasts, we compared that to treatment by the pore-forming peptide, alamethicin (20 μg), which induced immediate swelling of the matrix. The results of the treatment by alamethicin are shown in panel D. As shown, alamethicin led to completely swollen mitochondria, unlike the hypotonic treatment shown in panel C, in which the matrix and thus the inner mitochondrial membranes remained intact. From the above micrographs (A, B) we estimated that the crude mitochondrial extract contained >60% mitochondria, while the purification of this extract by Percoll gradient elevated the purity to >87%. The subsequent hypotonic treatment yielding mitoplasts is expected to purify the mitochondrial content further, however, at the expense of a partial loss of the outer mitochondrial membrane.

Legend to supplemental figure 1: TEM images of *Artemia franciscana* cysts mitochondrial and mitoplasts fractions. **A**: Crude mitochondria. **B**: Percoll-purified mitochondria. **C**: Mitoplasts. **D**: Alamethicin-treated Percoll-purified mitochondria. Red asterisks (*) indicate a mitochondrion (A,B, D) or a mitoplast (C). Horizontal bars on the lower right corner in each panel are 5 μm.

Legend to supplemental figure 2: Schematic overview of MS/MS^{ALL}. In the set mass range, Q1 is scanned in a unit-base step-wise fashion; precursor ions are fragmented in Q2 and product ions were scanned at high-resolution by TOF. Both High Resolution TOF MS and MS/MS spectra were recorded for *Artemia* cysts, mitochondria, and mitoplasts. An *Artemia* cyst sample is shown as an example here.

Supplementary figure 1
Click here to download high resolution image

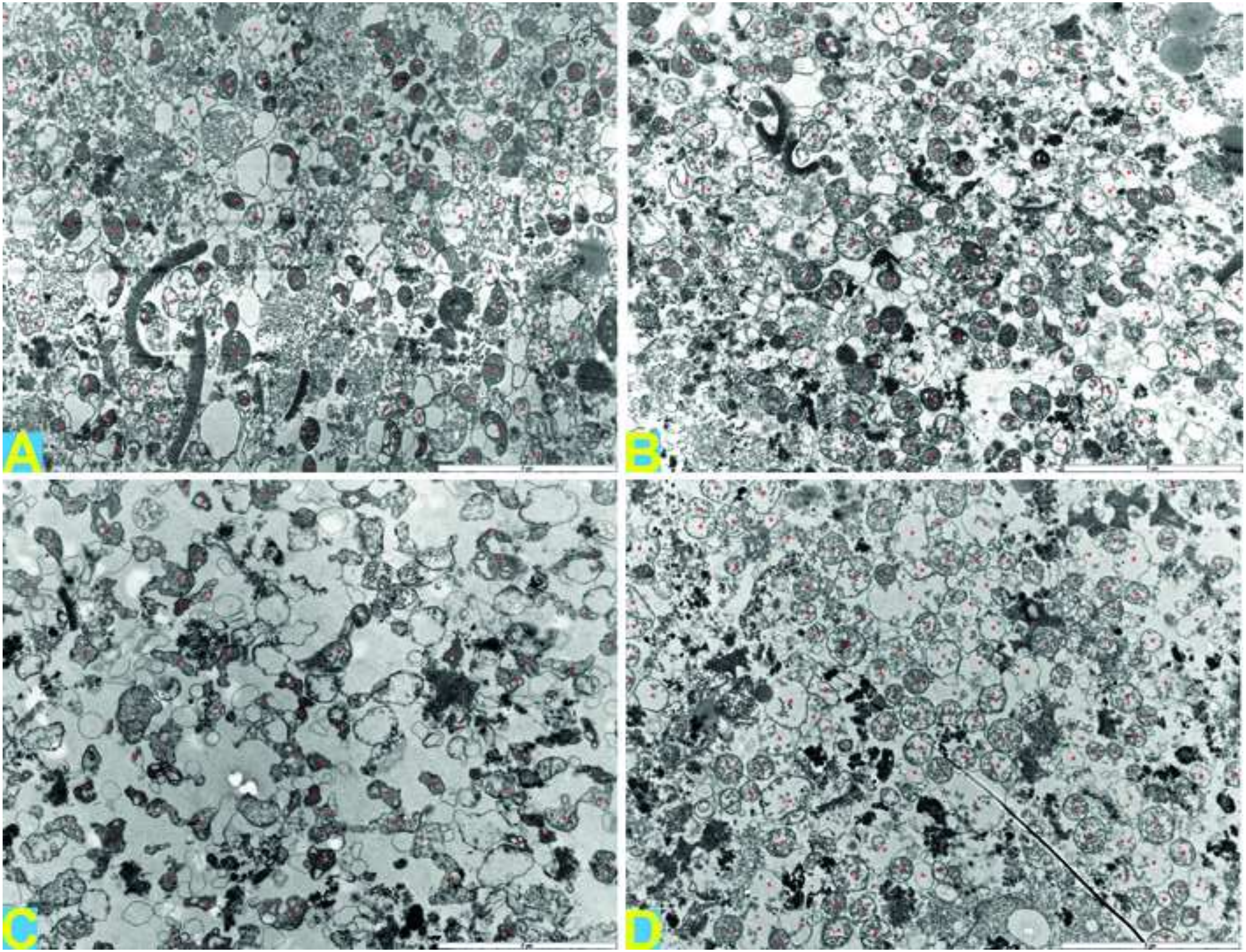

Supplementary figure 2

Click here to download Supplementary Material (for online publication): Supplementary Figure 2_R2.pdf

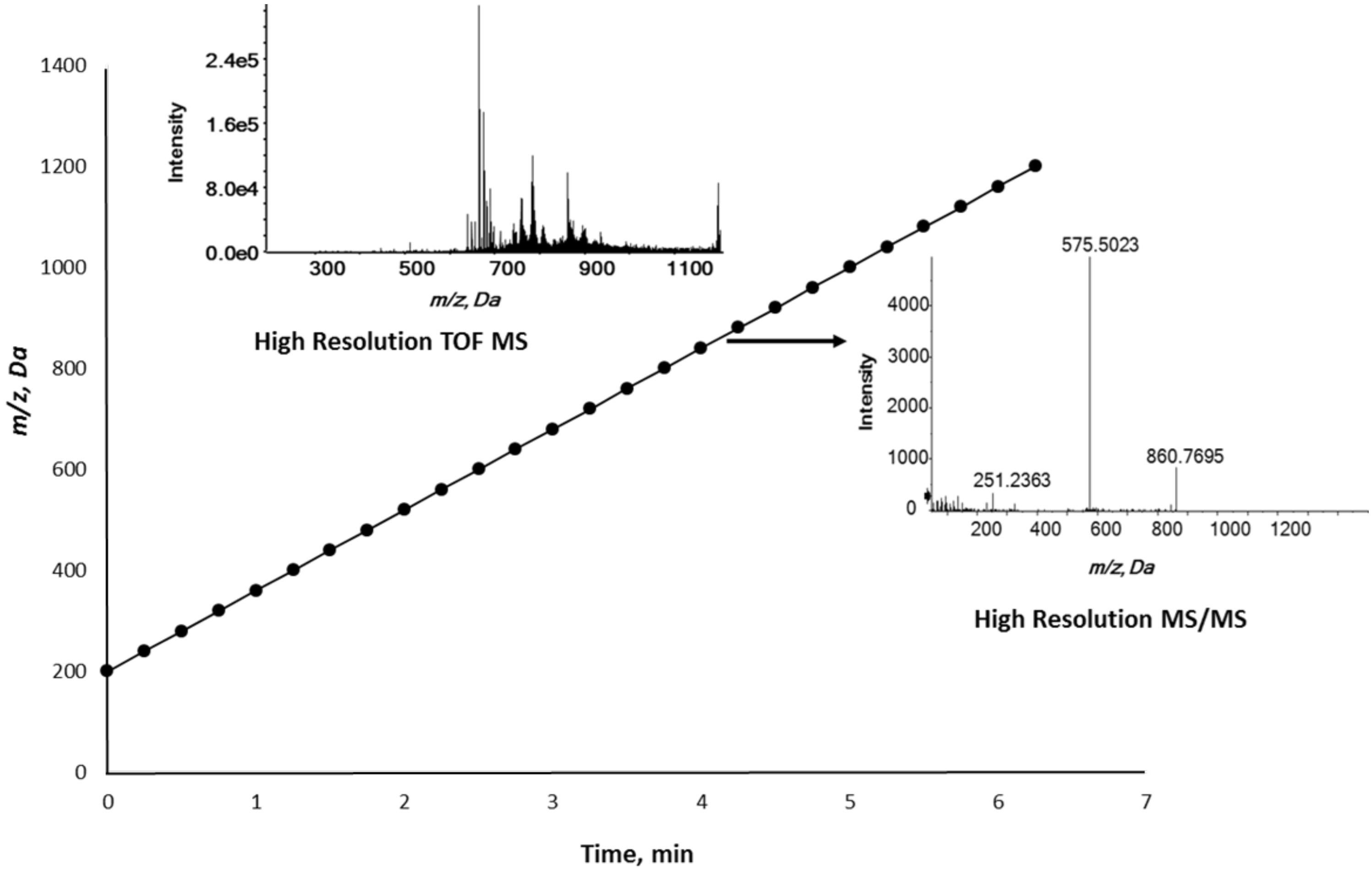

Supplementary tables
Click here to download Supplementary Material (for online publication): Suppl tables_R2.docx

Supplementary Table 1: Concentrations (in pmol/mg protein) of acylcarnitines (AC) in *Artemia* cysts, Percoll-purified mitochondria and mitoplasts. N.D.: not determined. Results shown are Mean +/- S.E.

$[M+H]^+$	Species	Artemia Cysts			Mitochondria			Mitoplasts		
282.13	AC_8:3	N.D.	±	N.D.	0.148	±	0.095	N.D.	±	N.D.
366.22	AC_14:3	0.507	±	0.144	0.088	±	0.088	N.D.	±	N.D.
368.22	AC_14:2	0.502	±	0.102	N.D.	±	N.D.	N.D.	±	N.D.
370.22	AC_14:1	1.397	±	0.217	0.070	±	0.070	0.079	±	0.079
372.22	AC_14:0	1.706	±	0.369	N.D.	±	N.D.	N.D.	±	N.D.
382.23	AC_14:3-OH	0.183	±	0.183	N.D.	±	N.D.	N.D.	±	N.D.
384.23	AC_14:2-OH	0.507	±	0.222	N.D.	±	N.D.	N.D.	±	N.D.
386.24	AC_14:1-OH	1.836	±	0.215	N.D.	±	N.D.	N.D.	±	N.D.
388.24	AC_14:0-OH	0.116	±	0.075	N.D.	±	N.D.	N.D.	±	N.D.
394.24	AC_16:3	0.655	±	0.271	N.D.	±	N.D.	N.D.	±	N.D.
396.25	AC_16:2	0.588	±	0.101	N.D.	±	N.D.	N.D.	±	N.D.
398.25	AC_16:1	4.118	±	0.792	N.D.	±	N.D.	N.D.	±	N.D.
400.25	AC_16:0	9.859	±	1.310	0.417	±	0.198	N.D.	±	N.D.
410.26	AC_16:3-OH	0.314	±	0.117	N.D.	±	N.D.	N.D.	±	N.D.
412.26	AC_16:2-OH	1.025	±	0.334	0.080	±	0.080	N.D.	±	N.D.
414.26	AC_16:1-OH	1.262	±	0.385	N.D.	±	N.D.	N.D.	±	N.D.
416.27	AC16:0-OH	0.094	±	0.053	0.199	±	0.129	0.173	±	0.110
422.27	AC_18:3	7.581	±	0.669	N.D.	±	N.D.	N.D.	±	N.D.
424.27	AC_18:2	4.802	±	0.157	0.006	±	0.006	N.D.	±	N.D.
426.28	AC_18:1	26.075	±	1.962	N.D.	±	N.D.	0.140	±	0.091
428.28	AC_18:0	7.312	±	0.729	0.838	±	0.280	0.111	±	0.111
438.29	AC_18:3-OH	0.757	±	0.263	0.101	±	0.101	N.D.	±	N.D.
440.29	AC_18:2-OH	0.806	±	0.312	0.086	±	0.086	N.D.	±	N.D.
442.29	AC_18:1-OH	0.741	±	0.254	0.066	±	0.066	N.D.	±	N.D.
444.29	AC_18:0-OH	N.D.	±	N.D.	N.D.	±	N.D.	0.063	±	0.063
448.30	AC_20:4	0.236	±	0.120	N.D.	±	N.D.	N.D.	±	N.D.
450.30	AC_20:3	0.223	±	0.174	N.D.	±	N.D.	N.D.	±	N.D.
452.30	AC_20:2	0.058	±	0.058	N.D.	±	N.D.	N.D.	±	N.D.
454.30	AC_20:1	0.582	±	0.176	N.D.	±	N.D.	N.D.	±	N.D.
456.31	AC_20:0	0.257	±	0.121	N.D.	±	N.D.	N.D.	±	N.D.
470.32	AC_20:1-OH	0.092	±	0.059	N.D.	±	N.D.	N.D.	±	N.D.
472.32	AC_20:0-OH/22:6	0.206	±	0.094	N.D.	±	N.D.	N.D.	±	N.D.
474.32	AC_22:5	0.210	±	0.096	N.D.	±	N.D.	N.D.	±	N.D.
476.33	AC_22:4	N.D.	±	N.D.	0.175	±	0.111	0.038	±	0.038
482.33	AC_22:1	0.178	±	0.082	0.255	±	0.115	N.D.	±	N.D.
484.33	AC_22:0	0.258	±	0.089	0.287	±	0.133	N.D.	±	N.D.
490.34	AC_22:5-OH	0.059	±	0.059	0.121	±	0.121	N.D.	±	N.D.
496.35	AC_22:2-OH	0.074	±	0.074	N.D.	±	N.D.	0.058	±	0.058
498.35	AC_22:1-OH	0.007	±	0.007	0.105	±	0.105	N.D.	±	N.D.
500.35	AC_22:0-OH/24:6	0.066	±	0.066	N.D.	±	N.D.	N.D.	±	N.D.
502.35	AC_24:5	0.169	±	0.108	0.186	±	0.120	N.D.	±	N.D.
508.36	AC_24:2	0.085	±	0.085	N.D.	±	N.D.	N.D.	±	N.D.
510.36	AC_24:1	0.215	±	0.164	0.083	±	0.083	0.316	±	0.145
512.36	AC_24:0	N.D.	±	N.D.	N.D.	±	N.D.	N.D.	±	N.D.

516.37	AC_24:6-OH	0.041	±	0.041	0.077	±	0.077	N.D.	±	N.D.
518.37	AC_24:5-OH	0.073	±	0.064	N.D.	±	N.D.	N.D.	±	N.D.
526.38	AC_24:1-OH	0.055	±	0.055	N.D.	±	N.D.	N.D.	±	N.D.
528.38	AC_24:0-OH/26:6	0.076	±	0.076	N.D.	±	N.D.	0.202	±	0.202
530.38	AC_26:5	0.413	±	0.263	0.642	±	0.436	0.355	±	0.173
532.38	AC_26:4	N.D.	±	N.D.	0.100	±	0.100	N.D.	±	N.D.
538.39	AC_26:1	0.069	±	0.069	0.126	±	0.126	N.D.	±	N.D.
540.39	AC_26:0	0.070	±	0.070	N.D.	±	N.D.	0.089	±	0.089
544.39	AC_26:6-OH	0.167	±	0.113	0.295	±	0.188	0.103	±	0.103
546.40	AC_26:5-OH	0.040	±	0.040	N.D.	±	N.D.	N.D.	±	N.D.
548.40	AC_26:4-OH	0.069	±	0.069	0.152	±	0.089	N.D.	±	N.D.
550.40	AC_26:3-OH	0.077	±	0.077	N.D.	±	N.D.	N.D.	±	N.D.
552.40	AC_26:2-OH	0.077	±	0.077	N.D.	±	N.D.	N.D.	±	N.D.
556.41	AC_26:0-OH	0.055	±	0.055	N.D.	±	N.D.	N.D.	±	N.D.

Supplementary Table 2: Concentrations (in pmol/mg protein) compared to the internal standard TAG_17:1-17:1-17:1 of cholesteryl esters (CE) in *Artemia* cysts, Percoll-purified mitochondria and mitoplasts. N.D.: not determined. Des: desmosterol. Results shown are Mean +/- S.E.

[M+NH4]+	**Species**	**Artemia Cysts**			**Mitochondria**			**Mitoplasts**		
558.41	CE_10:0	0.840	±	0.260	0.734	±	0.306	0.335	±	0.151
586.44	CE_12:0	0.035	±	0.035	N.D.	±	N.D.	0.032	±	0.032
614.46	CE_14:0	0.161	±	0.102	0.080	±	0.080	N.D.	±	N.D.
638.49	CE_16:2	3.957	±	0.616	0.898	±	0.129	0.461	±	0.149
640.49	CE_16:1	5.832	±	0.521	1.538	±	0.513	0.680	±	0.230
642.49	CE_16:0	1.445	±	0.424	1.442	±	0.857	0.211	±	0.109
664.51	CE_18:3	140.911	±	9.551	15.599	±	1.265	17.190	±	3.232
666.52	CE_18:2	49.363	±	4.537	52.570	±	38.809	18.300	±	6.623
668.52	CE_18:1	64.659	±	7.858	27.659	±	14.396	13.685	±	3.035
670.52	CE_18:0	1.641	±	0.570	0.893	±	0.245	1.059	±	0.572
688.54	CE_20:5	11.881	±	2.073	2.356	±	0.384	1.004	±	0.360
690.54	CE_20:4	34.619	±	2.893	8.974	±	4.261	3.794	±	0.832
692.54	CE_20:3	16.571	±	2.990	3.534	±	1.577	1.001	±	0.374
694.54	CE_20:2	6.993	±	0.720	1.736	±	0.655	1.034	±	0.343
696.55	CE_20:1	13.607	±	1.326	2.129	±	1.145	2.845	±	0.871
698.55	CE_20:0	4.028	±	0.849	1.758	±	0.371	2.136	±	0.812
714.56	CE_22:6	2.736	±	0.619	1.291	±	0.526	1.738	±	0.553
716.57	CE_22:5	2.283	±	0.446	0.976	±	0.259	1.303	±	0.364
718.57	CE_22:4	0.264	±	0.136	0.539	±	0.414	0.199	±	0.199
720.57	CE_22:3	0.620	±	0.140	N.D.	±	N.D.	0.140	±	0.140
722.57	CE_22:2	1.144	±	0.337	0.421	±	0.329	0.429	±	0.201
724.57	CE_22:1	1.963	±	0.396	0.880	±	0.256	0.448	±	0.288
726.58	CE_22:0	3.881	±	0.988	0.999	±	0.387	1.059	±	0.472
742.59	CE_24:6	1.819	±	0.629	0.127	±	0.094	0.332	±	0.170
744.59	CE_24:5	2.711	±	1.194	0.808	±	0.344	0.372	±	0.200
746.60	CE_24:4	0.652	±	0.306	0.813	±	0.310	N.D.	±	N.D.
748.60	CE_24:3	0.563	±	0.283	0.720	±	0.271	N.D.	±	N.D.
750.60	CE_24:2	0.393	±	0.154	0.602	±	0.313	0.064	±	0.064
752.60	CE_24:1	1.141	±	0.183	0.971	±	0.647	0.666	±	0.238
754.60	CE_24:0	1.802	±	0.731	0.165	±	0.083	0.529	±	0.242
584.43	Des_12:0	0.136	±	0.136	N.D.	±	N.D.	N.D.	±	N.D.
638.49	Des_16:1	0.136	±	0.136	0.020	±	0.020	N.D.	±	N.D.
640.49	Des_16:0	N.D.	±	N.D.	N.D.	±	N.D.	0.102	±	0.102
662.51	Des_18:3	1.397	±	0.502	0.114	±	0.114	0.338	±	0.226
664.51	Des_18:2	N.D.	±	N.D.	0.201	±	0.179	N.D.	±	N.D.
666.52	Des_18:1	0.688	±	0.272	0.118	±	0.081	0.135	±	0.123
668.52	Des_18:0	N.D.	±	N.D.	0.423	±	0.202	N.D.	±	N.D.
686.54	Des_20:5	0.148	±	0.148	0.019	±	0.019	0.097	±	0.097
688.54	Des_20:4	0.532	±	0.180	0.140	±	0.140	N.D.	±	N.D.
690.54	Des_20:3	0.123	±	0.109	N.D.	±	N.D.	N.D.	±	N.D.
692.54	Des_20:2	0.143	±	0.128	0.020	±	0.020	0.111	±	0.111
694.54	Des_20:1	0.715	±	0.430	0.265	±	0.265	0.088	±	0.088
696.55	Des_20:0	0.653	±	0.233	N.D.	±	N.D.	0.405	±	0.289

712.56	Des_22:6	0.992	±	0.381	0.637	±	0.315	0.729	±	0.358
714.56	Des_22:5	0.318	±	0.202	0.311	±	0.311	0.711	±	0.356
716.57	Des_22:4	0.565	±	0.275	N.D.	±	N.D.	N.D.	±	N.D.
718.57	Des_22:3	0.012	±	0.012	0.271	±	0.271	0.108	±	0.108
720.57	Des_22:2	N.D.	±	N.D.	0.133	±	0.133	N.D.	±	N.D.
722.57	Des_22:1	0.100	±	0.100	0.100	±	0.100	0.006	±	0.006
724.57	Des_22:0	0.144	±	0.144	N.D.	±	N.D.	N.D.	±	N.D.
740.59	Des_24:6	0.270	±	0.270	0.282	±	0.179	0.142	±	0.142
742.59	Des_24:5	0.455	±	0.179	0.636	±	0.458	0.291	±	0.205
744.59	Des_24:4	0.906	±	0.420	0.444	±	0.326	0.246	±	0.146
746.60	Des_24:3	0.293	±	0.173	0.147	±	0.147	N.D.	±	N.D.
748.60	Des_24:2	0.143	±	0.143	N.D.	±	N.D.	N.D.	±	N.D.
752.60	Des_24:0	0.183	±	0.154	N.D.	±	N.D.	N.D.	±	N.D.

Supplementary Table 3: Concentrations (in pmol/mg protein) of ceramides (Cer) in *Artemia* cysts, Percoll-purified mitochondria and mitoplasts. N.D.: not determined. Results shown are Mean +/- S.E.

$[M+H]^+$	Species	Artemia Cysts			Mitochondria			Mitoplasts		
564.41	Cer_d18:0/18:2	N.D.	±	N.D.	N.D.	±	N.D.	0.196	±	0.196
566.42	Cer_d18:0/18:1	N.D.	±	N.D.	0.367	±	0.367	N.D.	±	N.D.
568.42	Cer_d18:0/18:0	0.333	±	0.225	N.D.	±	N.D.	N.D.	±	N.D.
588.44	Cer_d18:0/20:4	N.D.	±	N.D.	N.D.	±	N.D.	0.208	±	0.208
624.47	Cer_d18:0/22:0	0.197	±	0.197	N.D.	±	N.D.	0.641	±	0.405
652.50	Cer_d18:0/24:0	0.198	±	0.198	N.D.	±	N.D.	N.D.	±	N.D.
678.53	Cer_d18:0/26:1	N.D.	±	N.D.	0.298	±	0.298	N.D.	±	N.D.
680.53	Cer_d18:0/26:0	N.D.	±	N.D.	N.D.	±	N.D.	0.508	±	0.508
482.33	Cer_d18:1/12:0	5.714	±	1.109	7.453	±	1.158	3.389	±	0.748
508.36	Cer_d18:1/14:1	0.408	±	0.192	0.302	±	0.191	0.826	±	0.542
536.39	Cer_d18:1/16:1	1.260	±	0.625	2.254	±	1.164	N.D.	±	N.D.
538.39	Cer_d18:1/16:0	0.215	±	0.215	0.359	±	0.359	0.199	±	0.199
562.41	Cer_d18:1/18:2	N.D.	±	N.D.	0.285	±	0.285	N.D.	±	N.D.
564.41	Cer_d18:1/18:1	0.090	±	0.090	0.533	±	0.348	N.D.	±	N.D.
566.42	Cer_d18:1/18:0	1.182	±	0.627	0.399	±	0.317	0.650	±	0.316
586.44	Cer_d18:1/20:4	0.263	±	0.175	N.D.	±	N.D.	0.212	±	0.212
590.44	Cer_d18:1/20:2	0.121	±	0.121	N.D.	±	N.D.	N.D.	±	N.D.
592.44	Cer_d18:1/20:1	N.D.	±	N.D.	0.215	±	0.215	N.D.	±	N.D.
594.44	Cer_d18:1/20:0	0.464	±	0.298	1.101	±	0.957	0.438	±	0.280
610.46	Cer_d18:1/22:6	0.457	±	0.457	N.D.	±	N.D.	N.D.	±	N.D.
616.47	Cer_d18:1/22:3	N.D.	±	N.D.	0.147	±	0.147	N.D.	±	N.D.
618.47	Cer_d18:1/22:2	0.270	±	0.270	0.724	±	0.460	N.D.	±	N.D.
620.47	Cer_d18:1/22:1	0.183	±	0.183	0.636	±	0.417	0.367	±	0.307
622.47	Cer_d18:1/22:0	4.120	±	1.355	1.320	±	0.771	2.664	±	1.001
648.50	Cer_d18:1/24:1	8.458	±	1.437	6.937	±	2.318	8.344	±	0.881
650.50	Cer_d18:1/24:0	0.502	±	0.386	1.839	±	0.590	1.649	±	0.728
676.53	Cer_d18:1/26:1	N.D.	±	N.D.	1.472	±	0.663	0.617	±	0.617
678.53	Cer_d18:1/26:0	N.D.	±	N.D.	0.846	±	0.538	N.D.	±	N.D.
506.36	Cer_d18:2/14:1	0.106	±	0.106	0.148	±	0.148	N.D.	±	N.D.
508.36	Cer_d18:2/14:0	0.248	±	0.248	N.D.	±	N.D.	N.D.	±	N.D.
534.38	Cer_d18:2/16:1	0.122	±	0.122	0.216	±	0.216	0.243	±	0.243
564.41	Cer_d18:2/18:0	0.200	±	0.149	0.363	±	0.363	0.429	±	0.429
584.43	Cer_d18:2/20:4	0.475	±	0.308	N.D.	±	N.D.	N.D.	±	N.D.
588.44	Cer_d18:2/20:2	N.D.	±	N.D.	0.374	±	0.374	N.D.	±	N.D.
590.44	Cer_d18:2/20:1	N.D.	±	N.D.	0.329	±	0.329	N.D.	±	N.D.
592.44	Cer_d18:2/20:0	0.046	±	0.046	0.374	±	0.374	N.D.	±	N.D.
608.46	Cer_d18:2/22:6	N.D.	±	N.D.	0.201	±	0.201	N.D.	±	N.D.
612.46	Cer_d18:2/22:4	0.047	±	0.047	N.D.	±	N.D.	N.D.	±	N.D.
616.47	Cer_d18:2/22:2	0.407	±	0.407	N.D.	±	N.D.	0.303	±	0.303
618.47	Cer_d18:2/22:1	0.158	±	0.158	N.D.	±	N.D.	N.D.	±	N.D.
620.47	Cer_d18:2/22:0	2.433	±	0.681	1.443	±	0.526	0.755	±	0.414
646.50	Cer_d18:2/24:1	0.201	±	0.201	0.235	±	0.235	N.D.	±	N.D.
648.50	Cer_d18:2/24:0	0.052	±	0.052	0.173	±	0.173	0.204	±	0.204
674.52	Cer_d18:2/26:1	N.D.	±	N.D.	0.167	±	0.167	N.D.	±	N.D.

Supplementary Table 4: Concentrations (in pmol/mg protein) of cardiolipins (CL), dilysocardiolipins (DLCL), and monolysocardiolipins (MLCL) in *Artemia* cysts, Percoll-purified mitochondria and mitoplasts. N.D.: not determined. For CL determination, all the fragments that would comprise the acyl chains were summed up and isomeric composition for the molecular species as the brutto nomenclature (carbon:double bond) is given. Results shown are Mean +/- S.E.

$[M-2H]^{-2}$	Species	Artemia Cysts			Mitochondria			Mitoplasts		
658.51	CL_62:3	34.180	±	14.750	51.441	±	24.203	83.921	±	42.248
659.51	CL_62:2	21.825	±	5.020	8.054	±	7.016	62.046	±	38.510
669.52	CL_64:6	16.576	±	7.093	36.264	±	10.789	121.125	±	38.690
670.52	CL_64:5	17.638	±	9.129	31.517	±	17.992	145.687	±	29.668
671.52	CL_64:4	22.164	±	11.485	14.015	±	5.024	151.222	±	59.061
672.52	CL_64:3	36.162	±	12.153	45.573	±	8.488	188.861	±	70.258
673.52	CL_64:2	66.841	±	19.430	19.793	±	9.394	48.227	±	24.256
674.52	CL_64:1	43.850	±	20.452	43.759	±	16.876	167.776	±	46.637
683.53	CL_66:6	15.843	±	7.978	52.510	±	37.039	47.676	±	15.361
684.53	CL_66:5	41.940	±	15.188	81.040	±	61.580	253.360	±	77.863
685.54	CL_66:4	33.872	±	17.669	14.640	±	9.895	728.170	±	329.505
686.54	CL_66:3	71.111	±	19.832	98.530	±	40.299	735.337	±	255.455
687.54	CL_66:2	22.404	±	15.451	37.512	±	8.041	491.763	±	207.950
688.54	CL_66:1	61.656	±	20.338	60.757	±	21.015	294.624	±	95.463
695.55	CL_68:8	64.212	±	26.003	55.610	±	16.004	278.805	±	167.040
696.55	CL_68:7	85.532	±	30.725	211.709	±	91.682	106.426	±	85.245
697.55	CL_68:6	99.904	±	35.480	132.824	±	29.138	141.631	±	63.767
698.55	CL_68:5	85.983	±	27.847	158.245	±	55.089	367.463	±	201.340
699.55	CL_68:4	140.832	±	47.222	391.116	±	174.054	432.345	±	122.710
700.55	CL_68:3	218.041	±	84.420	323.129	±	115.880	437.925	±	98.859
701.55	CL_68:2	187.474	±	77.412	292.054	±	148.569	168.983	±	65.138
702.55	CL_68:1	175.144	±	42.783	179.761	±	71.941	406.185	±	179.377
703.55	CL_68:0	65.069	±	13.482	96.795	±	56.744	178.683	±	139.459
704.55	CL_70:13	36.222	±	18.447	112.244	±	49.618	105.676	±	43.010
705.56	CL_70:12	34.780	±	9.319	62.658	±	45.246	223.701	±	157.190
706.56	CL_70:11	103.650	±	36.336	163.427	±	43.686	651.772	±	315.569
707.56	CL_70:10	174.057	±	71.696	256.470	±	144.962	602.570	±	296.369
708.56	CL_70:9	334.023	±	174.218	279.075	±	107.439	1274.436	±	369.225
709.56	CL_70:8	145.210	±	38.746	471.070	±	301.092	898.182	±	400.820
710.56	CL_70:7	152.221	±	37.460	337.083	±	129.986	584.000	±	326.620
711.56	CL_70:6	140.530	±	71.998	133.462	±	38.584	698.710	±	545.498
712.56	CL_70:5	179.894	±	104.049	291.521	±	118.581	880.145	±	246.604
713.56	CL_70:4	124.186	±	42.273	144.337	±	79.406	1359.246	±	720.177
714.56	CL_70:3	134.284	±	48.887	149.790	±	62.132	359.446	±	114.128
715.57	CL_70:2	66.225	±	21.606	148.606	±	64.243	530.749	±	229.753
716.57	CL_70:1	139.617	±	39.773	179.055	±	83.464	776.067	±	298.911
717.57	CL_70:0	84.877	±	27.930	59.278	±	25.171	986.642	±	443.833
718.57	CL_72:13	226.771	±	93.408	771.976	±	332.919	2732.397	±	1100.317
719.57	CL_72:12	421.017	±	152.967	398.114	±	218.217	9094.961	±	7202.475
720.57	CL_72:11	1082.941	±	264.484	1455.594	±	414.527	6709.414	±	2926.018
721.57	CL_72:10	1512.152	±	446.451	3133.453	±	1641.519	7360.046	±	2213.267
722.57	CL_72:9	1343.347	±	323.553	1436.210	±	628.502	3844.480	±	900.686

723.57	CL_72:8	1223.347	±	424.257	1710.036	±	901.697	3175.019	±	1149.929
724.57	CL_72:7	625.355	±	192.398	290.004	±	92.076	1763.317	±	828.823
725.58	CL_72:6	269.779	±	61.030	219.535	±	60.019	401.124	±	90.058
726.58	CL_72:5	51.055	±	16.947	183.255	±	77.414	368.223	±	182.672
727.58	CL_72:4	74.976	±	31.206	105.931	±	63.401	594.564	±	391.048
728.58	CL_72:3	102.748	±	37.697	187.325	±	82.719	454.956	±	132.904
729.58	CL_72:2	47.784	±	9.928	54.999	±	16.974	243.627	±	79.045
730.58	CL_72:1	149.200	±	39.414	101.721	±	38.565	386.578	±	181.827
731.58	CL_72:0	83.988	±	22.490	51.012	±	10.300	992.607	±	672.334
732.58	CL_74:13	139.998	±	30.496	75.805	±	22.042	458.838	±	148.743
733.58	CL_74:12	156.209	±	42.554	121.855	±	49.754	906.189	±	380.648
734.58	CL_74:11	120.142	±	46.130	163.081	±	77.532	472.582	±	104.464
735.59	CL_74:10	190.286	±	45.756	285.286	±	132.708	514.976	±	245.461
736.59	CL_74:9	223.250	±	45.164	194.291	±	105.764	840.539	±	464.895
737.59	CL_74:8	101.716	±	36.590	121.949	±	34.421	342.065	±	85.958
738.59	CL_74:7	60.192	±	27.334	159.369	±	56.144	181.988	±	60.084
739.59	CL_74:6	46.799	±	23.756	93.334	±	37.788	169.238	±	73.836
740.59	CL_74:5	86.624	±	16.511	76.542	±	26.927	81.696	±	38.703
741.59	CL_74:4	37.677	±	22.112	23.008	±	11.120	57.286	±	18.646
742.59	CL_74:3	45.202	±	17.710	64.274	±	25.257	192.200	±	116.978
743.59	CL_74:2	23.711	±	16.346	98.484	±	38.881	188.419	±	77.513
743.59	CL_74:1	25.428	±	7.959	101.575	±	66.674	263.837	±	152.627
744.59	CL_76:15	41.658	±	10.659	79.817	±	30.580	403.375	±	250.989
745.60	CL_76:14	33.668	±	13.117	34.113	±	19.235	65.775	±	31.436
746.60	CL_76:13	76.729	±	21.638	148.626	±	52.432	61.241	±	22.451
747.60	CL_76:12	39.191	±	9.331	94.928	±	33.319	99.640	±	47.872
748.60	CL_76:11	51.890	±	21.335	60.994	±	26.880	376.016	±	117.754
749.60	CL_76:10	33.755	±	16.271	57.032	±	24.690	301.450	±	88.761
750.60	CL_76:9	31.288	±	12.980	53.574	±	25.028	184.666	±	90.698
751.60	CL_76:8	28.499	±	10.946	42.985	±	27.715	38.488	±	19.658
752.60	CL_76:7	30.789	±	13.051	48.471	±	19.545	559.579	±	315.442
753.60	CL_76:6	28.897	±	7.058	38.957	±	14.699	111.586	±	49.876
754.60	CL_76:5	64.861	±	24.092	121.912	±	66.795	237.357	±	127.974
755.61	CL_76:4	38.762	±	17.044	79.018	±	33.079	59.832	±	37.483
756.61	CL_76:3	61.590	±	16.177	81.123	±	48.262	230.994	±	122.926
757.61	CL_76:2	76.424	±	27.703	65.670	±	44.345	199.381	±	73.383
758.61	CL_78:15	66.850	±	33.034	150.710	±	43.161	70.096	±	29.273
759.61	CL_78:14	54.308	±	13.095	25.779	±	13.472	219.659	±	102.435
760.61	CL_78:13	50.980	±	15.587	107.628	±	26.653	180.661	±	110.689
761.61	CL_78:12	43.207	±	18.775	36.396	±	7.466	127.943	±	78.411
762.61	CL_78:11	72.436	±	28.944	93.183	±	60.410	188.205	±	46.664
763.61	CL_78:10	33.553	±	23.353	38.230	±	12.623	327.127	±	287.109
764.61	CL_78:9	34.041	±	14.001	59.647	±	25.802	107.498	±	46.910
765.62	CL_78:8	35.111	±	16.148	48.226	±	21.490	156.405	±	98.627
766.62	CL_78:7	85.055	±	41.582	95.069	±	40.494	240.467	±	67.264
767.62	CL_78:6	24.770	±	19.034	47.511	±	22.710	89.028	±	34.681
768.62	CL_78:5	62.294	±	20.932	145.533	±	84.857	67.572	±	35.802
769.62	CL_78:4	22.149	±	9.204	17.046	±	8.014	42.394	±	31.880

770.62	CL_80:17	27.908	±	9.980	141.771	±	60.194	226.858	±	100.112
771.62	CL_80:16	36.025	±	15.556	40.357	±	16.228	208.162	±	129.090
772.62	CL_80:15	64.086	±	23.897	145.087	±	62.672	161.650	±	51.736
773.62	CL_80:14	35.160	±	17.384	144.374	±	103.068	184.102	±	57.204
774.62	CL_80:13	215.821	±	65.364	264.484	±	76.283	168.914	±	38.963
775.63	CL_80:12	140.461	±	37.425	92.224	±	35.068	207.512	±	36.930
776.63	CL_80:11	135.271	±	33.813	150.994	±	60.757	570.818	±	212.473
777.63	CL_80:10	47.290	±	19.632	13.042	±	6.001	254.564	±	100.310
778.63	CL_80:9	37.421	±	10.256	47.162	±	21.322	419.897	±	254.855
779.63	CL_80:8	49.486	±	18.424	44.339	±	15.151	181.558	±	124.671
780.63	CL_80:7	51.711	±	20.053	95.428	±	28.091	495.174	±	325.017
781.63	CL_80:6	48.213	±	11.050	82.829	±	35.785	166.738	±	64.589
782.63	CL_80:5	76.153	±	21.801	102.516	±	34.957	189.627	±	76.734
783.63	CL_82:18	35.226	±	9.805	23.166	±	9.009	59.543	±	26.712
784.63	CL_82:17	44.879	±	24.458	62.719	±	23.697	162.023	±	114.973
785.64	CL_82:16	61.425	±	31.053	44.628	±	19.504	261.038	±	177.060
786.64	CL_82:15	75.633	±	9.875	122.258	±	49.497	262.166	±	103.363
787.64	CL_82:14	40.245	±	14.845	114.223	±	81.444	56.586	±	25.709
788.64	CL_82:13	64.814	±	15.623	119.020	±	33.455	212.184	±	123.845
789.64	CL_82:12	83.804	±	14.617	80.541	±	25.240	305.968	±	155.042
790.64	CL_82:11	101.100	±	24.528	73.943	±	18.312	152.121	±	58.438
791.64	CL_82:10	37.645	±	13.957	45.047	±	25.401	114.852	±	70.796
792.64	CL_82:9	65.211	±	28.924	33.671	±	13.781	92.496	±	55.770
793.64	CL_82:8	47.170	±	15.057	38.071	±	21.412	95.413	±	46.706
794.64	CL_84:21	60.299	±	23.624	115.367	±	64.435	251.843	±	130.656
795.65	CL_84:20	53.660	±	19.003	50.572	±	29.208	42.305	±	19.566
796.65	CL_84:19	78.306	±	20.842	78.321	±	39.445	238.481	±	108.630
797.65	CL_84:18	71.673	±	25.539	88.500	±	41.291	200.635	±	152.056
798.65	CL_84:17	96.742	±	32.521	180.201	±	74.021	228.103	±	105.702
799.65	CL_84:16	28.643	±	10.887	69.411	±	40.197	123.489	±	51.233
800.65	CL_84:15	43.622	±	14.724	62.471	±	41.559	337.827	±	121.389
801.65	CL_84:14	34.944	±	15.448	138.659	±	56.561	244.361	±	214.902
802.65	CL_84:13	42.911	±	17.207	59.979	±	21.827	85.115	±	40.533
803.65	CL_84:12	20.253	±	8.005	19.121	±	8.691	110.268	±	46.680
804.65	CL_84:11	29.851	±	9.749	70.322	±	30.587	350.157	±	128.620
805.66	CL_84:10	79.246	±	22.230	70.597	±	22.615	2928.171	±	1853.371
806.66	CL_84:9	38.646	±	14.225	89.546	±	23.622	564.356	±	192.650
807.66	CL_86:22	42.265	±	16.324	82.947	±	31.155	227.391	±	73.159
808.66	CL_86:21	39.893	±	14.926	72.217	±	32.631	295.434	±	182.607
809.66	CL_86:20	39.104	±	10.506	94.430	±	72.124	122.132	±	44.948
810.66	CL_86:19	51.611	±	15.482	52.830	±	19.148	181.620	±	83.865
811.66	CL_86:18	48.121	±	10.818	31.926	±	14.749	99.323	±	40.179
812.66	CL_86:17	72.355	±	29.696	110.658	±	76.859	127.855	±	45.882
813.66	CL_86:16	38.597	±	17.112	29.482	±	15.012	243.068	±	117.348
814.66	CL_86:15	67.602	±	10.961	78.537	±	30.135	187.409	±	94.493
815.67	CL_86:14	57.099	±	25.781	65.980	±	18.521	233.770	±	201.726
816.67	CL_86:13	108.114	±	46.593	82.988	±	27.442	416.842	±	186.193
817.67	CL_86:12	85.148	±	57.493	32.807	±	14.539	177.837	±	107.494

818.67	CL_86:11	105.051	±	51.781	49.529	±	16.919	404.384	±	244.405
819.67	CL_88:24	65.797	±	12.360	56.593	±	29.874	111.039	±	47.735
820.67	CL_88:23	54.960	±	7.182	117.062	±	36.667	121.099	±	36.442
821.67	CL_88:22	59.399	±	19.941	95.657	±	32.790	444.407	±	222.507
822.67	CL_88:21	83.658	±	20.449	97.887	±	24.123	368.437	±	191.401
823.67	CL_88:20	53.428	±	13.571	74.273	±	25.878	386.966	±	225.146
824.67	CL_88:19	50.372	±	9.438	119.689	±	40.087	166.563	±	42.594
825.68	CL_88:18	35.762	±	14.695	96.898	±	26.137	126.105	±	54.258
826.68	CL_88:17	45.152	±	16.920	135.906	±	63.838	173.028	±	52.778
827.68	CL_88:16	31.723	±	10.529	58.590	±	28.751	265.744	±	112.620
832.68	CL_90:25	60.499	±	12.397	80.946	±	28.467	366.145	±	270.646
449.30	DLCL_34:2	3.353	±	2.011	N.D.	±	N.D.	63.946	±	53.857
450.30	DLCL_34:1	4.456	±	4.456	6.850	±	4.363	21.729	±	15.951
461.31	DLCL_36:4	12.706	±	5.987	12.420	±	8.228	29.998	±	19.797
462.31	DLCL_36:3	11.340	±	5.083	18.762	±	16.978	11.090	±	7.087
463.31	DLCL_36:2	15.317	±	8.566	5.961	±	3.086	15.128	±	15.128
464.31	DLCL_36:1	3.256	±	3.074	15.728	±	7.954	37.911	±	14.836
474.32	DLCL_38:5	0.563	±	0.563	6.382	±	4.050	4.989	±	4.989
475.33	DLCL_38:4	3.823	±	2.796	N.D.	±	N.D.	N.D.	±	N.D.
476.33	DLCL_38:3	14.044	±	7.974	0.287	±	0.287	1.417	±	1.417
477.33	DLCL_38_2	5.332	±	4.988	0.361	±	0.240	20.026	±	16.534
485.34	DLCL_40:8	4.437	±	3.219	0.238	±	0.238	9.010	±	6.212
486.34	DLCL_40:7	0.355	±	0.355	N.D.	±	N.D.	N.D.	±	N.D.
579.43	MLCL_52:5	13.523	±	9.793	3.150	±	2.863	81.727	±	55.435
580.43	MLCL_52:4	23.113	±	12.146	15.647	±	8.245	161.423	±	27.696
581.43	MLCL_52:3	7.205	±	3.601	10.524	±	10.064	86.518	±	31.275
582.43	MLCL_52:2	9.228	±	5.969	17.302	±	10.889	176.883	±	117.592
591.44	MLCL_54:7	110.637	±	50.081	54.671	±	19.576	43.516	±	27.739
592.44	MLCL_54:6	113.905	±	33.979	60.843	±	29.912	124.671	±	30.769
593.44	MLCL_54:5	95.352	±	26.018	96.135	±	43.653	233.182	±	91.182
594.44	MLCL_54:4	34.928	±	9.370	81.729	±	30.989	115.522	±	32.806
595.45	MLCL_54:3	23.571	±	14.941	31.857	±	17.268	166.851	±	90.943
596.45	MLCL_54:2	17.321	±	9.649	28.453	±	9.237	114.738	±	53.280
604.45	MLCL_56:8	26.115	±	14.615	26.489	±	21.869	48.705	±	22.517
605.46	MLCL_56:7	32.164	±	12.927	39.179	±	23.134	199.678	±	102.042
606.46	MLCL_56:6	20.426	±	6.998	3.522	±	1.447	167.791	±	120.783
607.46	MLCL_56:5	14.950	±	7.138	19.644	±	15.202	298.440	±	108.478
608.46	MLCL_56:4	22.712	±	15.394	4.783	±	2.998	163.726	±	67.783
616.47	MLCL_58:10	21.670	±	11.131	39.413	±	13.777	37.172	±	19.584
617.47	MLCL_58:9	5.039	±	2.470	19.631	±	14.537	35.874	±	18.775
618.47	MLCL_58:8	15.256	±	6.897	34.028	±	13.758	11.197	±	10.763

Supplementary Table 5: Concentrations (in pmol/mg protein) of coenzyme Q (CoQ) in *Artemia* cysts, Percoll-purified mitochondria and mitoplasts. N.D.: not determined. Only CoQ9 and CoQ10 –oxidized and reduced versions were analyzed, using a relevant internal standard TAG_17:1-17:1-17:1. Results shown are Mean +/- S.E.

$[M+NH4]^+$	**Species**	**Artemia Cysts**			**Mitochondria**			**Mitoplasts**		
880.73	CoQ10	93.507	±	6.197	179.296	±	26.857	226.277	±	80.895
882.73	CoQ10H2	14.349	±	1.079	28.359	±	5.459	32.207	±	13.787
812.66	CoQ9	0.473	±	0.203	0.531	±	0.222	0.250	±	0.159
814.66	CoQ9H2	0.140	±	0.140	0.663	±	0.318	N.D.	±	N.D.

Supplementary Table 6: Concentrations (in pmol/mg protein) of diacylglycerols (DAG) in *Artemia* cysts, Percoll-purified mitochondria and mitoplasts. N.D.: not determined. Results shown are Mean +/- S.E.

$[M+NH4]^+$	Species	Artemia Cysts			Mitochondria			Mitoplasts		
526.38	DAG_28:2	1.403	±	1.403	2.189	±	2.189	N.D.	±	N.D.
528.38	DAG_28:1	N.D.	±	N.D.	N.D.	±	N.D.	0.458	±	0.458
530.38	DAG_28:0	19.866	±	6.775	29.981	±	7.997	16.011	±	4.556
554.40	DAG_30:2	15.981	±	4.085	6.905	±	3.227	5.862	±	1.408
556.41	DAG_30:1	7.805	±	3.953	6.656	±	2.241	0.988	±	0.768
558.41	DAG_30:0	13.414	±	3.194	10.446	±	3.173	4.457	±	2.854
580.43	DAG_32:3	30.499	±	7.252	23.531	±	10.314	9.168	±	3.636
582.43	DAG_32:2	15.218	±	2.259	11.789	±	5.348	10.982	±	3.290
584.43	DAG_32:1	57.507	±	13.934	40.771	±	9.291	17.477	±	6.033
586.44	DAG_32:0	79.806	±	12.689	17.164	±	5.532	9.792	±	4.304
606.46	DAG_34:4	109.359	±	12.833	53.192	±	5.640	54.321	±	20.671
608.46	DAG_34:3	792.373	±	127.860	336.594	±	56.923	300.478	±	56.070
610.46	DAG_34:2	224.828	±	20.412	133.320	±	13.159	107.905	±	19.723
612.46	DAG_34:1	300.704	±	42.113	132.180	±	14.497	139.088	±	29.168
614.46	DAG_34:0	62.240	±	11.229	50.414	±	6.560	26.390	±	7.559
630.48	DAG_36:6	2.898	±	1.837	4.096	±	2.636	4.589	±	3.108
632.48	DAG_36:5	144.194	±	26.550	60.084	±	10.623	69.667	±	14.158
634.48	DAG_36:4	738.224	±	82.375	299.150	±	43.308	339.695	±	58.293
636.49	DAG_36:3	242.951	±	23.160	124.411	±	18.558	130.905	±	32.016
638.49	DAG_36:2	374.915	±	27.476	271.275	±	53.597	220.524	±	48.503
640.49	DAG_36:1	148.272	±	26.634	107.113	±	17.833	90.506	±	14.727
642.49	DAG_36:0	25.765	±	6.186	62.028	±	13.387	26.476	±	8.261
656.51	DAG_38:7	2.705	±	1.870	1.817	±	1.817	4.026	±	3.032
658.51	DAG_38:6	11.847	±	3.105	N.D.	±	N.D.	N.D.	±	N.D.
660.51	DAG_38:5	38.291	±	9.208	16.473	±	6.365	7.808	±	2.772
662.51	DAG_38:4	17.272	±	3.994	8.663	±	3.626	20.051	±	12.233
664.51	DAG_38:3	549.207	±	39.976	88.816	±	12.158	74.637	±	17.648
666.52	DAG_38:2	47.118	±	10.183	28.147	±	9.099	18.285	±	5.842
668.52	DAG_38:1	318.835	±	48.703	96.184	±	36.381	59.587	±	18.638
678.53	DAG_40:10	0.962	±	0.962	0.837	±	0.837	N.D.	±	N.D.
680.53	DAG_40:9	2.223	±	1.186	3.685	±	2.445	4.073	±	3.769
682.53	DAG_40:8	4.324	±	1.967	5.559	±	1.899	4.485	±	3.158
684.53	DAG_40:7	20.107	±	3.824	18.450	±	4.607	14.303	±	4.579
686.54	DAG_40:6	28.362	±	3.644	38.855	±	16.890	19.923	±	5.069
688.54	DAG_40:5	58.364	±	10.038	33.312	±	10.884	20.117	±	8.393
690.54	DAG_40:4	126.732	±	16.781	35.453	±	31.147	20.245	±	5.666
692.54	DAG_40:3	82.474	±	12.099	29.257	±	9.276	16.991	±	4.104
694.54	DAG_40:2	25.481	±	6.128	9.358	±	4.873	10.008	±	3.314
696.55	DAG_40:1	59.943	±	9.523	12.861	±	4.423	12.533	±	6.269
698.55	DAG_40:0	19.668	±	7.103	17.213	±	7.613	8.263	±	2.763
704.55	DAG_42:11	N.D.	±	N.D.	N.D.	±	N.D.	1.843	±	1.843
706.56	DAG_42:10	0.996	±	0.996	N.D.	±	N.D.	N.D.	±	N.D.
708.56	DAG_42:9	N.D.	±	N.D.	3.304	±	1.513	N.D.	±	N.D.
710.56	DAG_42:8	3.167	±	2.041	1.286	±	1.286	N.D.	±	N.D.

712.56	DAG_42:7	5.459	±	3.749	3.693	±	3.567	6.717	±	3.423
714.56	DAG_42:6	20.625	±	6.516	15.455	±	6.700	9.469	±	3.737
716.57	DAG_42:5	8.889	±	5.409	10.776	±	3.763	14.174	±	7.380
718.57	DAG_42:4	1.256	±	1.256	5.517	±	3.510	N.D.	±	N.D.
720.57	DAG_42:3	0.433	±	0.286	N.D.	±	N.D.	1.011	±	1.011
722.57	DAG_42:2	5.816	±	1.853	4.443	±	2.151	1.508	±	1.252
724.57	DAG_42:1	13.644	±	4.014	2.270	±	1.854	4.388	±	2.098

Supplementary Table 7: Concentrations (in pmol/mg protein) of free fatty acids (FFA) in *Artemia* cysts, Percoll-purified mitochondria and mitoplasts. N.D.: not determined. A stable water loss fragment from the deuterated palmitic acid standard was monitored and used for quantitation. Results shown are Mean +/- S.E.

$[M\text{-}H]^-$	**Species**	**Artemia Cysts**			**Mitochondria**			**Mitoplasts**		
227.08	FFA_14:0	886.90	±	318.35	972.34	±	294.33	1480.39	±	686.11
225.08	FFA_14:1	87.54	±	31.68	120.56	±	51.15	159.04	±	99.34
255.11	FFA_16:0	8842.40	±	2108.63	11869.59	±	1748.13	11624.12	±	1144.28
253.10	FFA_16:1	663.52	±	286.62	577.09	±	168.68	1036.59	±	520.03
283.13	FFA_18:0	23373.41	±	6148.49	105118.29	±	32781.39	24694.31	±	5747.26
281.13	FFA_18:1	22418.82	±	9632.87	7230.47	±	1678.53	6519.24	±	1716.78
279.13	FFA_18:2	2772.36	±	881.34	871.48	±	311.28	686.33	±	195.22
277.13	FFA_18:3	4155.84	±	1158.27	812.45	±	313.36	2570.81	±	1243.13
311.16	FFA_20:0	1847.27	±	393.52	1659.17	±	936.46	6406.84	±	5563.78
309.16	FFA_20:1	2153.80	±	1399.21	174.22	±	70.24	171.25	±	97.87
307.16	FFA_20:2	266.76	±	62.82	307.30	±	115.20	336.38	±	175.66
305.16	FFA_20:3	1627.01	±	405.85	1516.96	±	450.34	1536.51	±	515.68
303.15	FFA_20:4	3625.22	±	784.21	8462.53	±	4338.54	5491.98	±	1374.78
301.15	FFA_20:5	3641.98	±	983.89	4669.11	±	1699.72	6373.13	±	3724.27
339.19	FFA_22:0	2998.27	±	639.62	937.37	±	193.19	528.04	±	130.11
337.19	FFA_22:1	3029.62	±	679.86	2257.56	±	1204.43	879.99	±	376.96
335.19	FFA_22:2	137.41	±	45.80	59.80	±	38.48	478.42	±	470.45
333.18	FFA_22:3	4.10	±	2.92	125.08	±	85.89	19.44	±	12.56
331.18	FFA_22:4	82.68	±	35.67	131.51	±	47.50	79.93	±	41.04
329.18	FFA_22:5	6.04	±	5.22	27.27	±	15.71	200.58	±	134.51
327.18	FFA_22:6	28.34	±	22.05	50.74	±	45.55	114.77	±	60.38
367.22	FFA_24:0	2682.90	±	524.10	1194.68	±	243.33	1493.89	±	495.54
365.22	FFA_24:1	892.59	±	215.98	279.85	±	96.13	312.93	±	139.68
395.25	FFA_26:0	2886.89	±	961.13	599.32	±	162.00	472.86	±	214.17
393.24	FFA_26:1	658.36	±	182.58	183.54	±	107.95	1163.04	±	752.06

Supplementary Table 8: Concentrations (in pmol/mg protein) of glycolipids (monoHex (cerebroside), diHex, and triHex) in *Artemia* cysts, Percoll-purified mitochondria and mitoplasts. N.D.: not determined. Results shown are Mean +/- S.E.

[M+H]⁺	**Species**	**Artemia Cysts**			**Mitochondria**			**Mitoplasts**		
672.52	d18:0/14:1-MonoHex	0.199	±	0.199	0.580	±	0.261	0.016	±	0.016
674.52	d18:0/14:0-MonoHex	N.D.	±	N.D.	0.848	±	0.298	0.158	±	0.143
700.55	d18:0/16:1-MonoHex	0.354	±	0.224	0.165	±	0.165	0.759	±	0.488
702.55	d18:0/16:0-MonoHex	0.161	±	0.161	0.209	±	0.209	0.156	±	0.156
728.58	d18:0/18:1-MonoHex	0.194	±	0.194	N.D.	±	N.D.	N.D.	±	N.D.
750.60	d18:0/20:4-MonoHex	N.D.	±	N.D.	0.203	±	0.203	N.D.	±	N.D.
754.60	d18:0/20:2-MonoHex	0.167	±	0.167	N.D.	±	N.D.	N.D.	±	N.D.
756.61	d18:0/20:1-MonoHex	N.D.	±	N.D.	0.088	±	0.088	0.092	±	0.092
758.61	d18:0/20:0-MonoHex	0.112	±	0.112	0.217	±	0.217	N.D.	±	N.D.
776.63	d18:0/22:5-MonoHex	0.108	±	0.108	N.D.	±	N.D.	N.D.	±	N.D.
778.63	d18:0/22:4-MonoHex	N.D.	±	N.D.	0.184	±	0.184	N.D.	±	N.D.
786.64	d18:0/22:0-MonoHex	N.D.	±	N.D.	0.233	±	0.233	N.D.	±	N.D.
840.69	d18:0/26:1-MonoHex	0.303	±	0.303	N.D.	±	N.D.	N.D.	±	N.D.
842.69	d18:0/26:0-MonoHex	0.177	±	0.177	N.D.	±	N.D.	N.D.	±	N.D.
644.49	d18:1/12:0-MonoHex	N.D.	±	N.D.	0.099	±	0.099	N.D.	±	N.D.
670.52	d18:1/14:1-MonoHex	19.834	±	3.572	22.051	±	1.558	15.124	±	2.066
672.52	d18:1/14:0-MonoHex	0.354	±	0.265	0.215	±	0.215	0.227	±	0.151
698.55	d18:1/16:1-MonoHex	N.D.	±	N.D.	0.236	±	0.236	0.286	±	0.181
700.55	d18:1/16:0-MonoHex	N.D.	±	N.D.	0.723	±	0.563	0.721	±	0.289
722.57	d18:1/18:3-MonoHex	N.D.	±	N.D.	0.044	±	0.044	0.101	±	0.101
724.57	d18:1/18:2-MonoHex	0.078	±	0.078	0.075	±	0.075	0.182	±	0.182
726.58	d18:1/18:1-MonoHex	0.163	±	0.163	N.D.	±	N.D.	N.D.	±	N.D.
728.58	d18:1/18:0-MonoHex	0.269	±	0.269	0.478	±	0.306	N.D.	±	N.D.
746.60	d18:1/20:5-MonoHex	N.D.	±	N.D.	0.228	±	0.228	0.148	±	0.148
748.60	d18:1/20:4-MonoHex	0.120	±	0.120	0.463	±	0.294	N.D.	±	N.D.
750.60	d18:1/20:3-MonoHex	N.D.	±	N.D.	0.530	±	0.336	0.145	±	0.145
752.60	d18:1/20:2-MonoHex	0.281	±	0.183	0.169	±	0.169	0.205	±	0.168
754.60	d18:1/20:1-MonoHex	0.467	±	0.347	0.474	±	0.300	0.178	±	0.102
756.61	d18:1/20:0-MonoHex	N.D.	±	N.D.	0.213	±	0.213	N.D.	±	N.D.
772.62	d18:1/22:6-MonoHex	N.D.	±	N.D.	N.D.	±	N.D.	0.486	±	0.319
774.62	d18:1/22:5-MonoHex	0.085	±	0.085	0.226	±	0.226	0.035	±	0.035
776.63	d18:1/22:4-MonoHex	0.216	±	0.216	N.D.	±	N.D.	N.D.	±	N.D.
778.63	d18:1/22:3-MonoHex	0.296	±	0.205	0.442	±	0.294	0.157	±	0.157
780.63	d18:1/22:2-MonoHex	N.D.	±	N.D.	0.215	±	0.215	0.238	±	0.238
782.63	d18:1/22:1-MonoHex	N.D.	±	N.D.	0.608	±	0.309	0.610	±	0.194
784.63	d18:1/22:0-MonoHex	N.D.	±	N.D.	N.D.	±	N.D.	0.658	±	0.331
810.66	d18:1/24:1-MonoHex	1.437	±	0.611	1.995	±	0.640	1.586	±	0.660
812.66	d18:1/24:0-MonoHex	0.527	±	0.255	0.431	±	0.275	0.436	±	0.200
838.69	d18:1/26:1-MonoHex	N.D.	±	N.D.	N.D.	±	N.D.	0.372	±	0.238
840.69	d18:1/26:0-MonoHex	N.D.	±	N.D.	N.D.	±	N.D.	0.417	±	0.263
642.49	d18:2/12:0-MonoHex	0.157	±	0.157	N.D.	±	N.D.	0.046	±	0.046
668.52	d18:2/14:1-MonoHex	0.526	±	0.238	N.D.	±	N.D.	0.711	±	0.236
670.52	d18:2/14:0-MonoHex	0.158	±	0.158	0.231	±	0.231	N.D.	±	N.D.
696.55	d18:2/16:1-MonoHex	0.346	±	0.219	0.477	±	0.354	0.909	±	0.293

720.57	d18:2/18:3-MonoHex	0.163	±	0.163	N.D.	±	N.D.	N.D.	±	N.D.
722.57	d18:2/18:2-MonoHex	0.179	±	0.179	N.D.	±	N.D.	N.D.	±	N.D.
724.57	d18:2/18:1-MonoHex	N.D.	±	N.D.	0.213	±	0.213	0.300	±	0.225
726.58	d18:2/18:0-MonoHex	N.D.	±	N.D.	0.405	±	0.258	0.178	±	0.178
744.59	d18:2/20:5-MonoHex	0.373	±	0.373	0.217	±	0.217	N.D.	±	N.D.
750.60	d18:2/20:2-MonoHex	0.190	±	0.190	N.D.	±	N.D.	N.D.	±	N.D.
752.60	d18:2/20:1-MonoHex	N.D.	±	N.D.	0.526	±	0.342	0.148	±	0.148
754.60	d18:2/20:0-MonoHex	0.344	±	0.344	N.D.	±	N.D.	0.054	±	0.054
770.62	d18:2/22:6-MonoHex	0.202	±	0.202	0.577	±	0.265	1.073	±	0.397
772.62	d18:2/22:5-MonoHex	0.048	±	0.048	0.159	±	0.159	N.D.	±	N.D.
774.62	d18:2/22:4-MonoHex	N.D.	±	N.D.	N.D.	±	N.D.	0.148	±	0.148
778.63	d18:2/22:2-MonoHex	N.D.	±	N.D.	N.D.	±	N.D.	0.041	±	0.041
780.63	d18:2/22:1-MonoHex	0.162	±	0.162	0.415	±	0.271	0.386	±	0.244
782.63	d18:2/22:0-MonoHex	0.640	±	0.454	0.290	±	0.290	N.D.	±	N.D.
808.66	d18:2/24:1-MonoHex	0.053	±	0.053	0.461	±	0.231	0.189	±	0.189
836.69	d18:2/26:1-MonoHex	0.178	±	0.178	0.261	±	0.261	N.D.	±	N.D.
838.69	d18:2/26:0-MonoHex	0.377	±	0.377	0.114	±	0.114	N.D.	±	N.D.
862.71	d18:0/16:1-DiHex	0.291	±	0.291	N.D.	±	N.D.	0.146	±	0.146
864.71	d18:0/16:0-DiHex	0.445	±	0.345	N.D.	±	N.D.	N.D.	±	N.D.
886.74	d18:0/18:3-DiHex	0.099	±	0.099	N.D.	±	N.D.	N.D.	±	N.D.
888.74	d18:0/18:2-DiHex	0.198	±	0.198	N.D.	±	N.D.	N.D.	±	N.D.
890.74	d18:0/18:1-DiHex	0.347	±	0.347	N.D.	±	N.D.	N.D.	±	N.D.
892.74	d18:0/18:0-DiHex	0.480	±	0.275	N.D.	±	N.D.	N.D.	±	N.D.
916.77	d18:0/20:2-DiHex	0.183	±	0.183	0.307	±	0.232	N.D.	±	N.D.
920.77	d18:0/20:0-DiHex	0.194	±	0.194	N.D.	±	N.D.	N.D.	±	N.D.
946.80	d18:0/22:1-DiHex	N.D.	±	N.D.	0.220	±	0.220	N.D.	±	N.D.
806.66	d18:1/12:0-DiHex	0.466	±	0.225	0.419	±	0.419	0.145	±	0.145
832.68	d18:1/14:1-DiHex	0.183	±	0.183	0.338	±	0.226	N.D.	±	N.D.
834.68	d18:1/14:0-DiHex	0.190	±	0.190	N.D.	±	N.D.	0.145	±	0.145
860.71	d18:1/16:1-DiHex	0.569	±	0.266	0.222	±	0.222	0.188	±	0.188
862.71	d18:1/16:0-DiHex	1.249	±	0.186	0.659	±	0.258	0.174	±	0.174
884.73	d18:1/18:3-DiHex	0.581	±	0.202	0.097	±	0.097	0.033	±	0.033
886.74	d18:1/18:2-DiHex	0.190	±	0.190	0.383	±	0.383	0.193	±	0.149
888.74	d18:1/18:1-DiHex	0.414	±	0.207	0.238	±	0.238	0.113	±	0.113
890.74	d18:1/18:0-DiHex	0.545	±	0.262	0.650	±	0.297	0.039	±	0.039
908.76	d18:1/20:5-DiHex	0.472	±	0.316	N.D.	±	N.D.	0.043	±	0.043
912.76	d18:1/20:3-DiHex	N.D.	±	N.D.	N.D.	±	N.D.	0.250	±	0.181
914.76	d18:1/20:2-DiHex	0.286	±	0.198	0.103	±	0.103	N.D.	±	N.D.
916.77	d18:1/20:1-DiHex	N.D.	±	N.D.	0.236	±	0.236	N.D.	±	N.D.
918.77	d18:1/20:0-DiHex	0.088	±	0.088	N.D.	±	N.D.	N.D.	±	N.D.
934.78	d18:1/22:6-DiHex	0.215	±	0.215	N.D.	±	N.D.	0.398	±	0.252
936.79	d18:1/22:5-DiHex	N.D.	±	N.D.	0.307	±	0.307	N.D.	±	N.D.
938.79	d18:1/22:4-DiHex	0.198	±	0.126	N.D.	±	N.D.	N.D.	±	N.D.
940.79	d18:1/22:3-DiHex	0.198	±	0.198	0.130	±	0.130	N.D.	±	N.D.
942.79	d18:1/22:2-DiHex	0.180	±	0.180	0.368	±	0.368	N.D.	±	N.D.
944.79	d18:1/22:1-DiHex	N.D.	±	N.D.	0.228	±	0.228	N.D.	±	N.D.
946.80	d18:1/22:0-DiHex	0.181	±	0.181	N.D.	±	N.D.	N.D.	±	N.D.
972.82	d18:1/24:1-DiHex	N.D.	±	N.D.	0.233	±	0.233	N.D.	±	N.D.

974.82	d18:1/24:0-DiHex	0.092	±	0.092	N.D.	±	N.D.	N.D.	±	N.D.
1000.85	d18:1/26:1-DiHex	N.D.	±	N.D.	0.404	±	0.259	N.D.	±	N.D.
1002.85	d18:1/26:0-DiHex	N.D.	±	N.D.	N.D.	±	N.D.	0.346	±	0.220
830.68	d18:2/14:1-DiHex	0.154	±	0.154	N.D.	±	N.D.	N.D.	±	N.D.
832.68	d18:2/14:0-DiHex	0.819	±	0.396	N.D.	±	N.D.	0.308	±	0.308
858.71	d18:2/16:1-DiHex	1.842	±	0.837	0.104	±	0.104	0.165	±	0.165
860.71	d18:2/16:0-DiHex	2.312	±	0.578	0.477	±	0.302	0.223	±	0.152
882.73	d18:2/18:3-DiHex	0.563	±	0.393	0.174	±	0.174	N.D.	±	N.D.
884.73	d18:2/18:2-DiHex	0.936	±	0.345	0.619	±	0.444	0.149	±	0.149
886.74	d18:2/18:1-DiHex	0.162	±	0.162	0.222	±	0.222	0.147	±	0.147
888.74	d18:2/18:0-DiHex	1.262	±	0.211	N.D.	±	N.D.	N.D.	±	N.D.
908.76	d18:2/20:4-DiHex	0.530	±	0.237	N.D.	±	N.D.	N.D.	±	N.D.
910.76	d18:2/20:3-DiHex	0.050	±	0.050	0.289	±	0.193	N.D.	±	N.D.
912.76	d18:2/20:2-DiHex	0.950	±	0.464	0.269	±	0.175	0.172	±	0.172
914.76	d18:2/20:1-DiHex	0.169	±	0.169	0.396	±	0.290	N.D.	±	N.D.
916.77	d18:2/20:0-DiHex	0.547	±	0.367	N.D.	±	N.D.	N.D.	±	N.D.
932.78	d18:2/22:6-DiHex	N.D.	±	N.D.	0.220	±	0.220	N.D.	±	N.D.
934.78	d18:2/22:5-DiHex	0.193	±	0.193	0.307	±	0.307	N.D.	±	N.D.
938.79	d18:2/22:3-DiHex	N.D.	±	N.D.	N.D.	±	N.D.	0.058	±	0.058
940.79	d18:2/22:2-DiHex	0.682	±	0.682	N.D.	±	N.D.	N.D.	±	N.D.
942.79	d18:2/22:1-DiHex	0.399	±	0.210	0.157	±	0.157	N.D.	±	N.D.
944.79	d18:2/22:0-DiHex	0.180	±	0.180	0.390	±	0.390	N.D.	±	N.D.
998.85	d18:2/26:1-DiHex	N.D.	±	N.D.	0.320	±	0.320	N.D.	±	N.D.
1000.85	d18:2/26:0-DiHex	N.D.	±	N.D.	0.197	±	0.197	N.D.	±	N.D.
970.82	d18:0/12:0-TriHex	N.D.	±	N.D.	0.231	±	0.231	N.D.	±	N.D.
1024.87	d18:0/16:1-TriHex	0.373	±	0.373	N.D.	±	N.D.	N.D.	±	N.D.
1048.90	d18:0/18:3-TriHex	0.112	±	0.112	N.D.	±	N.D.	N.D.	±	N.D.
1098.95	d18:0/22:6-TriHex	N.D.	±	N.D.	N.D.	±	N.D.	0.177	±	0.177
1100.95	d18:0/22:5-TriHex	0.193	±	0.193	0.402	±	0.270	0.138	±	0.121
1104.95	d18:0/22:3-TriHex	N.D.	±	N.D.	N.D.	±	N.D.	0.021	±	0.021
968.82	d18:1/12:0-TriHex	N.D.	±	N.D.	0.189	±	0.189	0.150	±	0.150
1022.87	d18:1/16:1-TriHex	N.D.	±	N.D.	N.D.	±	N.D.	0.112	±	0.112
1048.90	d18:1/18:2-TriHex	N.D.	±	N.D.	N.D.	±	N.D.	0.170	±	0.170
1050.90	d18:1/18:1-TriHex	0.110	±	0.110	N.D.	±	N.D.	N.D.	±	N.D.
1072.92	d18:1/20:4-TriHex	N.D.	±	N.D.	0.507	±	0.321	0.039	±	0.039
1074.92	d18:1/20:3-TriHex	N.D.	±	N.D.	N.D.	±	N.D.	0.650	±	0.298
1098.95	d18:1/22:5-TriHex	0.296	±	0.200	0.410	±	0.259	N.D.	±	N.D.
1100.95	d18:1/22:4-TriHex	N.D.	±	N.D.	N.D.	±	N.D.	0.225	±	0.225
1102.95	d18:1/22:3-TriHex	N.D.	±	N.D.	0.115	±	0.115	N.D.	±	N.D.
1104.95	d18:1/22:2-TriHex	N.D.	±	N.D.	N.D.	±	N.D.	0.288	±	0.288
1106.96	d18:1/22:1-TriHex	N.D.	±	N.D.	0.107	±	0.107	N.D.	±	N.D.
1134.98	d18:1/24:1-TriHex	0.403	±	0.403	N.D.	±	N.D.	0.273	±	0.273
1136.99	d18:1/24:0-TriHex	0.329	±	0.214	0.185	±	0.185	N.D.	±	N.D.
1165.01	d18:1/26:0-TriHex	N.D.	±	N.D.	0.265	±	0.265	N.D.	±	N.D.
966.82	d18:2/12:0-TriHex	N.D.	±	N.D.	0.151	±	0.151	N.D.	±	N.D.
992.84	d18:2/14:1-TriHex	N.D.	±	N.D.	0.292	±	0.292	N.D.	±	N.D.
1044.89	d18:2/18:3-TriHex	N.D.	±	N.D.	N.D.	±	N.D.	0.205	±	0.205
1050.90	d18:2/18:0-TriHex	N.D.	±	N.D.	0.108	±	0.108	N.D.	±	N.D.

1068.92	d18:2/20:5-TriHex	N.D.	±	N.D.	0.257	±	0.257	N.D.	±	N.D.
1072.92	d18:2/20:3-TriHex	N.D.	±	N.D.	0.250	±	0.250	N.D.	±	N.D.
1102.95	d18:2/22:2-TriHex	N.D.	±	N.D.	N.D.	±	N.D.	0.057	±	0.057
1104.95	d18:2/22:1-TriHex	N.D.	±	N.D.	N.D.	±	N.D.	0.225	±	0.225

Supplementary Table 9: Concentrations (in pmol/mg protein) of phosphatidic acids (PA) and lysophosphatidic acids (LPA) in *Artemia* cysts, Percoll-purified mitochondria and mitoplasts. N.D.: not determined. p(carbond:double bond) indicates a plasmalogen species. Results shown are Mean +/- S.E.

$[M\text{-}H]^-$	Species	Artemia Cysts			Mitochondria			Mitoplasts		
353.20	LPA_12:0	N.D.	±	N.D.	0.688	±	0.688	N.D.	±	N.D.
409.26	LPA_16:0	8.813	±	8.813	22.710	±	14.394	N.D.	±	N.D.
437.29	LPA_18:0	10.034	±	10.034	5.492	±	5.492	4.565	±	4.168
435.29	LPA_18:1	5.968	±	5.968	N.D.	±	N.D.	N.D.	±	N.D.
431.28	LPA_18:3	N.D.	±	N.D.	2.173	±	2.173	N.D.	±	N.D.
457.31	LPA_20:4	26.135	±	24.226	N.D.	±	N.D.	3.280	±	2.995
421.27	LPA_p18:0	N.D.	±	N.D.	1.435	±	1.435	N.D.	±	N.D.
535.39	PA_10:0/14:0	55.140	±	33.761	4.752	±	3.279	N.D.	±	N.D.
563.41	PA_12:0/14:0	100.307	±	50.428	58.994	±	37.409	37.005	±	33.781
591.44	PA_14:0/14:0	316.551	±	92.677	163.969	±	67.687	95.123	±	49.337
617.47	PA_14:0/16:1	134.674	±	89.477	27.312	±	18.659	80.347	±	73.346
647.50	PA_14:0/18:0	301.772	±	185.998	222.652	±	127.470	84.303	±	34.030
645.50	PA_14:0/18:1	367.691	±	204.988	128.975	±	47.660	255.047	±	139.512
643.49	PA_14:0/18:2	49.390	±	30.109	31.387	±	19.922	N.D.	±	N.D.
641.49	PA_14:0/18:3	95.230	±	45.766	74.631	±	36.179	59.262	±	54.098
675.53	PA_14:0/20:0	51.625	±	28.286	N.D.	±	N.D.	5.405	±	4.934
673.52	PA_14:0/20:1	118.301	±	30.523	54.396	±	38.868	107.396	±	53.285
671.52	PA_14:0/20:2	10.445	±	7.716	15.691	±	14.677	103.407	±	82.566
669.52	PA_14:0/20:3	20.875	±	14.646	23.448	±	14.499	N.D.	±	N.D.
667.52	PA_14:0/20:4	117.820	±	30.017	12.540	±	8.465	12.357	±	7.713
703.55	PA_14:0/22:0	109.730	±	45.832	89.491	±	40.370	35.283	±	32.209
701.55	PA_14:0/22:1	156.244	±	79.457	120.355	±	61.240	82.111	±	53.266
647.50	PA_16:0/16:0	577.858	±	257.473	276.605	±	187.149	244.957	±	115.632
645.50	PA_16:0/16:1	323.912	±	115.247	99.970	±	26.673	233.777	±	68.104
675.53	PA_16:0/18:0	243.825	±	87.658	250.754	±	57.899	83.929	±	58.395
673.52	PA_16:0/18:1	398.283	±	87.231	875.154	±	397.624	325.162	±	140.296
671.52	PA_16:0/18:2	200.085	±	63.324	335.411	±	140.886	817.071	±	661.450
669.52	PA_16:0/18:3	295.448	±	80.871	458.816	±	102.414	168.566	±	79.737
703.55	PA_16:0/20:0	286.217	±	111.000	47.613	±	17.002	1276.065	±	1093.945
701.55	PA_16:0/20:1	142.285	±	65.162	225.507	±	155.469	253.913	±	161.392
699.55	PA_16:0/20:2	387.402	±	191.742	79.914	±	22.369	113.649	±	58.174
697.55	PA_16:0/20:3	193.461	±	32.968	229.749	±	124.436	181.186	±	93.409
695.55	PA_16:0/20:4	420.298	±	251.442	233.023	±	89.217	890.826	±	662.500
693.54	PA_16:0/20:5	88.639	±	31.431	58.657	±	41.463	1246.737	±	1100.293
731.58	PA_16:0/22:0	449.471	±	174.305	288.272	±	115.840	362.925	±	211.097
729.58	PA_16:0/22:1	338.729	±	163.246	59.900	±	36.716	85.987	±	41.430
727.58	PA_16:0/22:2	276.599	±	102.766	138.864	±	44.854	57.867	±	52.825
725.58	PA_16:0/22:3	148.382	±	65.594	216.057	±	38.473	30.404	±	21.901
723.57	PA_16:0/22:4	439.676	±	172.833	70.034	±	28.888	97.572	±	60.572
721.57	PA_16:0/22:5	435.723	±	250.956	50.233	±	33.310	879.343	±	687.527
719.57	PA_16:0/22:6	463.448	±	130.818	55.665	±	15.165	123.468	±	64.890
703.55	PA_18:0/18:0	417.021	±	136.815	246.131	±	88.733	2.258	±	2.061
701.55	PA_18:0/18:1	461.076	±	153.112	636.408	±	225.086	352.203	±	145.400

699.55	PA_18:0/18:2	466.079	±	185.125	69.498	±	32.550	367.360	±	227.148
699.55	PA_18:1/18:1	329.122	±	167.110	174.996	±	43.998	571.298	±	404.969
697.55	PA_18:0/18:3	466.271	±	112.109	365.763	±	92.744	2695.998	±	2156.231
731.58	PA_18:0/20:0	207.661	±	117.989	88.485	±	35.685	104.653	±	51.375
729.58	PA_18:0/20:1	195.775	±	118.611	90.743	±	44.554	63.129	±	47.615
727.58	PA_18:0/20:2	182.262	±	55.465	202.179	±	109.047	1176.376	±	1043.505
725.58	PA_18:0/20:3	267.683	±	111.250	124.649	±	29.666	19.544	±	11.495
723.57	PA_18:0/20:4	258.887	±	69.767	109.591	±	72.018	71.167	±	47.617
721.57	PA_18:0/20:5	106.387	±	40.968	45.147	±	25.568	47.202	±	36.018
759.61	PA_18:0/22:0	318.779	±	88.809	258.432	±	79.634	849.124	±	564.730
757.61	PA_18:0/22:1	269.885	±	60.689	120.249	±	45.318	173.430	±	90.106
755.61	PA_18:0/22:2	391.672	±	138.181	154.064	±	41.771	1293.590	±	1147.479
753.60	PA_18:0/22:3	229.826	±	115.959	241.542	±	83.388	89.872	±	41.562
751.60	PA_18:0/22:4	506.192	±	376.776	112.072	±	45.230	44.710	±	23.229
749.60	PA_18:0/22:5	222.631	±	103.486	297.368	±	145.823	141.939	±	53.696
747.60	PA_18:0/22:6	335.212	±	102.633	286.647	±	148.837	43.503	±	38.912
695.55	PA_18:1/18:3	658.086	±	310.798	386.456	±	169.991	51.797	±	32.602
725.58	PA_18:1/20:2	486.101	±	159.131	493.718	±	233.369	284.117	±	151.267
721.57	PA_18:1/20:4	1119.373	±	612.474	481.911	±	179.177	1441.168	±	733.091
757.61	PA_18:1/22:0	704.432	±	161.440	228.256	±	67.021	248.640	±	188.417
755.61	PA_18:2/22:0	307.419	±	75.928	40.091	±	25.697	744.609	±	597.629
757.61	PA_20:0/20:1	14.443	±	9.137	N.D.	±	N.D.	N.D.	±	N.D.
755.61	PA_20:0/20:2	19.658	±	12.488	N.D.	±	N.D.	N.D.	±	N.D.
753.60	PA_20:0/20:3	22.148	±	14.028	15.505	±	15.505	N.D.	±	N.D.
751.60	PA_20:0/20:4	33.685	±	33.049	1.496	±	1.496	5.749	±	5.248
749.60	PA_20:0/20:5	27.909	±	27.909	16.668	±	16.668	74.395	±	67.913
787.64	PA_20:0/22:0	N.D.	±	N.D.	0.168	±	0.168	12.328	±	7.128
785.64	PA_20:0/22:1	8.703	±	7.119	16.370	±	16.370	N.D.	±	N.D.
783.63	PA_20:0/22:2	25.115	±	25.115	N.D.	±	N.D.	N.D.	±	N.D.
781.63	PA_20:0/22:3	10.279	±	10.279	N.D.	±	N.D.	N.D.	±	N.D.
785.64	PA_20:1/22:0	91.764	±	83.992	29.844	±	26.974	5.868	±	5.356
783.63	PA_20:2/22:0	12.327	±	10.695	19.994	±	19.994	5.868	±	5.356
781.63	PA_20:3/22:0	11.508	±	11.508	N.D.	±	N.D.	N.D.	±	N.D.
815.67	PA_22:0/22:0	N.D.	±	N.D.	9.439	±	9.439	10.060	±	9.183
811.66	PA_22:0/22:2	37.808	±	37.808	N.D.	±	N.D.	5.988	±	5.466
809.66	PA_22:0/22:3	40.385	±	32.403	8.206	±	8.206	N.D.	±	N.D.
807.66	PA_22:0/22:4	21.034	±	21.034	N.D.	±	N.D.	51.441	±	46.959
659.51	PA_p16:0/18:0	63.108	±	47.901	72.419	±	54.875	10.859	±	9.913
657.51	PA_p16:0/18:1	1.410	±	0.913	N.D.	±	N.D.	3.802	±	3.471
655.51	PA_p16:0/18:2	12.660	±	12.660	39.951	±	28.302	N.D.	±	N.D.
679.53	PA_p16:0/20:4	19.383	±	12.749	1.435	±	1.435	N.D.	±	N.D.
631.48	PA_p18:0/14:0	29.870	±	16.806	17.906	±	7.850	23.455	±	16.067
659.51	PA_p18:0/16:0	151.103	±	59.705	61.199	±	39.516	160.870	±	72.690
687.54	PA_p18:0/18:0	64.396	±	40.297	35.845	±	20.682	86.599	±	58.693
685.54	PA_p18:0/18:1	62.702	±	37.089	109.121	±	83.197	1251.028	±	794.481
683.53	PA_p18:0/18:2	48.997	±	28.101	N.D.	±	N.D.	N.D.	±	N.D.
715.57	PA_p18:0/20:0	N.D.	±	N.D.	15.867	±	15.867	N.D.	±	N.D.
705.56	PA_p18:0/20:5	N.D.	±	N.D.	11.140	±	11.140	57.867	±	52.825

Supplementary Table 10: Concentrations (in pmol/mg protein) of phosphatidylcholines (PC) and lysophosphatidylcholines (LPC) in *Artemia* cysts, Percoll-purified mitochondria and mitoplasts. N.D.: not determined. O-(carbon:double bond) indicates a plasmalogen species. Results shown are Mean +/- S.E.

$[M+H]^+$	**Species**	**Artemia Cysts**			**Mitochondria**			**Mitoplasts**		
412.26	LPC_10:0	5.980	±	1.056	7.657	±	2.124	5.280	±	0.715
440.29	LPC_12:0	0.546	±	0.263	0.739	±	0.464	0.676	±	0.676
468.32	LPC_14:0	11.008	±	2.420	12.018	±	3.212	6.625	±	1.214
466.32	LPC_14:1	342.393	±	10.354	323.199	±	17.756	258.339	±	15.826
496.35	LPC_16:0	205.680	±	15.821	135.055	±	19.434	103.157	±	15.457
494.34	LPC_16:1	22.811	±	1.204	18.008	±	5.347	11.276	±	1.530
524.37	LPC_18:0	194.019	±	13.196	157.363	±	23.406	118.607	±	16.690
522.37	LPC_18:1	386.942	±	36.434	329.713	±	69.067	237.272	±	34.237
520.37	LPC_18:2	58.559	±	3.790	38.036	±	9.685	29.525	±	5.104
518.37	LPC_18:3	175.047	±	14.087	72.938	±	13.469	43.088	±	8.805
552.40	LPC_20:0	5.300	±	1.648	2.394	±	0.774	2.945	±	0.720
550.40	LPC_20:1	14.099	±	1.623	10.886	±	2.123	9.949	±	1.090
548.40	LPC_20:2	5.670	±	1.891	7.189	±	2.221	3.933	±	0.918
546.40	LPC_20:3	10.079	±	1.713	10.444	±	3.572	3.416	±	1.534
544.39	LPC_20:4	7.103	±	0.907	4.482	±	1.135	2.725	±	1.246
542.39	LPC_20:5	9.048	±	1.838	5.126	±	1.439	2.488	±	0.680
580.43	LPC_22:0	10.153	±	0.624	8.074	±	1.401	4.301	±	1.415
578.43	LPC_22:1	6.667	±	0.558	4.301	±	0.915	3.127	±	0.885
576.43	LPC_22:2	2.773	±	0.515	1.348	±	0.604	1.825	±	0.863
574.42	LPC_22:3	1.313	±	0.372	1.369	±	0.895	0.093	±	0.093
572.42	LPC_22:4	1.890	±	0.645	1.230	±	0.279	0.511	±	0.251
570.42	LPC_22:5	13.348	±	1.866	18.942	±	4.775	9.352	±	2.277
568.42	LPC_22:6	4.358	±	1.175	9.438	±	0.540	3.948	±	0.871
608.46	LPC_24:0	40.240	±	3.893	56.690	±	9.069	28.828	±	3.077
606.46	LPC_24:1	22.720	±	2.715	26.800	±	2.208	12.845	±	1.819
636.49	LPC_26:0	99.153	±	4.686	117.684	±	11.693	69.572	±	5.653
634.48	LPC_26:1	79.643	±	5.404	111.585	±	8.592	57.584	±	5.559
454.30	LPC_O-14:0	0.371	±	0.251	1.348	±	0.765	0.302	±	0.193
452.30	LPC_O-14:1	1.838	±	1.135	1.204	±	0.444	0.942	±	0.545
482.33	LPC_O-16:0	10.060	±	0.802	3.145	±	1.345	1.564	±	0.503
480.33	LPC_O-16:1	1.540	±	0.356	1.774	±	0.567	0.497	±	0.224
508.36	LPC_O-18:1	15.040	±	2.673	9.972	±	2.852	6.890	±	1.987
538.39	LPC_O-20:0	17.434	±	2.234	10.690	±	3.124	8.300	±	1.587
536.39	LPC_O-20:1	8.087	±	1.875	6.258	±	1.322	4.402	±	1.579
566.42	LPC_O-22:0	20.561	±	1.821	30.199	±	1.887	20.877	±	1.962
564.41	LPC_O-22:1	6.309	±	0.708	5.895	±	1.508	4.663	±	0.519
622.47	PC_24:0	13.539	±	0.719	13.901	±	1.032	9.896	±	1.001
620.47	PC_24:1	52.898	±	1.785	99.051	±	9.473	76.497	±	7.770
650.50	PC_26:0	69.289	±	3.974	65.416	±	3.067	50.954	±	4.260
648.50	PC_26:1	703.530	±	32.822	612.710	±	9.600	596.989	±	15.934
678.53	PC_28:0	76.316	±	2.511	68.167	±	4.122	57.280	±	2.617
676.53	PC_28:1	1289.161	±	24.452	1241.526	±	24.663	1306.974	±	14.108
706.56	PC_30:0	110.024	±	6.174	76.550	±	4.965	57.314	±	7.417

704.55	PC_30:1	144.294	±	9.865	77.319	±	5.112	57.308	±	7.521
702.55	PC_30:2	95.684	±	4.673	41.245	±	2.577	30.674	±	4.130
700.55	PC_30:3	37.047	±	3.020	27.218	±	1.988	19.924	±	1.922
734.58	PC_32:0	513.399	±	38.687	341.718	±	32.270	277.166	±	37.958
732.58	PC_32:1	1030.327	±	69.735	587.800	±	54.067	454.890	±	58.678
730.58	PC_32:2	297.963	±	17.272	161.024	±	17.588	117.088	±	16.570
728.58	PC_32:3	440.660	±	20.350	233.769	±	13.312	168.997	±	18.500
726.58	PC_32:4	353.817	±	15.763	202.432	±	14.929	148.906	±	18.269
762.61	PC_34:0	1112.014	±	55.671	723.021	±	58.044	526.242	±	82.682
760.61	PC_34:1	7738.905	±	456.815	4915.736	±	398.948	3865.778	±	558.964
758.61	PC_34:2	3449.128	±	186.074	2080.242	±	216.644	1757.925	±	250.162
756.61	PC_34:3	7593.250	±	362.151	4740.506	±	446.644	3833.307	±	518.969
754.60	PC_34:4	3766.571	±	214.559	2541.288	±	275.856	2105.936	±	266.744
752.60	PC_34:5	920.694	±	35.210	600.579	±	38.654	463.765	±	57.146
750.60	PC_34:6	240.053	±	17.653	124.125	±	8.451	97.733	±	8.969
790.64	PC_36:0/PC_O-38:7	235.018	±	13.411	178.520	±	11.819	138.309	±	21.749
788.64	PC_36:1	1553.687	±	85.860	1386.071	±	120.503	1019.076	±	161.003
786.64	PC_36:2	3890.815	±	190.949	3189.836	±	246.906	2290.982	±	368.780
784.63	PC_36:3	8178.157	±	403.725	6524.077	±	546.825	4930.396	±	673.879
782.63	PC_36:4	14166.475	±	622.773	10639.654	±	1161.382	8292.801	±	1093.327
780.63	PC_36:5	8367.207	±	428.555	6559.572	±	726.617	5005.828	±	650.302
778.63	PC_36:6	3015.987	±	170.781	1623.404	±	146.874	1260.739	±	173.568
776.63	PC_36:7	1300.008	±	80.371	807.148	±	52.913	626.934	±	95.689
818.67	PC_38:0/PC_O-40:7	102.248	±	10.063	75.533	±	5.490	55.432	±	9.396
816.67	PC_38:1	149.539	±	14.558	116.867	±	7.357	96.781	±	12.837
814.66	PC_38:2	246.375	±	16.219	190.911	±	13.684	163.742	±	22.213
812.66	PC_38:3	327.061	±	15.546	267.449	±	25.006	221.869	±	30.484
810.66	PC_38:4	711.454	±	46.741	666.535	±	62.118	471.402	±	68.298
808.66	PC_38:5	1278.177	±	98.494	1277.281	±	119.650	961.420	±	150.450
806.66	PC_38:6	1475.688	±	79.693	1229.980	±	143.567	924.764	±	138.011
804.65	PC_38:7/PC_O-38:0	668.318	±	36.763	431.303	±	33.881	325.582	±	44.232
802.65	PC_38:8/PC_O-38:1	344.053	±	20.940	267.610	±	22.754	207.355	±	25.697
846.70	PC_40:0/PC_O-42:7	88.152	±	7.724	62.133	±	4.666	51.798	±	9.515
844.69	PC_40:1	74.664	±	6.199	50.724	±	2.583	42.463	±	5.917
826.68	PC_40:10/PC_O-40:3	101.146	±	8.408	85.871	±	7.499	67.702	±	9.529
842.69	PC_40:2	57.884	±	3.041	41.340	±	3.649	33.752	±	4.489
840.69	PC_40:3	64.863	±	5.963	44.955	±	5.061	39.585	±	6.567
838.69	PC_40:4	60.810	±	5.565	51.123	±	6.591	43.060	±	6.849
836.69	PC_40:5	107.511	±	6.185	75.588	±	5.656	55.946	±	7.323
834.68	PC_40:6	149.369	±	12.930	141.406	±	12.730	108.595	±	12.467
832.68	PC_40:7/PC_O-40:0	237.334	±	20.332	215.312	±	19.732	161.167	±	19.999
830.68	PC_40:8/PC_O-	343.853	±	25.511	321.079	±	16.763	220.195	±	22.760

	40:1									
828.68	PC_40:9/PC_O-40:2	206.809	±	19.259	196.589	±	7.882	153.572	±	22.883
874.72	PC_42:0/PC_O-44:7	26.197	±	2.631	17.536	±	1.065	15.222	±	2.794
872.72	PC_42:1	23.006	±	2.898	17.308	±	1.310	14.592	±	2.649
854.70	PC_42:10/PC_O-42:3	55.497	±	4.177	49.604	±	3.542	36.704	±	3.891
852.70	PC_42:11	45.544	±	2.715	44.380	±	3.005	34.008	±	4.557
870.72	PC_42:2	23.079	±	2.355	14.727	±	2.039	12.670	±	1.494
868.72	PC_42:3	21.124	±	1.060	16.879	±	1.209	14.256	±	2.106
866.72	PC_42:4	24.479	±	2.586	21.247	±	1.697	16.448	±	2.399
864.71	PC_42:5	36.833	±	2.817	23.545	±	2.652	19.255	±	3.425
862.71	PC_42:6	39.999	±	2.824	31.065	±	2.508	22.632	±	3.195
860.71	PC_42:7/PC_O-42:0	36.120	±	4.080	31.646	±	2.300	22.731	±	3.138
858.71	PC_42:8/PC_O-42:1	35.705	±	2.808	33.837	±	0.846	25.232	±	3.776
856.71	PC_42:9/PC_O-42:2	41.299	±	3.493	41.780	±	3.692	30.481	±	3.874
902.75	PC_44:0	11.123	±	1.339	12.198	±	0.886	7.007	±	1.102
900.75	PC_44:1	9.928	±	0.909	10.240	±	1.289	9.325	±	1.025
882.73	PC_44:10/PC_O-44:3	20.589	±	1.290	16.975	±	2.286	10.192	±	1.593
880.73	PC_44:11/PC_O-44:4	21.755	±	2.982	24.998	±	3.059	15.946	±	1.531
878.73	PC_44:12/PC_O-44:5	45.537	±	4.417	44.524	±	3.850	27.785	±	1.768
898.75	PC_44:2	21.701	±	1.318	20.248	±	0.513	20.017	±	1.443
896.75	PC_44:3	10.990	±	0.980	9.057	±	1.010	6.253	±	1.694
894.74	PC_44:4	9.640	±	0.586	8.109	±	1.271	7.677	±	1.241
892.74	PC_44:5	9.152	±	0.906	9.726	±	0.840	6.638	±	1.028
890.74	PC_44:6	10.967	±	1.282	8.395	±	0.995	7.301	±	1.666
888.74	PC_44:7/PC_O-44:0	14.126	±	1.788	9.547	±	1.476	8.011	±	0.717
886.74	PC_44:8/PC_O-44:1	11.552	±	1.044	9.306	±	0.817	7.386	±	1.058
884.73	PC_44:9/PC_O-44:2	11.285	±	0.892	9.775	±	1.817	7.461	±	1.218
664.51	PC_O-28:0	24.036	±	3.343	14.110	±	0.858	14.258	±	1.651
662.51	PC_O-28:1	35.997	±	1.101	28.864	±	1.861	26.467	±	1.181
660.51	PC_O-28:2	104.584	±	1.729	102.451	±	4.395	110.117	±	2.824
692.54	PC_O-30:0	43.993	±	2.130	26.573	±	1.652	18.590	±	3.519
690.54	PC_O-30:1	45.725	±	1.934	35.765	±	1.905	30.202	±	1.789
688.54	PC_O-30:2	23.570	±	1.876	15.919	±	1.502	14.384	±	1.087
720.57	PC_O-32:0	118.768	±	8.390	77.458	±	7.364	55.366	±	7.565
718.57	PC_O-32:1	214.721	±	11.605	90.620	±	5.133	65.956	±	8.927
716.57	PC_O-32:2	67.885	±	3.427	37.720	±	3.925	30.537	±	4.330
748.60	PC_O-34:0	370.544	±	26.012	204.754	±	21.995	163.283	±	21.617
746.60	PC_O-34:1	861.576	±	54.383	398.593	±	32.310	313.779	±	42.923

744.59	PC_O-34:2	368.949	±	13.791	182.894	±	16.466	138.933	±	18.952
742.59	PC_O-34:3	497.014	±	33.155	208.740	±	18.219	178.335	±	22.298
740.59	PC_O-34:4	261.659	±	10.957	127.114	±	9.573	108.825	±	12.881
776.63	PC_O-36:0	1300.008	±	80.371	807.148	±	52.913	626.934	±	95.689
774.62	PC_O-36:1	1056.688	±	69.806	667.180	±	43.994	497.062	±	71.904
772.62	PC_O-36:2	759.754	±	47.048	523.286	±	47.932	401.830	±	59.676
770.62	PC_O-36:3	1396.551	±	81.714	938.619	±	84.011	755.819	±	105.441
768.62	PC_O-36:4	1030.958	±	68.390	646.018	±	58.285	524.141	±	71.870
766.62	PC_O-36:5	311.438	±	14.928	203.840	±	22.246	170.143	±	22.454
764.61	PC_O-36:6	156.923	±	11.514	97.356	±	8.436	77.062	±	10.608
800.65	PC_O-38:2	271.383	±	19.846	204.531	±	16.163	148.931	±	26.302
798.65	PC_O-38:3	372.539	±	17.065	266.596	±	18.409	225.091	±	33.445
796.65	PC_O-38:4	425.596	±	24.198	309.360	±	19.900	243.383	±	33.651
794.64	PC_O-38:5	253.362	±	11.107	209.029	±	16.738	160.489	±	20.221
792.64	PC_O-38:6	126.843	±	6.591	90.820	±	6.298	70.093	±	8.682
824.67	PC_O-40:4	55.521	±	5.136	52.144	±	2.459	42.088	±	6.062
822.67	PC_O-40:5	81.412	±	8.421	59.544	±	4.462	47.419	±	5.983
820.67	PC_O-40:6	83.480	±	8.584	63.747	±	5.876	51.108	±	7.596
852.70	PC_O-42:4	45.544	±	2.715	44.380	±	3.005	34.008	±	4.557
850.70	PC_O-42:5	69.552	±	7.380	44.946	±	3.978	34.869	±	5.096
848.70	PC_O-42:6	83.673	±	8.498	60.176	±	7.570	47.316	±	6.067
876.73	PC_O-44:6	36.616	±	3.377	39.097	±	2.082	24.474	±	3.662

Supplementary Table 11: Concentrations (in pmol/mg protein) of phosphatidylethanolamines (PE) and lysophosphatidylethanolamines (LPE) in *Artemia* cysts, Percoll-purified mitochondria and mitoplasts. O-(carbon:double bond) indicates a plasmalogen species. Results shown are Mean +/- S.E.

$[M+H]^+$	Species	Artemia Cysts			Mitochondria			Mitoplasts		
370.22	LPE_10:0	4.594	±	4.594	N.D.	±	N.D.	N.D.	±	N.D.
398.25	LPE_12:0	4.124	±	4.124	4.104	±	4.104	N.D.	±	N.D.
454.30	LPE_16:0	30.685	±	7.423	76.908	±	12.730	55.948	±	16.796
452.30	LPE_16:1	1417.534	±	223.187	1219.868	±	124.393	1334.998	±	194.968
482.33	LPE_18:0	51.516	±	8.875	294.972	±	89.188	186.864	±	33.567
480.33	LPE_18:1	395.852	±	67.377	712.865	±	116.899	696.982	±	130.599
478.33	LPE_18:2	32.841	±	11.240	19.052	±	7.651	29.894	±	19.389
476.33	LPE_18:3	44.617	±	4.126	35.375	±	17.863	28.729	±	12.986
508.36	LPE_20:1	18.240	±	8.833	48.052	±	27.073	26.261	±	13.866
506.36	LPE_20:2	5.116	±	5.116	N.D.	±	N.D.	6.405	±	6.405
504.35	LPE_20:3	3.377	±	3.377	20.615	±	15.639	20.117	±	14.866
502.35	LPE_20:4	5.116	±	5.116	9.628	±	6.369	12.364	±	7.909
500.35	LPE_20:5	4.742	±	4.742	8.192	±	8.192	N.D.	±	N.D.
538.39	LPE_22:0	3.062	±	3.062	N.D.	±	N.D.	N.D.	±	N.D.
530.38	LPE_22:4	N.D.	±	N.D.	4.820	±	4.820	N.D.	±	N.D.
526.38	LPE_22:6	0.569	±	0.569	7.450	±	6.147	N.D.	±	N.D.
578.43	PE_24:1	0.024	±	0.024	0.779	±	0.427	N.D.	±	N.D.
608.46	PE_26:0	0.907	±	0.577	0.516	±	0.516	N.D.	±	N.D.
606.46	PE_26:1	2.649	±	1.471	11.140	±	3.005	5.349	±	2.023
636.49	PE_28:0	0.399	±	0.399	1.726	±	0.916	2.533	±	0.599
634.48	PE_28:1	1.653	±	0.626	3.134	±	1.569	0.898	±	0.579
632.48	PE_28:2	N.D.	±	N.D.	0.250	±	0.250	0.883	±	0.801
664.51	PE_30:0	6.652	±	3.022	4.891	±	1.682	1.631	±	0.373
662.51	PE_30:1	33.379	±	4.230	29.485	±	5.564	28.760	±	2.703
660.51	PE_30:2	2.645	±	1.082	2.108	±	0.672	2.502	±	0.530
658.51	PE_30:3	0.906	±	0.844	1.307	±	0.877	0.435	±	0.435
692.54	PE_32:0	29.983	±	2.914	30.802	±	3.367	29.507	±	7.259
690.54	PE_32:1	2196.825	±	109.789	2219.146	±	97.849	2047.774	±	107.887
686.54	PE_32:3	48.006	±	4.668	31.123	±	4.212	19.579	±	3.469
684.53	PE_32:4	35.209	±	4.069	17.039	±	3.222	11.045	±	0.965
720.57	PE_34:0	55.519	±	1.271	50.945	±	10.339	27.565	±	5.248
718.57	PE_34:1	589.113	±	40.199	460.750	±	64.005	315.437	±	29.001
716.57	PE_34:2	584.776	±	26.670	444.841	±	43.111	340.153	±	42.147
714.56	PE_34:3	1398.008	±	88.369	903.596	±	108.642	647.681	±	92.771
712.56	PE_34:4	819.761	±	48.964	646.441	±	59.003	506.891	±	72.694
710.56	PE_34:5	1214.155	±	128.294	977.350	±	71.916	1168.630	±	36.768
708.56	PE_34:6	48.966	±	6.186	15.540	±	1.520	10.216	±	1.756
748.60	PE_36:0	70.873	±	7.512	90.054	±	11.174	63.355	±	9.893
746.60	PE_36:1	1128.477	±	77.128	1069.555	±	129.960	800.526	±	109.441
744.59	PE_36:2	4077.367	±	182.168	4304.616	±	541.329	3093.649	±	353.062
742.59	PE_36:3	4419.613	±	131.864	4260.660	±	490.542	3311.509	±	435.296
740.59	PE_36:4	6686.543	±	499.443	6536.664	±	912.261	5291.378	±	630.214
738.59	PE_36:5	3402.350	±	210.717	3946.200	±	498.255	2927.200	±	312.795

736.59	PE_36:6	849.569	±	34.479	616.663	±	73.988	512.652	±	70.523
734.58	PE_36:7/PE_O-36:0	277.748	±	34.966	212.790	±	17.419	168.302	±	21.284
776.63	PE_38:0/PE_O-40:7	3.282	±	0.478	4.124	±	1.955	0.121	±	0.121
774.62	PE_38:1	31.562	±	2.456	30.414	±	2.800	19.893	±	3.284
772.62	PE_38:2	130.720	±	3.611	118.019	±	17.719	86.383	±	17.167
770.62	PE_38:3	168.898	±	11.760	210.301	±	25.360	164.400	±	25.644
768.62	PE_38:4	511.197	±	28.692	476.199	±	65.968	377.489	±	50.561
766.62	PE_38:5	821.749	±	52.551	840.102	±	99.064	726.405	±	94.504
764.61	PE_38:6	1022.868	±	60.152	1013.435	±	133.480	794.992	±	101.126
762.61	PE_38:7/PE_O-38:0	546.671	±	24.819	455.048	±	56.568	401.539	±	44.466
760.61	PE_38:8/PE_O-38:1	306.216	±	25.834	267.177	±	33.410	213.749	±	30.305
804.65	PE_40:0/PE_O-42:7	1.417	±	0.717	1.798	±	0.835	0.774	±	0.490
802.65	PE_40:1	5.087	±	1.466	2.791	±	1.021	1.516	±	0.797
784.63	PE_40:10/PE_O-40:3	24.987	±	4.946	18.028	±	1.650	12.111	±	2.914
800.65	PE_40:2	22.469	±	4.013	12.651	±	3.405	7.253	±	1.769
798.65	PE_40:3	27.501	±	2.133	30.472	±	6.261	13.253	±	2.011
796.65	PE_40:4	13.055	±	4.014	19.329	±	5.407	10.995	±	2.217
794.64	PE_40:5	23.012	±	3.543	23.254	±	3.303	15.324	±	2.889
792.64	PE_40:6	40.175	±	3.396	42.258	±	5.892	32.594	±	4.496
790.64	PE_40:7/PE_O-40:0	63.395	±	11.418	54.404	±	7.693	47.938	±	3.871
788.64	PE_40:8/PE_O-40:1	68.990	±	8.454	70.223	±	13.617	58.057	±	10.017
786.64	PE_40:9/PE_O-40:2	67.299	±	8.706	71.317	±	11.729	40.195	±	5.759
832.68	PE_42:0/PE_O-44:7	1.557	±	0.945	1.085	±	0.687	N.D.	±	N.D.
830.68	PE_42:1	0.812	±	0.812	1.021	±	0.651	0.625	±	0.484
812.66	PE_42:10/PE_O-42:3	32.213	±	3.211	22.967	±	5.685	14.433	±	3.301
810.66	PE_42:11/PE_O-42:4	18.567	±	3.997	14.754	±	2.699	9.512	±	1.924
828.68	PE_42:2	2.182	±	0.824	1.516	±	0.576	0.433	±	0.433
826.68	PE_42:3	6.621	±	1.745	4.382	±	1.994	3.347	±	2.488
824.67	PE_42:4	5.058	±	1.239	9.150	±	2.365	7.127	±	2.535
822.67	PE_42:5	16.017	±	4.400	23.540	±	5.673	8.132	±	1.982
820.67	PE_42:6	20.123	±	3.035	16.426	±	3.785	10.292	±	3.703
818.67	PE_42:7/PE_O-42:0	42.154	±	4.002	39.983	±	9.153	26.996	±	6.405
816.67	PE_42:8/PE_O-42:1	32.166	±	1.957	48.937	±	6.280	33.007	±	6.822
814.66	PE_42:9/PE_O-42:2	20.335	±	3.746	11.648	±	2.957	10.719	±	2.381
860.71	PE_44:0	0.419	±	0.419	N.D.	±	N.D.	N.D.	±	N.D.
840.69	PE_44:10/PE_O-44:3	7.546	±	1.875	8.423	±	3.300	5.648	±	2.727
838.69	PE_44:11/PE_O-44:4	10.124	±	2.799	9.410	±	2.141	7.051	±	1.831
836.69	PE_44:12/PE_O-44:5	6.380	±	1.275	5.622	±	1.649	3.677	±	1.938
854.70	PE_44:3	0.985	±	0.623	N.D.	±	N.D.	0.848	±	0.537
852.70	PE_44:4	1.201	±	0.559	0.447	±	0.284	N.D.	±	N.D.
850.70	PE_44:5	0.828	±	0.598	2.741	±	1.084	1.919	±	0.797
848.70	PE_44:6	2.050	±	1.046	2.240	±	1.195	3.202	±	1.585
846.70	PE_44:7/PE_O-44:0	3.097	±	1.424	5.535	±	1.550	2.058	±	1.116
844.69	PE_44:8/PE_O-44:1	3.149	±	1.622	1.977	±	1.245	4.120	±	1.423
842.69	PE_44:9/PE_O-44:2	7.904	±	1.422	2.116	±	1.121	3.010	±	1.394
622.47	PE_O-28:0	N.D.	±	N.D.	0.200	±	0.200	N.D.	±	N.D.
650.50	PE_O-30:0	0.338	±	0.338	0.934	±	0.934	N.D.	±	N.D.
648.50	PE_O-30:1	0.431	±	0.431	2.188	±	0.866	0.408	±	0.408

646.50	PE_O-30:2	0.255	±	0.255	0.230	±	0.230	0.435	±	0.435
678.53	PE_O-32:0	1.059	±	0.777	0.953	±	0.605	0.280	±	0.280
676.53	PE_O-32:1	2.414	±	0.786	0.431	±	0.236	0.477	±	0.362
674.52	PE_O-32:2	1.328	±	0.604	N.D.	±	N.D.	N.D.	±	N.D.
706.56	PE_O-34:0	4.037	±	1.132	1.848	±	0.848	N.D.	±	N.D.
704.55	PE_O-34:1	16.332	±	3.340	6.898	±	1.719	3.501	±	1.353
702.55	PE_O-34:2	9.238	±	2.096	6.114	±	2.468	0.842	±	0.546
700.55	PE_O-34:3	17.722	±	1.306	10.161	±	2.629	3.443	±	0.835
698.55	PE_O-34:4	9.576	±	0.997	3.435	±	1.248	1.905	±	0.480
732.58	PE_O-36:1	44.777	±	9.232	39.288	±	4.970	22.492	±	3.513
730.58	PE_O-36:2	45.077	±	5.531	36.193	±	3.665	30.391	±	4.009
728.58	PE_O-36:3	86.340	±	9.969	77.623	±	12.093	46.545	±	10.295
726.58	PE_O-36:4	58.590	±	8.128	57.316	±	9.650	26.939	±	4.111
724.57	PE_O-36:5	18.150	±	3.845	17.393	±	2.536	8.712	±	2.712
722.57	PE_O-36:6	9.185	±	2.337	8.501	±	2.458	10.579	±	2.902
758.61	PE_O-38:2	12.936	±	2.093	16.842	±	4.533	7.992	±	2.190
756.61	PE_O-38:3	15.019	±	3.361	14.045	±	0.998	9.196	±	1.950
754.60	PE_O-38:4	32.459	±	9.261	24.118	±	3.725	19.983	±	3.217
752.60	PE_O-38:5	29.764	±	5.088	28.128	±	4.149	24.023	±	4.640
750.60	PE_O-38:6	50.522	±	4.146	61.712	±	11.282	43.930	±	4.892
748.60	PE_O-38:7/PE_36:0	56.585	±	8.878	76.924	±	10.858	57.652	±	7.013
782.63	PE_O-40:4	2.130	±	0.968	2.082	±	1.078	0.991	±	0.507
780.63	PE_O-40:5	2.536	±	1.273	2.932	±	2.078	1.878	±	1.571
778.63	PE_O-40:6	4.500	±	1.581	6.447	±	2.474	5.086	±	1.987
808.66	PE_O-42:5	2.022	±	0.607	1.152	±	0.755	0.444	±	0.444
806.66	PE_O-42:6	2.586	±	0.955	0.806	±	0.538	0.784	±	0.539
834.68	PE_O-44:6	1.141	±	0.569	0.946	±	0.602	1.551	±	0.700

Supplementary Table 12: Concentrations (in pmol/mg protein) of phosphatidylglycerols (PG) and lysophosphatidylglycerols (LPG)in *Artemia* cysts, Percoll-purified mitochondria and mitoplasts. N.D.: not determined. p(carbon:double bond) indicates a plasmalogen species. a(carbon:double bond) indicates an alkylenyl species. Results shown are Mean +/- S.E.

$[M-H]^-$	Species	Artemia Cysts			Mitochondria			Mitoplasts		
399.25	LPG_10:0	N.D.	±	N.D.	2.922	±	2.009	N.D.	±	N.D.
427.28	LPG_12:0	N.D.	±	N.D.	N.D.	±	N.D.	0.014	±	0.014
455.31	LPG_14:0	1.565	±	0.880	N.D.	±	N.D.	1.275	±	1.275
483.33	LPG_16:0	3.252	±	0.834	6.548	±	2.574	N.D.	±	N.D.
481.33	LPG_16:1	1.980	±	1.110	N.D.	±	N.D.	N.D.	±	N.D.
511.36	LPG_18:0	3.077	±	1.419	20.123	±	12.738	7.489	±	5.916
509.36	LPG_18:1	8.635	±	1.659	7.592	±	3.477	2.369	±	2.369
507.36	LPG_18:2	4.212	±	1.679	N.D.	±	N.D.	N.D.	±	N.D.
505.36	LPG_18:3	1.359	±	0.892	N.D.	±	N.D.	N.D.	±	N.D.
539.39	LPG_20:0	N.D.	±	N.D.	0.377	±	0.377	N.D.	±	N.D.
537.39	LPG_20:1	1.916	±	1.227	N.D.	±	N.D.	N.D.	±	N.D.
531.38	LPG_20:4	2.528	±	2.308	N.D.	±	N.D.	1.748	±	1.748
565.42	LPG_22:1	1.009	±	0.921	N.D.	±	N.D.	N.D.	±	N.D.
595.45	LPG_24:0	0.770	±	0.703	N.D.	±	N.D.	N.D.	±	N.D.
593.44	LPG_24:1	1.636	±	0.964	N.D.	±	N.D.	N.D.	±	N.D.
621.47	LPG_26:1	N.D.	±	N.D.	N.D.	±	N.D.	0.832	±	0.832
853.70	PG_20:3/22:1	5.470	±	3.488	8.928	±	5.697	6.921	±	4.500
851.70	PG_20:3/22:2	7.581	±	3.492	1.550	±	1.550	3.840	±	3.840
849.70	PG_20:3/22:3	9.286	±	6.550	4.711	±	2.474	0.668	±	0.668
847.70	PG_20:3/22:4	6.052	±	1.354	6.490	±	3.115	4.470	±	4.079
609.46	PG_10:0/14:0	0.793	±	0.724	N.D.	±	N.D.	0.168	±	0.168
609.46	PG_12:0/12:0	N.D.	±	N.D.	N.D.	±	N.D.	1.418	±	1.418
665.52	PG_14:0/14:0	28.549	±	12.917	36.316	±	15.389	19.583	±	9.745
693.54	PG_14:0/16:0	7.091	±	1.930	11.639	±	4.092	15.130	±	11.285
691.54	PG_14:0/16:1	8.053	±	2.708	6.390	±	4.071	14.382	±	6.520
721.57	PG_14:0/18:0	13.924	±	2.037	14.975	±	7.814	100.921	±	83.542
719.57	PG_14:0/18:1	48.494	±	24.139	37.540	±	6.128	54.532	±	22.269
717.57	PG_14:0/18:2	10.916	±	3.699	4.106	±	2.634	3.542	±	2.356
715.57	PG_14:0/18:3	6.831	±	2.181	121.495	±	44.178	4.824	±	2.446
749.60	PG_14:0/20:0	18.353	±	3.696	24.153	±	8.762	8.637	±	3.462
747.60	PG_14:0/20:1	4.434	±	1.244	12.337	±	4.917	N.D.	±	N.D.
745.60	PG_14:0/20:2	6.368	±	2.615	5.826	±	3.685	2.520	±	2.348
743.59	PG_14:0/20:3	6.876	±	2.226	6.356	±	2.975	1.046	±	1.046
741.59	PG_14:0/20:4	10.504	±	5.903	10.790	±	5.986	8.371	±	5.392
739.59	PG_14:0/20:5	10.778	±	5.227	29.340	±	16.965	1.704	±	0.936
777.63	PG_14:0/22:0	7.507	±	2.737	4.297	±	2.768	5.642	±	5.642
775.63	PG_14:0/22:1	8.240	±	2.850	11.183	±	5.213	N.D.	±	N.D.
773.62	PG_14:0/22:2	2.575	±	1.743	12.809	±	6.835	N.D.	±	N.D.
771.62	PG_14:0/22:3	3.882	±	1.007	3.980	±	2.044	2.088	±	2.088
769.62	PG_14:0/22:4	4.385	±	2.482	14.732	±	4.416	1.258	±	1.046
767.62	PG_14:0/22:5	19.863	±	7.883	10.563	±	3.646	2.498	±	1.670
765.62	PG_14:0/22:6	4.577	±	1.956	19.297	±	7.760	6.155	±	3.730

721.57	PG_16:0/16:0	21.020	±	5.368	26.129	±	10.809	19.127	±	8.215
719.57	PG_16:0/16:1	35.430	±	10.999	18.786	±	3.257	25.715	±	8.584
749.60	PG_16:0/18:0	34.401	±	7.732	118.508	±	38.635	29.631	±	11.385
747.60	PG_16:0/18:1	309.432	±	28.735	1455.679	±	456.570	526.668	±	285.774
745.60	PG_16:0/18:2	224.062	±	49.022	249.721	±	79.071	48.743	±	16.866
743.59	PG_16:0/18:3	483.400	±	190.859	265.256	±	45.154	203.513	±	44.714
777.63	PG_16:0/20:0	50.524	±	5.218	62.733	±	10.262	19.816	±	7.657
775.63	PG_16:0/20:1	34.685	±	4.750	78.514	±	27.883	8.704	±	4.287
773.62	PG_16:0/20:2	21.708	±	4.160	63.867	±	18.705	17.717	±	4.719
771.62	PG_16:0/20:3	45.397	±	8.845	61.773	±	21.593	57.479	±	28.600
769.62	PG_16:0/20:4	85.085	±	24.674	53.379	±	21.178	50.401	±	16.046
767.62	PG_16:0/20:5	112.389	±	20.503	80.772	±	12.407	30.780	±	16.279
805.66	PG_16:0/22:0	88.903	±	8.639	211.031	±	111.990	157.908	±	49.740
803.65	PG_16:0/22:1	69.400	±	4.240	57.272	±	15.476	46.637	±	18.425
801.65	PG_16:0/22:2	60.668	±	5.461	43.365	±	12.025	27.824	±	8.348
799.65	PG_16:0/22:3	40.644	±	6.559	72.677	±	40.579	5.342	±	3.555
797.65	PG_16:0/22:4	92.782	±	17.575	181.072	±	81.619	23.963	±	5.302
795.65	PG_16:0/22:5	180.280	±	22.624	538.680	±	174.571	205.414	±	89.015
793.64	PG_16:0/22:6	365.426	±	25.979	563.902	±	305.638	275.523	±	70.831
717.57	PG_16:1/16:1	92.640	±	20.746	106.559	±	25.973	72.463	±	21.875
747.60	PG_16:1/18:0	43.006	±	8.686	189.138	±	43.228	81.637	±	56.826
745.60	PG_16:1/18:1	948.151	±	250.427	991.074	±	314.674	262.160	±	83.324
743.59	PG_16:1/18:2	1160.602	±	397.832	567.746	±	49.417	469.862	±	88.813
741.59	PG_16:1/18:3	245.816	±	102.473	153.331	±	19.626	146.878	±	65.740
775.63	PG_16:1/20:0	20.366	±	3.154	38.092	±	17.493	16.256	±	4.725
773.62	PG_16:1/20:1	12.037	±	2.051	43.747	±	16.646	11.799	±	6.655
771.62	PG_16:1/20:2	55.008	±	20.739	49.773	±	19.555	12.872	±	6.734
769.62	PG_16:1/20:3	449.660	±	183.457	347.478	±	96.804	245.075	±	44.109
767.62	PG_16:1/20:4	1030.558	±	186.214	874.729	±	173.443	691.797	±	265.953
765.62	PG_16:1/20:5	34.998	±	15.210	40.364	±	13.906	9.788	±	3.782
803.65	PG_16:1/22:0	55.460	±	9.051	61.445	±	16.110	40.581	±	20.514
801.65	PG_16:1/22:1	21.363	±	5.967	43.260	±	6.237	23.761	±	5.442
799.65	PG_16:1/22:2	17.081	±	3.035	32.656	±	11.681	5.883	±	4.046
797.65	PG_16:1/22:3	28.930	±	5.760	61.137	±	29.530	9.720	±	5.098
795.65	PG_16:1/22:4	47.446	±	6.522	229.755	±	93.448	67.237	±	34.924
793.64	PG_16:1/22:5	72.648	±	8.045	213.666	±	118.298	121.538	±	48.602
791.64	PG_16:1/22:6	108.939	±	22.023	193.520	±	73.644	105.559	±	54.986
777.63	PG_18:0/18:0	25.764	±	6.658	35.318	±	9.066	14.548	±	7.329
775.63	PG_18:0/18:1	136.602	±	11.206	399.245	±	119.494	61.755	±	20.876
773.62	PG_18:0/18:2	57.548	±	7.167	197.643	±	59.651	60.863	±	22.027
771.62	PG_18:0/18:3	188.202	±	49.404	233.155	±	70.100	83.951	±	26.576
805.66	PG_18:0/20:0	27.062	±	3.174	105.852	±	55.343	65.190	±	37.956
803.65	PG_18:0/20:1	17.984	±	5.235	42.652	±	10.911	13.795	±	8.119
801.65	PG_18:0/20:2	14.644	±	1.451	29.232	±	6.140	39.871	±	29.196
799.65	PG_18:0/20:3	19.620	±	2.449	52.586	±	30.654	5.161	±	3.909
797.65	PG_18:0/20:4	42.204	±	7.259	92.668	±	39.488	28.260	±	12.464
795.65	PG_18:0/20:5	49.490	±	7.704	138.719	±	40.423	54.041	±	30.656
833.68	PG_18:0/22:0	54.368	±	17.346	47.824	±	10.438	94.625	±	30.011

831.68	PG_18:0/22:1	39.806	±	15.114	41.372	±	14.710	10.902	±	5.095
829.68	PG_18:0/22:2	30.194	±	5.474	38.162	±	10.637	15.317	±	10.943
827.68	PG_18:0/22:3	28.003	±	12.246	35.351	±	9.828	34.200	±	19.876
825.68	PG_18:0/22:4	22.768	±	3.780	53.146	±	18.876	101.181	±	57.996
823.67	PG_18:0/22:5	62.182	±	13.377	61.644	±	13.319	55.069	±	29.565
821.67	PG_18:0/22:6	110.217	±	26.874	199.283	±	57.978	125.821	±	29.740
773.62	PG_18:1/18:1	103.664	±	11.762	413.959	±	130.461	74.426	±	25.733
771.62	PG_18:1/18:2	136.679	±	21.075	176.698	±	52.908	99.004	±	25.796
769.62	PG_18:1/18:3	367.637	±	133.983	342.805	±	84.093	164.143	±	24.307
803.65	PG_18:1/20:0	120.759	±	8.597	165.453	±	17.153	122.421	±	49.458
801.65	PG_18:1/20:1	99.091	±	6.237	175.022	±	36.550	59.320	±	18.905
799.65	PG_18:1/20:2	89.762	±	12.461	215.257	±	122.397	69.494	±	19.730
797.65	PG_18:1/20:3	126.178	±	22.319	240.382	±	104.312	59.521	±	14.157
795.65	PG_18:1/20:4	158.008	±	26.782	580.468	±	201.142	178.149	±	73.118
793.64	PG_18:1/20:5	218.891	±	26.460	379.873	±	192.175	160.240	±	54.112
831.68	PG_18:1/22:0	255.592	±	120.333	135.567	±	31.276	44.447	±	14.297
829.68	PG_18:1/22:1	104.487	±	14.613	99.530	±	16.491	36.132	±	18.354
827.68	PG_18:1/22:2	150.911	±	59.605	95.408	±	13.706	78.434	±	21.465
825.68	PG_18:1/22:3	126.035	±	21.890	233.537	±	105.420	214.333	±	76.246
823.67	PG_18:1/22:4	248.375	±	53.869	211.164	±	59.024	146.109	±	79.535
821.67	PG_18:1/22:5	225.855	±	46.944	499.319	±	194.721	173.621	±	60.249
769.62	PG_18:2/18:2	34.759	±	12.558	43.928	±	15.640	4.937	±	3.176
767.62	PG_18:2/18:3	171.795	±	27.770	131.022	±	29.964	141.756	±	63.165
801.65	PG_18:2/20:0	26.710	±	3.314	30.966	±	7.624	26.572	±	16.027
799.65	PG_18:2/20:1	30.655	±	5.729	80.751	±	48.637	4.405	±	2.919
797.65	PG_18:2/20:2	36.128	±	10.079	116.193	±	52.363	21.886	±	6.372
795.65	PG_18:2/20:3	24.236	±	5.008	79.374	±	21.402	22.910	±	15.618
791.64	PG_18:2/20:5	64.172	±	13.306	149.029	±	64.026	80.082	±	63.636
829.68	PG_18:2/22:0	46.678	±	4.729	64.356	±	11.457	35.389	±	14.736
827.68	PG_18:2/22:1	40.300	±	15.524	28.358	±	8.108	18.427	±	8.888
825.68	PG_18:2/22:2	26.775	±	7.561	39.078	±	22.104	71.469	±	48.184
823.67	PG_18:2/22:3	73.098	±	16.354	38.955	±	8.278	34.607	±	19.385
821.67	PG_18:2/22:4	83.407	±	7.800	201.816	±	76.181	59.784	±	18.806
819.67	PG_18:2/22:5	89.828	±	13.827	238.141	±	98.592	269.478	±	148.306
765.62	PG_18:3/18:3	237.755	±	45.422	243.967	±	117.424	102.771	±	34.994
799.65	PG_18:3/20:0	75.336	±	7.188	148.896	±	88.265	22.755	±	7.863
797.65	PG_18:3/20:1	118.966	±	24.260	250.996	±	106.280	43.701	±	17.084
795.65	PG_18:3/20:2	87.133	±	15.455	259.462	±	103.884	75.129	±	48.206
793.64	PG_18:3/20:3	70.916	±	5.530	129.931	±	59.154	68.791	±	27.318
791.64	PG_18:3/20:4	171.326	±	46.236	392.585	±	175.437	143.460	±	95.918
789.64	PG_18:3/20:5	300.353	±	117.279	468.542	±	215.526	99.400	±	27.347
827.68	PG_18:3/22:0	321.696	±	131.098	230.800	±	46.700	208.274	±	70.441
825.68	PG_18:3/22:1	114.358	±	13.009	185.574	±	93.297	198.505	±	83.254
823.67	PG_18:3/22:2	126.722	±	33.012	49.560	±	20.568	49.321	±	28.585
821.67	PG_18:3/22:3	119.207	±	29.828	228.415	±	89.472	64.306	±	30.623
819.67	PG_18:3/22:4	222.012	±	10.857	564.789	±	205.709	409.170	±	154.913
817.67	PG_18:3/22:5	541.531	±	169.568	520.875	±	117.624	258.842	±	64.907
815.67	PG_18:3/22:6	664.682	±	29.766	981.056	±	281.667	407.092	±	75.719

831.68	PG_20:0/20:1	5.464	±	1.735	8.126	±	4.203	1.090	±	1.090
829.68	PG_20:0/20:2	0.213	±	0.151	3.889	±	2.624	1.475	±	1.475
827.68	PG_20:0/20:3	7.143	±	2.102	10.105	±	3.270	N.D.	±	N.D.
825.68	PG_20:0/20:4	4.778	±	1.786	8.572	±	2.814	1.230	±	1.230
823.67	PG_20:0/20:5	6.731	±	2.138	3.587	±	2.304	1.411	±	1.411
861.71	PG_20:0/22:0	0.358	±	0.298	N.D.	±	N.D.	N.D.	±	N.D.
859.71	PG_20:0/22:1	0.729	±	0.666	N.D.	±	N.D.	N.D.	±	N.D.
857.71	PG_20:0/22:2	0.720	±	0.657	N.D.	±	N.D.	N.D.	±	N.D.
855.71	PG_20:0/22:3	0.295	±	0.269	N.D.	±	N.D.	N.D.	±	N.D.
853.70	PG_20:0/22:4	1.572	±	0.883	1.419	±	1.419	N.D.	±	N.D.
851.70	PG_20:0/22:5	3.886	±	1.518	2.841	±	1.899	N.D.	±	N.D.
849.70	PG_20:0/22:6	4.941	±	2.170	2.513	±	2.513	5.996	±	5.996
829.68	PG_20:1/20:1	4.623	±	1.946	5.171	±	3.427	N.D.	±	N.D.
827.68	PG_20:1/20:2	6.638	±	1.383	6.085	±	4.982	34.034	±	33.485
825.68	PG_20:1/20:3	5.709	±	1.590	11.796	±	6.561	38.739	±	32.665
823.67	PG_20:1/20:4	7.046	±	2.656	16.365	±	8.285	9.294	±	5.521
821.67	PG_20:1/20:5	6.474	±	2.408	16.804	±	7.766	7.359	±	4.282
859.71	PG_20:1/22:0	1.758	±	1.279	3.830	±	2.748	3.406	±	2.154
857.71	PG_20:1/22:1	2.232	±	1.355	6.120	±	2.366	N.D.	±	N.D.
855.71	PG_20:1/22:2	0.968	±	0.884	3.136	±	3.136	N.D.	±	N.D.
853.70	PG_20:1/22:3	3.181	±	1.703	4.187	±	3.350	2.957	±	1.871
851.70	PG_20:1/22:4	2.281	±	0.793	7.898	±	3.061	1.786	±	1.786
849.70	PG_20:1/22:5	1.214	±	0.699	3.900	±	3.900	6.978	±	5.089
847.70	PG_20:1/22:6	13.553	±	4.371	26.699	±	14.958	6.045	±	5.987
823.67	PG_20:2/20:3	5.658	±	2.687	2.534	±	2.534	9.813	±	6.846
821.67	PG_20:2/20:4	5.642	±	1.513	14.297	±	6.220	3.084	±	1.961
819.67	PG_20:2/20:5	6.743	±	2.245	19.034	±	5.733	0.201	±	0.201
857.71	PG_20:2/22:0	0.955	±	0.871	0.788	±	0.788	N.D.	±	N.D.
855.71	PG_20:2/22:1	1.478	±	0.800	N.D.	±	N.D.	24.212	±	24.212
853.70	PG_20:2/22:2	2.406	±	0.907	0.635	±	0.635	4.088	±	4.088
851.70	PG_20:2/22:3	3.043	±	1.173	1.432	±	1.432	0.450	±	0.450
849.70	PG_20:2/22:4	1.134	±	1.035	N.D.	±	N.D.	2.890	±	1.944
847.70	PG_20:2/22:5	2.866	±	1.118	7.915	±	5.348	N.D.	±	N.D.
845.70	PG_20:2/22:6	5.719	±	2.001	9.382	±	7.024	5.439	±	4.167
821.67	PG_20:3/20:3	2.561	±	2.338	2.451	±	2.451	0.793	±	0.793
819.67	PG_20:3/20:4	4.741	±	1.544	14.833	±	4.405	13.827	±	6.911
817.67	PG_20:3/20:5	10.209	±	2.051	10.071	±	4.343	7.549	±	5.779
855.71	PG_20:3/22:0	5.218	±	1.682	4.711	±	4.711	3.399	±	3.399
845.70	PG_20:3/22:5	3.672	±	2.321	16.520	±	8.276	N.D.	±	N.D.
815.67	PG_20:4/20:5	11.716	±	4.519	32.913	±	6.867	10.755	±	5.581
853.70	PG_20:4/22:0	13.482	±	2.735	21.865	±	7.315	25.440	±	8.867
851.70	PG_20:4/22:1	8.501	±	2.793	10.956	±	2.700	7.162	±	3.541
849.70	PG_20:4/22:2	1.726	±	1.418	5.942	±	4.037	2.681	±	1.703
847.70	PG_20:4/22:3	3.140	±	1.195	20.101	±	6.054	2.334	±	2.334
845.70	PG_20:4/22:4	18.675	±	3.848	29.476	±	14.706	7.502	±	5.883
843.69	PG_20:4/22:5	17.552	±	3.237	51.754	±	22.557	19.604	±	17.142
813.66	PG_20:5/20:5	7.955	±	2.455	9.421	±	1.961	19.553	±	8.496
851.70	PG_20:5/22:0	13.740	±	5.273	15.661	±	4.781	13.388	±	12.118

849.70	PG_20:5/22:1	11.098	±	4.366	5.960	±	5.960	11.787	±	10.773
847.70	PG_20:5/22:2	2.195	±	1.244	9.043	±	4.054	1.958	±	1.430
845.70	PG_20:5/22:3	4.047	±	1.298	14.228	±	7.935	2.805	±	1.781
843.69	PG_20:5/22:4	7.134	±	1.351	38.297	±	14.646	16.996	±	16.996
841.69	PG_20:5/22:5	22.785	±	3.139	38.404	±	19.234	13.036	±	6.924
839.69	PG_20:5/22:6	55.487	±	17.328	52.692	±	28.165	35.944	±	25.040
889.74	PG_22:0/22:0	2.152	±	1.284	1.854	±	1.854	N.D.	±	N.D.
887.74	PG_22:0/22:1	1.102	±	1.006	N.D.	±	N.D.	N.D.	±	N.D.
885.74	PG_22:0/22:2	0.974	±	0.889	0.633	±	0.633	N.D.	±	N.D.
879.73	PG_22:0/22:5	0.735	±	0.671	N.D.	±	N.D.	N.D.	±	N.D.
877.73	PG_22:0/22:6	0.987	±	0.901	N.D.	±	N.D.	1.059	±	1.059
885.74	PG_22:1/22:1	N.D.	±	N.D.	N.D.	±	N.D.	3.871	±	3.871
883.73	PG_22:1/22:2	1.944	±	1.166	1.099	±	1.099	N.D.	±	N.D.
881.73	PG_22:1/22:3	0.707	±	0.645	1.759	±	1.144	N.D.	±	N.D.
877.73	PG_22:1/22:5	N.D.	±	N.D.	0.959	±	0.855	N.D.	±	N.D.
879.73	PG_22:2/22:3	N.D.	±	N.D.	N.D.	±	N.D.	2.874	±	2.874
875.73	PG_22:2/22:5	N.D.	±	N.D.	N.D.	±	N.D.	1.742	±	1.742
873.72	PG_22:2/22:6	N.D.	±	N.D.	0.044	±	0.044	N.D.	±	N.D.
873.72	PG_22:4/22:4	0.447	±	0.408	N.D.	±	N.D.	N.D.	±	N.D.
869.72	PG_22:4/22:6	0.765	±	0.698	1.448	±	1.448	N.D.	±	N.D.
869.72	PG_22:5/22:5	1.975	±	1.803	N.D.	±	N.D.	N.D.	±	N.D.
867.72	PG_22:5/22:6	0.166	±	0.152	1.367	±	1.367	5.348	±	5.348
865.72	PG_22:6/22:6	4.242	±	1.636	N.D.	±	N.D.	1.469	±	1.469
679.53	PG_a16:0/14:0	279.468	±	85.980	125.971	±	18.943	73.309	±	23.936
707.56	PG_a16:0/16:0	26.886	±	11.896	12.008	±	3.935	10.003	±	7.288
735.59	PG_a16:0/18:0	10.647	±	4.789	23.404	±	12.074	23.299	±	14.239
755.61	PG_a16:0/20:4	3.899	±	2.758	2.583	±	2.395	N.D.	±	N.D.
707.56	PG_a18:0/14:0	2.307	±	1.303	1.892	±	1.892	N.D.	±	N.D.
735.59	PG_a18:0/16:0	41.694	±	12.657	47.133	±	27.969	47.977	±	25.978
763.61	PG_a18:0/18:0	16.841	±	2.165	9.912	±	5.189	20.209	±	15.795
783.63	PG_a18:0/20:4	0.995	±	0.629	0.885	±	0.885	N.D.	±	N.D.
819.67	PG_a18:0/22:0	0.948	±	0.866	N.D.	±	N.D.	N.D.	±	N.D.
735.59	PG_a20:0/14:0	72.832	±	22.209	84.655	±	44.923	214.586	±	99.158
763.61	PG_a20:0/16:0	65.779	±	8.722	58.429	±	17.133	90.449	±	31.581
791.64	PG_a20:0/18:0	35.300	±	3.471	94.667	±	34.492	38.456	±	21.100
819.67	PG_a20:0/20:0	1.111	±	1.014	1.806	±	1.806	0.284	±	0.284
811.66	PG_a20:0/20:4	2.135	±	1.088	6.409	±	4.053	1.568	±	1.568
847.70	PG_a20:0/22:0	1.024	±	0.935	N.D.	±	N.D.	N.D.	±	N.D.
835.69	PG_a20:0/22:6	1.505	±	0.843	1.078	±	1.078	N.D.	±	N.D.
677.53	PG_p16:0/14:0	167.129	±	30.365	180.704	±	23.653	148.351	±	32.850
705.56	PG_p16:0/16:0	12.484	±	1.225	13.150	±	4.881	5.668	±	4.112
703.55	PG_p16:0/16:1	15.572	±	1.248	14.686	±	6.228	35.755	±	24.042
733.58	PG_p16:0/18:0	23.468	±	6.873	11.003	±	6.497	13.677	±	9.825
731.58	PG_p16:0/18:1	6.324	±	1.644	3.443	±	1.998	1.753	±	1.540
729.58	PG_p16:0/18:2	25.274	±	11.587	13.605	±	7.014	1.623	±	1.149
727.58	PG_p16:0/18:3	58.262	±	24.537	109.154	±	52.276	6.778	±	3.998
761.61	PG_p16:0/20:0	1.167	±	1.065	N.D.	±	N.D.	0.159	±	0.159
759.61	PG_p16:0/20:1	0.251	±	0.229	N.D.	±	N.D.	N.D.	±	N.D.

757.61	PG_p16:0/20:2	N.D.	±	N.D.	N.D.	±	N.D.	0.190	±	0.190
755.61	PG_p16:0/20:3	0.311	±	0.284	N.D.	±	N.D.	0.088	±	0.088
753.60	PG_p16:0/20:4	7.052	±	2.463	2.089	±	2.089	0.190	±	0.190
751.60	PG_p16:0/20:5	1.807	±	1.650	1.083	±	0.676	1.450	±	1.450
789.64	PG_p16:0/22:0	0.141	±	0.129	N.D.	±	N.D.	N.D.	±	N.D.
787.64	PG_p16:0/22:1	0.917	±	0.837	N.D.	±	N.D.	N.D.	±	N.D.
783.63	PG_p16:0/22:3	0.455	±	0.416	N.D.	±	N.D.	N.D.	±	N.D.
779.63	PG_p16:0/22:5	N.D.	±	N.D.	0.336	±	0.336	N.D.	±	N.D.
705.56	PG_p18:0/14:0	4.255	±	1.863	1.281	±	1.281	N.D.	±	N.D.
733.58	PG_p18:0/16:0	40.130	±	15.021	27.785	±	15.169	82.835	±	24.087
731.58	PG_p18:0/16:1	30.741	±	8.740	89.969	±	42.757	76.546	±	42.529
761.61	PG_p18:0/18:0	18.591	±	5.585	29.985	±	3.798	67.926	±	35.521
759.61	PG_p18:0/18:1	34.274	±	7.497	52.009	±	15.270	39.226	±	23.316
757.61	PG_p18:0/18:2	20.271	±	5.680	6.792	±	2.221	12.188	±	7.124
755.61	PG_p18:0/18:3	43.605	±	12.102	15.286	±	3.499	6.150	±	3.305
789.64	PG_p18:0/20:0	0.262	±	0.239	0.718	±	0.718	N.D.	±	N.D.
787.64	PG_p18:0/20:1	2.290	±	2.091	1.820	±	1.820	N.D.	±	N.D.
785.64	PG_p18:0/20:2	N.D.	±	N.D.	N.D.	±	N.D.	1.383	±	1.383
783.63	PG_p18:0/20:3	N.D.	±	N.D.	2.659	±	2.659	13.350	±	6.005
781.63	PG_p18:0/20:4	3.030	±	0.915	1.759	±	1.473	1.602	±	1.602
779.63	PG_p18:0/20:5	2.546	±	0.886	2.919	±	2.000	2.305	±	2.305
817.67	PG_p18:0/22:0	0.750	±	0.685	N.D.	±	N.D.	N.D.	±	N.D.
815.67	PG_p18:0/22:1	N.D.	±	N.D.	N.D.	±	N.D.	0.198	±	0.198
811.66	PG_p18:0/22:3	1.147	±	0.673	2.792	±	1.850	N.D.	±	N.D.
809.66	PG_p18:0/22:4	N.D.	±	N.D.	2.698	±	2.698	N.D.	±	N.D.
807.66	PG_p18:0/22:5	0.633	±	0.578	N.D.	±	N.D.	0.392	±	0.392
805.66	PG_p18:0/22:6	N.D.	±	N.D.	N.D.	±	N.D.	58.119	±	55.159
733.58	PG_p20:0/14:0	102.056	±	33.327	71.761	±	28.317	531.075	±	255.465
761.61	PG_p20:0/16:0	47.188	±	8.538	49.802	±	23.380	64.993	±	35.446
759.61	PG_p20:0/16:1	23.670	±	6.443	46.328	±	23.209	59.635	±	32.984
789.64	PG_p20:0/18:0	43.394	±	19.031	104.178	±	41.222	35.110	±	12.602
787.64	PG_p20:0/18:1	97.109	±	42.929	113.405	±	30.143	66.431	±	21.075
785.64	PG_p20:0/18:2	19.902	±	3.552	45.626	±	11.990	15.469	±	7.610
783.63	PG_p20:0/18:3	81.838	±	19.920	55.243	±	19.941	36.677	±	17.881
817.67	PG_p20:0/20:0	0.665	±	0.607	N.D.	±	N.D.	N.D.	±	N.D.
815.67	PG_p20:0/20:1	1.198	±	1.094	5.013	±	2.266	1.763	±	1.384
813.66	PG_p20:0/20:2	2.047	±	1.151	N.D.	±	N.D.	2.862	±	2.862
811.66	PG_p20:0/20:3	2.333	±	1.426	9.347	±	6.325	18.187	±	16.984
809.66	PG_p20:0/20:4	1.882	±	0.885	8.245	±	2.877	39.179	±	32.658
807.66	PG_p20:0/20:5	1.670	±	1.524	9.845	±	4.488	N.D.	±	N.D.
845.70	PG_p20:0/22:0	N.D.	±	N.D.	2.753	±	2.753	N.D.	±	N.D.
843.69	PG_p20:0/22:1	0.750	±	0.685	4.549	±	2.917	1.965	±	1.965
839.69	PG_p20:0/22:3	N.D.	±	N.D.	0.616	±	0.616	N.D.	±	N.D.
837.69	PG_p20:0/22:4	N.D.	±	N.D.	3.236	±	2.115	9.869	±	6.996
835.69	PG_p20:0/22:5	N.D.	±	N.D.	0.691	±	0.691	0.402	±	0.402
833.68	PG_p20:0/22:6	0.828	±	0.756	N.D.	±	N.D.	1.714	±	1.714

Supplementary Table 13: Concentrations (in pmol/mg protein) of phosphatidylinositols (PI) and lysophosphatidylinositols (LPI) in *Artemia* cysts, Percoll-purified mitochondria and mitoplasts. N.D.: not determined. p(carbon:double bond) indicates a plasmalogen species. a(carbon:double bond) indicates an alkylenyl species. Results shown are Mean +/- S.E.

[M-H]$^-$	**Species**	**Artemia Cysts**			**Mitochondria**			**Mitoplasts**		
487.34	LPI_10:0	N.D.	±	N.D.	N.D.	±	N.D.	1.261	±	1.261
515.37	LPI_12:0	N.D.	±	N.D.	N.D.	±	N.D.	0.937	±	0.937
543.39	LPI_14:0	1.086	±	0.700	N.D.	±	N.D.	N.D.	±	N.D.
569.42	LPI_16:1	0.479	±	0.479	N.D.	±	N.D.	2.791	±	2.224
571.42	LPI_16:0	1.460	±	0.924	15.547	±	3.702	9.439	±	4.844
593.44	LPI_18:3	2.739	±	1.354	3.336	±	2.328	0.999	±	0.999
597.45	LPI_18:1	4.103	±	2.076	4.162	±	4.162	1.367	±	1.367
599.45	LPI_18:0	5.273	±	1.798	11.423	±	6.960	0.959	±	0.669
611.46	LPI_p20:0	0.514	±	0.514	3.151	±	1.787	31.053	±	29.074
617.47	LPI_20:5	1.153	±	0.730	0.034	±	0.034	N.D.	±	N.D.
619.47	LPI_20:4	0.059	±	0.059	N.D.	±	N.D.	0.649	±	0.649
621.47	LPI_20:3	0.163	±	0.163	2.644	±	2.644	N.D.	±	N.D.
625.48	LPI_20:1	0.324	±	0.324	1.493	±	1.493	N.D.	±	N.D.
643.49	LPI_22:6	0.141	±	0.141	N.D.	±	N.D.	N.D.	±	N.D.
647.50	LPI_22:4	N.D.	±	N.D.	1.217	±	1.217	N.D.	±	N.D.
655.51	LPI_22:0	N.D.	±	N.D.	1.525	±	1.525	N.D.	±	N.D.
753.60	PI_14:0/14:0	5.857	±	2.306	8.466	±	4.117	2.664	±	2.454
779.63	PI_14:0/16:1	20.165	±	5.423	40.883	±	14.078	26.655	±	13.522
781.63	PI_14:0/16:0	39.114	±	4.994	54.027	±	14.019	28.571	±	12.835
805.66	PI_14:0/18:2	35.260	±	7.162	185.753	±	95.961	138.204	±	42.953
805.66	PI_16:1/16:1	34.385	±	4.030	154.043	±	97.732	83.336	±	43.469
807.66	PI_14:0/18:1	160.483	±	40.109	292.793	±	123.748	176.721	±	41.384
807.66	PI_16:0/16:1	103.398	±	25.612	141.701	±	41.653	144.390	±	52.618
809.66	PI_14:0/18:0	44.081	±	9.551	81.959	±	34.598	54.290	±	28.971
809.66	PI_16:0/16:0	83.591	±	20.460	103.524	±	37.756	107.916	±	35.242
831.68	PI_14:0/20:3	16.963	±	7.704	8.741	±	4.475	3.590	±	2.790
831.68	PI_16:0/18:3	390.137	±	151.759	206.613	±	27.156	87.654	±	34.278
831.68	PI_16:1/18:2	78.361	±	37.414	64.254	±	18.297	25.359	±	11.946
833.68	PI_14:0/20:2	16.985	±	4.369	7.051	±	3.734	0.427	±	0.427
833.68	PI_16:1/18:1	587.243	±	188.441	385.404	±	55.271	359.283	±	67.215
833.68	PI_16:0/18:2	163.688	±	29.483	105.085	±	20.310	37.886	±	14.077
835.69	PI_14:0/20:1	11.357	±	2.861	10.992	±	5.670	5.583	±	2.955
835.69	PI_16:1/18:0	191.509	±	43.225	250.381	±	12.708	148.577	±	48.100
835.69	PI_16:0/18:1	181.294	±	47.090	164.338	±	21.620	93.995	±	20.754
837.69	PI_14:0/20:0	7.410	±	2.517	7.260	±	4.028	6.970	±	6.970
837.69	PI_16:0/18:0	173.437	±	62.694	101.920	±	35.877	91.178	±	42.763
849.70	PI_p16:0/20:0	3.995	±	2.046	2.438	±	2.438	5.817	±	5.817
849.70	PI_p18:0/18:0	33.515	±	6.877	50.164	±	18.763	56.333	±	35.503
849.70	PI_p20:0/16:0	115.971	±	22.567	95.616	±	31.319	84.302	±	23.626
857.71	PI_14:0/22:4	10.634	±	3.495	6.394	±	4.930	7.113	±	7.113
857.71	PI_16:1/20:3	35.023	±	8.302	23.810	±	3.142	10.133	±	4.747
857.71	PI_16:0/20:4	71.539	±	8.046	59.817	±	10.439	11.831	±	5.780

857.71	PI_18:1/18:3	1269.157	±	160.032	1077.320	±	128.153	408.784	±	103.737
857.71	PI_18:2/18:2	30.992	±	2.490	16.679	±	7.831	13.713	±	6.872
859.71	PI_14:0/22:3	18.524	±	2.159	3.807	±	2.408	4.418	±	1.995
859.71	PI_16:1/20:2	57.232	±	11.958	50.137	±	26.025	32.177	±	16.160
859.71	PI_16:0/20:3	102.419	±	7.086	82.267	±	39.874	46.275	±	13.053
859.71	PI_18:0/18:3	1262.904	±	315.096	1221.203	±	470.388	699.263	±	96.766
859.71	PI_18:1/18:2	454.049	±	107.865	442.223	±	156.096	220.952	±	50.678
861.71	PI_14:0/22:2	4.569	±	2.319	7.342	±	3.431	3.780	±	2.420
861.71	PI_16:1/20:1	46.929	±	16.309	70.486	±	19.565	39.418	±	15.745
861.71	PI_16:0/20:2	103.419	±	9.766	64.761	±	25.910	42.914	±	13.559
861.71	PI_18:0/18:2	422.269	±	109.858	464.293	±	165.042	312.094	±	66.291
861.71	PI_18:1/18:1	341.997	±	90.196	341.979	±	138.058	201.504	±	55.921
863.71	PI_14:0/22:1	10.874	±	1.500	9.181	±	3.810	13.537	±	8.430
863.71	PI_16:1/20:0	32.574	±	7.460	22.238	±	8.493	6.467	±	3.829
863.71	PI_16:0/20:1	102.327	±	20.865	77.603	±	18.263	22.737	±	11.564
863.71	PI_18:0/18:1	490.916	±	141.196	335.487	±	93.687	207.553	±	56.666
865.72	PI_14:0/22:0	4.756	±	1.714	6.117	±	3.098	6.353	±	3.638
865.72	PI_16:0/20:0	58.969	±	10.131	29.690	±	5.244	36.577	±	17.759
865.72	PI_18:0/18:0	165.005	±	50.122	132.879	±	61.036	82.360	±	34.783
865.72	PI_p16:0/22:6	3.430	±	1.577	N.D.	±	N.D.	1.426	±	1.426
871.72	PI_p16:0/22:3	N.D.	±	N.D.	N.D.	±	N.D.	N.D.	±	N.D.
871.72	PI_p18:0/20:3	2.679	±	2.196	1.924	±	1.228	4.019	±	1.875
871.72	PI_p20:0/18:3	102.526	±	21.173	65.176	±	10.490	25.551	±	11.084
871.72	PI_a18:0/20:4	3.584	±	1.748	11.687	±	5.664	2.788	±	2.093
873.72	PI_p16:0/22:2	N.D.	±	N.D.	0.043	±	0.043	N.D.	±	N.D.
873.72	PI_p18:0/20:2	3.474	±	1.923	N.D.	±	N.D.	100.739	±	90.273
873.72	PI_p20:0/18:2	44.621	±	10.698	35.558	±	11.661	19.596	±	11.080
883.73	PI_16:1/22:4	128.736	±	15.711	149.231	±	12.892	155.979	±	65.850
883.73	PI_16:0/22:5	98.903	±	10.818	16.454	±	6.440	27.233	±	9.986
883.73	PI_18:1/20:4	300.643	±	73.497	149.651	±	10.841	175.321	±	43.577
883.73	PI_18:0/20:5	80.832	±	18.033	59.309	±	7.724	33.940	±	17.218
883.73	PI_18:2/20:3	55.777	±	12.363	13.495	±	4.197	15.451	±	7.488
883.73	PI_18:3/20:2	147.314	±	23.692	27.391	±	5.173	97.145	±	59.243
885.74	PI_16:1/22:3	86.551	±	6.864	103.598	±	26.377	63.252	±	16.504
885.74	PI_16:0/22:4	101.215	±	7.223	59.101	±	14.066	24.485	±	13.173
885.74	PI_18:1/20:3	215.211	±	21.302	169.429	±	32.809	111.650	±	60.730
885.74	PI_18:0/20:4	197.163	±	65.383	198.914	±	49.020	78.750	±	30.126
885.74	PI_18:2/20:2	38.089	±	5.273	22.227	±	9.887	26.434	±	16.663
885.74	PI_18:3/20:1	237.170	±	44.840	214.173	±	41.271	137.305	±	55.254
887.74	PI_16:1/22:2	26.445	±	4.232	27.525	±	8.789	15.861	±	7.241
887.74	PI_16:0/22:3	86.774	±	13.088	53.176	±	4.098	36.318	±	17.447
887.74	PI_18:1/20:2	121.156	±	11.331	79.626	±	15.026	46.428	±	26.798
887.74	PI_18:0/20:3	59.833	±	8.247	52.633	±	14.610	51.354	±	32.620
887.74	PI_18:2/20:1	49.898	±	11.664	56.706	±	10.003	44.198	±	31.189
887.74	PI_18:3/20:0	102.057	±	4.841	58.609	±	6.435	41.241	±	30.315
889.74	PI_16:1/22:1	31.961	±	10.640	15.326	±	6.140	12.244	±	5.319
889.74	PI_16:0/22:2	60.040	±	8.384	32.225	±	9.295	42.614	±	14.365
889.74	PI_18:1/20:1	151.860	±	42.067	143.763	±	28.526	165.820	±	110.020

889.74	PI_18:0/20:2	73.476	±	18.510	58.081	±	14.341	39.707	±	20.508
889.74	PI_18:2/20:0	46.829	±	15.919	26.619	±	9.686	22.793	±	17.247
891.74	PI_16:1/22:0	82.335	±	25.819	101.529	±	19.408	63.790	±	22.373
891.74	PI_16:0/22:1	87.350	±	21.042	147.247	±	31.568	273.494	±	104.259
891.74	PI_18:1/20:0	100.104	±	18.804	119.024	±	49.579	34.871	±	17.517
891.74	PI_18:0/20:1	56.795	±	11.147	62.520	±	10.685	16.006	±	5.652
893.74	PI_16:0/22:0	52.814	±	18.456	44.365	±	6.814	26.661	±	12.228
893.74	PI_18:0/20:0	28.602	±	9.648	39.274	±	8.554	17.424	±	6.826
893.74	PI_p18:0/22:6	1.010	±	1.010	1.982	±	1.982	N.D.	±	N.D.
911.76	PI_18:3/22:2	109.047	±	4.000	38.561	±	11.118	16.343	±	6.256
911.76	PI_18:2/22:3	45.907	±	7.052	28.936	±	2.233	1.519	±	0.972
911.76	PI_18:1/22:4	197.573	±	15.508	86.233	±	20.660	37.676	±	23.432
911.76	PI_18:0/22:5	17.545	±	2.666	22.034	±	8.083	1.199	±	1.157
911.76	PI_20:0/20:5	8.908	±	2.309	6.130	±	3.143	N.D.	±	N.D.
911.76	PI_20:1/20:4	31.519	±	4.690	24.534	±	9.073	4.927	±	1.765
911.76	PI_20:2/20:3	8.341	±	3.327	13.247	±	7.772	0.209	±	0.209
913.76	PI_18:3/22:1	87.415	±	15.368	37.712	±	9.253	21.690	±	8.856
913.76	PI_18:2/22:2	39.783	±	9.295	15.239	±	8.878	8.908	±	4.278
913.76	PI_18:1/22:3	159.296	±	17.413	66.759	±	13.884	48.485	±	20.868
913.76	PI_18:0/22:4	35.260	±	1.897	25.670	±	11.048	11.104	±	6.319
913.76	PI_20:0/20:4	6.437	±	2.312	11.278	±	6.031	6.660	±	4.219
913.76	PI_20:1/20:3	16.422	±	2.423	4.560	±	2.126	1.349	±	1.238
913.76	PI_20:2/20:2	1.590	±	1.590	0.512	±	0.512	N.D.	±	N.D.
915.77	PI_18:3/22:0	52.946	±	4.310	88.933	±	40.094	100.917	±	61.671
915.77	PI_18:2/22:1	20.068	±	3.192	38.540	±	13.842	8.855	±	4.033
915.77	PI_18:1/22:2	100.010	±	10.007	137.392	±	48.843	23.377	±	10.254
915.77	PI_18:0/22:3	42.688	±	5.371	43.188	±	21.085	15.254	±	6.130
915.77	PI_20:0/20:3	4.460	±	1.394	3.676	±	3.676	N.D.	±	N.D.
915.77	PI_20:1/20:2	3.681	±	1.329	2.586	±	2.586	36.059	±	34.343
917.77	PI_18:2/22:0	16.691	±	2.781	21.522	±	10.173	38.183	±	33.973
917.77	PI_18:1/22:1	106.590	±	22.997	135.009	±	51.213	95.056	±	30.976
917.77	PI_18:0/22:2	39.152	±	5.953	64.344	±	35.229	29.283	±	12.204
917.77	PI_20:0/20:2	2.324	±	1.565	5.705	±	5.150	0.886	±	0.886
917.77	PI_20:1/20:1	0.633	±	0.601	5.200	±	2.381	N.D.	±	N.D.
931.78	PI__20:3/22:6	8.684	±	2.126	6.045	±	3.160	N.D.	±	N.D.
931.78	PI_20:4/22:5	2.830	±	1.945	1.612	±	1.612	N.D.	±	N.D.
931.78	PI_20:5/22:4	2.387	±	1.157	7.964	±	3.905	N.D.	±	N.D.
931.78	PI_p20:0/22:1	1.559	±	1.324	1.462	±	1.462	N.D.	±	N.D.
941.79	PI_20:0/22:4	N.D.	±	N.D.	1.435	±	1.435	N.D.	±	N.D.
941.79	PI_20:1/22:3	0.993	±	0.639	2.320	±	1.488	N.D.	±	N.D.
941.79	PI_20:2/22:2	1.169	±	0.801	N.D.	±	N.D.	N.D.	±	N.D.
941.79	PI__20:3/22:1	3.429	±	1.815	2.687	±	2.687	2.808	±	1.984
941.79	PI_20:4/22:0	2.310	±	1.071	5.471	±	1.926	1.683	±	1.683
943.79	PI_20:0/22:3	0.644	±	0.644	N.D.	±	N.D.	N.D.	±	N.D.
943.79	PI_20:1/22:2	5.147	±	2.217	N.D.	±	N.D.	N.D.	±	N.D.
943.79	PI_20:2/22:1	1.763	±	1.151	N.D.	±	N.D.	N.D.	±	N.D.
943.79	PI_20:3/22:0	3.063	±	1.521	N.D.	±	N.D.	6.179	±	6.179

Supplementary Table 14: Concentrations (in pmol/mg protein) of phosphatidylserines (PS) and lysophosphatidylserines (LPS) in *Artemia* cysts, Percoll-purified mitochondria and mitoplasts. N.D.: not determined. p(carbon:double bond) indicates a plasmalogen species. a(carbon:double bond) indicates an alkylenyl species. Results shown are Mean +/- S.E.

$[M\text{-}H]^-$	**Species**		**Artemia Cysts**			**Mitochondria**			**Mitoplasts**	
440.29	LPS_12:0	N.D.	±	N.D.	7.618	±	7.618	N.D.	±	N.D.
468.32	LPS_14:0	35.190	±	28.810	58.816	±	22.067	18.548	±	18.548
494.34	LPS_16:1	4.939	±	3.227	20.383	±	19.036	81.892	±	52.298
496.35	LPS_16:0	58.463	±	19.251	35.511	±	27.957	57.413	±	41.863
518.37	LPS_18:3	32.001	±	23.971	2.414	±	2.414	N.D.	±	N.D.
520.37	LPS_18:2	15.667	±	15.153	16.081	±	16.081	N.D.	±	N.D.
522.37	LPS_18:1	33.970	±	16.215	48.473	±	29.641	53.621	±	26.238
524.37	LPS_18:0	36.256	±	23.271	253.099	±	90.158	24.511	±	17.261
542.39	LPS_20:5	5.988	±	3.841	N.D.	±	N.D.	N.D.	±	N.D.
544.39	LPS_20:4	16.376	±	15.420	13.597	±	8.819	37.775	±	24.265
552.40	LPS_20:0	15.562	±	15.562	6.999	±	6.999	21.626	±	21.626
578.43	LPS_22:1	N.D.	±	N.D.	11.492	±	11.492	1.419	±	1.419
580.43	LPS_22:0	14.878	±	14.878	N.D.	±	N.D.	N.D.	±	N.D.
606.46	LPS_24:1	8.189	±	8.189	N.D.	±	N.D.	N.D.	±	N.D.
608.46	LPS_24:0	4.381	±	4.381	N.D.	±	N.D.	20.631	±	20.631
650.50	PS_12:0/14:0	98.621	±	60.617	46.952	±	22.063	70.776	±	41.771
730.58	PS_14:0/18:2	79.628	±	16.793	24.987	±	12.277	388.505	±	214.946
730.58	PS_16:1/16:1	1873.378	±	578.019	1840.430	±	149.845	8881.254	±	4509.601
732.58	PS_14:0/18:1	172.572	±	73.371	220.905	±	62.467	449.016	±	179.739
732.58	PS_16:0/16:1	324.243	±	92.700	327.401	±	96.854	1729.558	±	433.701
734.58	PS_16:0/16:0	166.136	±	57.716	245.495	±	107.458	396.362	±	214.557
758.61	PS_14:0/20:2	64.792	±	25.152	97.472	±	69.707	120.706	±	42.486
758.61	PS_16:1/18:1	538.884	±	118.331	657.494	±	178.832	1716.357	±	1079.955
758.61	PS_16:0/18:2	462.402	±	95.235	403.486	±	189.247	1049.421	±	736.108
760.61	PS_14:0/20:1	32.162	±	23.347	75.385	±	27.742	17.400	±	17.400
760.61	PS_16:0/18:1	676.869	±	101.375	695.109	±	173.533	3269.493	±	1263.883
762.61	PS_16:0/18:0	1063.945	±	381.840	439.834	±	88.402	1224.227	±	351.325
776.63	PS_a16:0/20:0	18.390	±	18.390	9.498	±	9.498	N.D.	±	N.D.
776.63	PS_a18:0/18:0	249.845	±	152.958	475.270	±	159.815	211.740	±	80.523
782.63	PS_14:0/22:4	167.738	±	76.494	11.765	±	11.765	75.243	±	38.235
782.63	PS_16:1/20:3	549.324	±	125.954	176.724	±	49.472	223.946	±	126.509
782.63	PS_16:0/20:4	625.525	±	165.009	190.104	±	52.550	577.502	±	317.579
782.63	PS_18:1/18:3	3206.060	±	1325.095	860.679	±	103.338	1298.500	±	745.744
782.63	PS_18:2/18:2	463.220	±	208.114	262.298	±	53.180	558.967	±	301.826
784.63	PS_14:0/22:3	340.669	±	186.767	77.275	±	38.399	157.311	±	75.136
784.63	PS_16:1/20:2	993.504	±	404.339	325.449	±	82.110	1663.197	±	759.216
784.63	PS_16:0/20:3	1537.264	±	757.486	373.166	±	101.127	1208.192	±	495.801
784.63	PS_18:1/18:2	2072.761	±	854.431	1272.330	±	442.902	3587.544	±	1078.122
786.64	PS_16:1/20:1	446.522	±	81.863	295.869	±	49.038	878.682	±	466.867
786.64	PS_16:0/20:2	630.364	±	142.401	247.383	±	48.553	558.107	±	360.294
786.64	PS_18:0/18:2	651.432	±	156.056	434.754	±	49.236	990.753	±	397.217
786.64	PS_18:1/18:1	1055.009	±	196.215	799.532	±	124.069	1035.783	±	370.353
788.64	PS_16:0/20:1	974.880	±	126.070	1062.598	±	202.650	716.174	±	150.777

788.64	PS_18:0/18:1	1449.558	±	173.580	2026.445	±	386.655	2896.658	±	456.555
790.64	PS_18:0/18:0	315.324	±	74.133	685.237	±	135.044	1005.301	±	469.794
790.64	PS_p16:0/22:6	13.721	±	7.130	36.561	±	20.608	284.069	±	222.388
810.66	PS_18:0/20:4	543.837	±	206.380	996.188	±	382.215	1897.056	±	483.993
812.66	PS_16:0/22:3	4302.048	±	1162.322	3472.079	±	1259.119	5911.670	±	2679.791
812.66	PS_18:1/20:2	1153.304	±	269.712	1046.863	±	299.076	1116.288	±	600.709
812.66	PS_18:2/20:1	310.656	±	112.756	359.258	±	106.612	585.946	±	337.771
814.66	PS_18:1/20:1	1614.123	±	150.665	1606.537	±	533.701	3467.313	±	1212.208
814.66	PS_18:2/20:0	1037.448	±	70.469	563.134	±	191.351	1460.901	±	380.424
816.67	PS_18:0/20:1	636.592	±	73.629	576.190	±	92.695	692.215	±	225.844
818.67	PS_p18:0/22:6	26.108	±	19.025	12.253	±	12.253	N.D.	±	N.D.
838.69	PS_18:3/22:1	5820.871	±	1681.410	2326.223	±	813.986	2235.767	±	711.662
838.69	PS_18:1/22:3	8494.654	±	2466.142	5403.340	±	1716.862	6762.831	±	2062.207
838.69	PS_18:0/22:4	239.559	±	78.866	187.774	±	36.647	528.422	±	262.540
838.69	PS_20:1/20:3	106.709	±	40.279	97.342	±	54.191	78.496	±	78.496
838.69	PS_20:2/20:2	6.756	±	3.792	N.D.	±	N.D.	N.D.	±	N.D.
840.69	PS_18:0/22:3	2425.767	±	612.020	4174.169	±	1693.996	2236.657	±	581.706
840.69	PS_20:1/20:2	26.229	±	9.474	79.117	±	48.564	26.618	±	26.618
842.69	PS_20:1/20:1	87.014	±	50.139	113.163	±	66.316	6.388	±	6.388
858.71	PS_20:2/22:6	30.472	±	19.625	32.045	±	20.478	N.D.	±	N.D.
858.71	PS__20:3/22:5	72.358	±	25.332	35.746	±	22.621	N.D.	±	N.D.
858.71	PS_20:4/22:4	69.401	±	26.292	63.040	±	24.048	18.093	±	18.093
858.71	PS_20:5/22:3	31.652	±	26.671	56.529	±	22.956	297.409	±	292.195

Supplementary Table 15: Concentrations (in pmol/mg protein) of sphingomyelins (SM) in *Artemia* cysts, Percoll-purified mitochondria and mitoplasts. N.D.: not determined. Results shown are Mean +/- S.E.

$[M+H]^+$	Species	Artemia Cysts			Mitochondria			Mitoplasts		
649.50	SM_d18:0/12:0	25.289	±	13.284	18.505	±	15.173	11.548	±	9.350
675.53	SM_d18:0/14:1	N.D.	±	N.D.	8.168	±	8.168	N.D.	±	N.D.
705.56	SM_d18:0/16:0	N.D.	±	N.D.	N.D.	±	N.D.	10.107	±	10.107
751.60	SM_d18:0/20:5	11.360	±	7.198	N.D.	±	N.D.	N.D.	±	N.D.
757.61	SM_d18:0/20:2	N.D.	±	N.D.	N.D.	±	N.D.	12.020	±	12.020
777.63	SM_d18:0/22:6	N.D.	±	N.D.	N.D.	±	N.D.	11.383	±	11.383
787.64	SM_d18:0/22:1	21.317	±	15.123	N.D.	±	N.D.	N.D.	±	N.D.
789.64	SM_d18:0/22:0	22.339	±	14.782	12.741	±	12.741	0.996	±	0.996
817.67	SM_d18:0/24:0	7.054	±	7.054	N.D.	±	N.D.	N.D.	±	N.D.
845.70	SM_d18:0/26:0	56.136	±	20.979	N.D.	±	N.D.	N.D.	±	N.D.
673.52	SM_d18:1/14:1	12.875	±	12.875	31.109	±	21.715	18.295	±	18.295
675.53	SM_d18:1/14:0	10.148	±	10.148	N.D.	±	N.D.	N.D.	±	N.D.
701.55	SM_d18:1/16:1	N.D.	±	N.D.	11.838	±	11.838	N.D.	±	N.D.
725.58	SM_d18:1/18:3	14.261	±	14.261	10.027	±	10.027	10.007	±	10.007
727.58	SM_d18:1/18:2	9.497	±	9.497	N.D.	±	N.D.	21.342	±	13.552
729.58	SM_d18:1/18:1	51.333	±	25.454	N.D.	±	N.D.	N.D.	±	N.D.
731.58	SM_d18:1/18:0	25.935	±	17.061	9.015	±	9.015	9.840	±	9.840
749.60	SM_d18:1/20:5	7.309	±	7.309	N.D.	±	N.D.	N.D.	±	N.D.
751.60	SM_d18:1/20:4	N.D.	±	N.D.	11.585	±	11.585	10.530	±	10.530
753.60	SM_d18:1/20:3	10.006	±	10.006	N.D.	±	N.D.	22.731	±	22.731
755.61	SM_d18:1/20:2	10.856	±	10.856	28.088	±	17.928	10.044	±	10.044
757.61	SM_d18:1/20:1	4.872	±	4.872	38.099	±	19.143	16.978	±	16.978
759.61	SM_d18:1/20:0	23.006	±	10.928	N.D.	±	N.D.	10.363	±	10.363
775.63	SM_d18:1/22:6	N.D.	±	N.D.	4.562	±	4.562	N.D.	±	N.D.
777.63	SM_d18:1/22:5	N.D.	±	N.D.	21.500	±	21.500	12.620	±	10.055
779.63	SM_d18:1/22:4	6.796	±	6.796	N.D.	±	N.D.	N.D.	±	N.D.
781.63	SM_d18:1/22:3	N.D.	±	N.D.	25.204	±	15.986	33.377	±	23.406
783.63	SM_d18:1/22:2	5.544	±	5.544	46.125	±	20.846	8.705	±	8.705
785.64	SM_d18:1/22:1	87.691	±	36.674	82.763	±	27.620	36.980	±	22.170
787.64	SM_d18:1/22:0	29.394	±	14.110	13.381	±	13.381	N.D.	±	N.D.
813.66	SM_d18:1/24:1	6.835	±	6.835	36.028	±	17.457	10.460	±	10.460
815.67	SM_d18:1/24:0	40.475	±	27.440	22.683	±	14.385	N.D.	±	N.D.
841.69	SM_d18:1/26:1	N.D.	±	N.D.	19.040	±	15.826	N.D.	±	N.D.
843.69	SM_d18:1/26:0	N.D.	±	N.D.	16.564	±	16.564	N.D.	±	N.D.
645.50	SM_d18:2/12:0	11.167	±	11.167	N.D.	±	N.D.	N.D.	±	N.D.
671.52	SM_d18:2/14:1	2.932	±	2.932	5.912	±	5.912	18.076	±	18.076
673.52	SM_d18:2/14:0	13.894	±	13.894	N.D.	±	N.D.	N.D.	±	N.D.
701.55	SM_d18:2/16:0	13.413	±	10.250	106.008	±	35.632	30.452	±	15.972
723.57	SM_d18:2/18:3	3.353	±	3.353	N.D.	±	N.D.	N.D.	±	N.D.
727.58	SM_d18:2/18:1	10.636	±	10.636	10.027	±	10.027	N.D.	±	N.D.
729.58	SM_d18:2/18:0	N.D.	±	N.D.	7.707	±	7.707	N.D.	±	N.D.
747.60	SM_d18:2/20:5	13.695	±	13.695	N.D.	±	N.D.	N.D.	±	N.D.
749.60	SM_d18:2/20:4	N.D.	±	N.D.	N.D.	±	N.D.	7.750	±	7.750
753.60	SM_d18:2/20:2	13.516	±	13.516	34.985	±	16.463	11.058	±	11.058

755.61	SM_d18:2/20:1	N.D.	±	N.D.	11.358	±	11.358	25.556	±	16.534
757.61	SM_d18:2/20:0	N.D.	±	N.D.	10.235	±	10.235	N.D.	±	N.D.
773.62	SM_d18:2/22:6	N.D.	±	N.D.	15.909	±	15.909	N.D.	±	N.D.
779.63	SM_d18:2/22:3	N.D.	±	N.D.	9.848	±	9.848	N.D.	±	N.D.
781.63	SM_d18:2/22:2	N.D.	±	N.D.	10.547	±	10.547	4.209	±	4.209
783.63	SM_d18:2/22:1	14.855	±	14.855	40.980	±	26.310	N.D.	±	N.D.
785.64	SM_d18:2/22:0	14.855	±	14.855	19.004	±	12.108	10.576	±	10.576
811.66	SM_d18:2/24:1	N.D.	±	N.D.	N.D.	±	N.D.	15.648	±	15.648
839.69	SM_d18:2/26:1	23.391	±	14.800	13.082	±	13.082	N.D.	±	N.D.
841.69	SM_d18:2/26:0	84.411	±	28.798	8.359	±	8.359	N.D.	±	N.D.
647.50	SM_d16:0/14:1	N.D.	±	N.D.	11.496	±	11.496	12.495	±	12.495
753.60	SM_d16:0/22:4	26.084	±	26.084	N.D.	±	N.D.	11.240	±	11.240
757.61	SM_d16:0/22:2	N.D.	±	N.D.	N.D.	±	N.D.	9.703	±	9.703
759.61	SM_d16:0/22:1	8.607	±	8.607	N.D.	±	N.D.	11.383	±	11.383
761.61	SM_d16:0/22:0	N.D.	±	N.D.	N.D.	±	N.D.	14.515	±	14.515
787.64	SM_d16:0/24:1	10.139	±	10.139	N.D.	±	N.D.	N.D.	±	N.D.
817.67	SM_d16:0/26:0	12.886	±	12.886	13.933	±	13.933	N.D.	±	N.D.
619.47	SM_d16:1/12:0	42.639	±	27.285	N.D.	±	N.D.	N.D.	±	N.D.
645.50	SM_d16:1/14:1	9.909	±	9.909	N.D.	±	N.D.	N.D.	±	N.D.
647.50	SM_d16:1/14:0	11.401	±	11.401	10.842	±	10.842	N.D.	±	N.D.
673.52	SM_d16:1/16:1	9.413	±	9.413	2.620	±	2.620	N.D.	±	N.D.
675.53	SM_d16:1/16:0	5.122	±	5.122	N.D.	±	N.D.	14.422	±	14.422
697.55	SM_d16:1/18:3	N.D.	±	N.D.	2.021	±	2.021	N.D.	±	N.D.
699.55	SM_d16:1/18:2	12.644	±	10.582	5.268	±	5.268	N.D.	±	N.D.
701.55	SM_d16:1/18:1	115.148	±	43.654	29.466	±	16.463	37.009	±	24.129
703.55	SM_d16:1/18:0	30.685	±	15.714	53.583	±	25.670	24.569	±	13.419
725.58	SM_d16:1/20:3	N.D.	±	N.D.	N.D.	±	N.D.	7.228	±	7.228
727.58	SM_d16:1/20:2	N.D.	±	N.D.	N.D.	±	N.D.	19.226	±	19.226
729.58	SM_d16:1/20:1	N.D.	±	N.D.	28.330	±	19.015	N.D.	±	N.D.
731.58	SM_d16:1/20:0	N.D.	±	N.D.	25.291	±	25.291	4.573	±	4.573
749.60	SM_d16:1/22:5	22.227	±	22.227	16.993	±	16.993	N.D.	±	N.D.
751.60	SM_d16:1/22:4	N.D.	±	N.D.	42.439	±	26.845	N.D.	±	N.D.
753.60	SM_d16:1/22:3	N.D.	±	N.D.	34.782	±	18.218	4.337	±	4.337
755.61	SM_d16:1/22:2	57.540	±	21.101	23.487	±	17.682	N.D.	±	N.D.
757.61	SM_d16:1/22:1	380.884	±	166.754	175.774	±	39.016	228.900	±	54.538
759.61	SM_d16:1/22:0	384.957	±	156.670	207.721	±	82.855	134.336	±	29.461
785.64	SM_d16:1/24:1	51.837	±	26.044	24.329	±	21.589	N.D.	±	N.D.
787.64	SM_d16:1/24:0	15.390	±	15.390	N.D.	±	N.D.	15.808	±	15.808
815.67	SM_d16:1/26:0	N.D.	±	N.D.	N.D.	±	N.D.	20.677	±	20.677
731.58	SM_d20:0/16:1	10.636	±	10.636	N.D.	±	N.D.	2.502	±	2.502
789.64	SM_d20:0/20:0	N.D.	±	N.D.	N.D.	±	N.D.	9.157	±	9.157
811.66	SM_d20:0/22:3	N.D.	±	N.D.	5.299	±	5.299	N.D.	±	N.D.
817.67	SM_d20:0/22:0	N.D.	±	N.D.	N.D.	±	N.D.	7.160	±	7.160
701.55	SM_d20:1/14:1	N.D.	±	N.D.	6.144	±	6.144	N.D.	±	N.D.
753.60	SM_d20:1/18:3	14.556	±	14.556	N.D.	±	N.D.	N.D.	±	N.D.
759.61	SM_d20:1/18:0	N.D.	±	N.D.	10.445	±	10.445	N.D.	±	N.D.
787.64	SM_d20:1/20:0	14.915	±	9.456	N.D.	±	N.D.	N.D.	±	N.D.
811.66	SM_d20:1/22:2	7.995	±	7.995	6.189	±	6.189	N.D.	±	N.D.

841.69	SM_d20:1/24:1	N.D.	±	N.D.	11.235	±	11.235	N.D.	±	N.D.
843.69	SM_d20:1/24:0	N.D.	±	N.D.	N.D.	±	N.D.	20.677	±	20.677
871.72	SM_d20:1/26:0	11.223	±	11.223	N.D.	±	N.D.	N.D.	±	N.D.

Supplementary Table 16: Concentrations (in pmol/mg protein) of triacylglycerols (TAG) in *Artemia* cysts, Percoll-purified mitochondria and mitoplasts. For TAG determination, all the fragments that would comprise the acyl chains were summed up and isomeric composition for the molecular species as the brutto nomenclature (carbon:double bond) is given. N.D.: not determined. Results shown are Mean +/- S.E.

$[M+NH4]^+$	Species	Artemia Cysts			Mitochondria			Mitoplasts		
684.53	TAG_38:0	4.453	±	0.999	5.964	±	0.594	2.510	±	0.600
704.55	TAG_40:4	0.277	±	0.175	0.234	±	0.148	0.069	±	0.069
706.56	TAG_40:3	1.750	±	0.446	0.394	±	0.244	0.412	±	0.261
708.56	TAG_40:2	1.710	±	0.279	1.938	±	0.532	0.233	±	0.122
710.56	TAG_40:1	3.637	±	1.046	3.476	±	0.692	3.519	±	0.826
712.56	TAG_40:0	138.291	±	15.399	124.264	±	12.254	138.103	±	10.821
732.58	TAG_42:4	11.640	±	1.352	3.305	±	0.499	4.295	±	0.747
734.58	TAG_42:3	13.828	±	1.686	12.751	±	1.929	8.146	±	0.869
736.59	TAG_42:2	15.265	±	0.501	14.188	±	1.505	10.749	±	1.142
738.59	TAG_42:1	44.922	±	5.535	34.774	±	5.510	25.872	±	2.005
740.59	TAG_42:0	27.257	±	1.677	22.268	±	3.532	15.487	±	2.153
756.61	TAG_44:6	11.555	±	1.928	10.211	±	1.031	8.498	±	2.145
762.61	TAG_44:3	38.392	±	4.367	40.210	±	3.654	44.058	±	5.321
764.61	TAG_44:2	26.834	±	1.243	21.423	±	1.982	19.801	±	1.459
766.62	TAG_44:1	21.622	±	1.640	8.124	±	0.816	5.053	±	1.288
768.62	TAG_44:0	10.321	±	1.203	4.159	±	0.915	4.626	±	0.682
786.64	TAG_46:5	14.710	±	1.654	1.475	±	0.390	1.282	±	0.439
788.64	TAG_46:4	54.345	±	2.636	13.250	±	1.768	12.733	±	1.971
790.64	TAG_46:3	143.342	±	5.355	22.717	±	1.923	22.164	±	1.763
792.64	TAG_46:2	53.744	±	3.305	13.383	±	1.265	10.105	±	1.582
794.64	TAG_46:1	73.734	±	3.948	20.744	±	2.202	11.768	±	2.557
796.65	TAG_46:0	18.877	±	1.069	9.792	±	0.859	8.585	±	0.793
810.66	TAG_48:7	26.782	±	1.769	11.169	±	1.198	9.705	±	1.987
812.66	TAG_48:6	126.981	±	12.016	35.682	±	2.781	22.912	±	3.163
814.66	TAG_48:5	232.278	±	13.742	24.229	±	2.928	24.989	±	4.359
816.67	TAG_48:4	821.335	±	62.036	99.765	±	10.186	73.471	±	10.637
818.67	TAG_48:3	1846.500	±	93.827	207.450	±	21.366	157.119	±	22.913
820.67	TAG_48:2	471.994	±	21.417	72.941	±	8.771	61.149	±	8.752
822.67	TAG_48:1	307.507	±	12.626	70.052	±	8.364	48.774	±	8.909
824.67	TAG_48:0	50.822	±	3.732	21.699	±	2.515	8.068	±	1.255
836.69	TAG_50:8	63.482	±	4.761	8.488	±	1.376	7.780	±	1.957
838.69	TAG_50:7	840.353	±	38.745	83.990	±	10.930	81.800	±	7.744
840.69	TAG_50:6	1296.524	±	97.000	131.075	±	13.230	102.625	±	14.720
842.69	TAG_50:5	2376.974	±	142.153	230.387	±	26.384	170.561	±	22.845
844.69	TAG_50:4	5441.862	±	195.119	545.810	±	64.448	422.030	±	60.811
846.70	TAG_50:3	5923.590	±	480.636	771.227	±	80.512	561.379	±	77.832
848.70	TAG_50:2	1867.802	±	103.967	286.505	±	29.607	231.027	±	33.920
850.70	TAG_50:1	795.040	±	61.777	192.581	±	22.199	141.746	±	18.731
852.70	TAG_50:0	74.552	±	4.592	23.425	±	3.949	14.628	±	1.384
862.71	TAG_52:9	607.304	±	46.943	55.430	±	7.061	53.079	±	8.248
864.71	TAG_52:8	1531.702	±	70.438	114.942	±	14.642	116.503	±	15.573
866.72	TAG_52:7	3075.006	±	265.359	275.766	±	33.127	252.200	±	23.439

868.72	TAG_52:6	5536.309	±	207.582	516.833	±	52.349	455.063	±	45.618
870.72	TAG_52:5	8693.497	±	523.281	714.381	±	99.663	739.232	±	89.580
872.72	TAG_52:4	12849.125	±	892.921	1636.508	±	140.968	1373.093	±	175.820
874.72	TAG_52:3	6537.106	±	228.425	778.749	±	80.627	631.878	±	75.692
876.73	TAG_52:2	2659.765	±	73.209	500.970	±	67.481	381.678	±	42.710
878.73	TAG_52:1	415.309	±	22.846	98.736	±	13.921	58.998	±	6.650
880.73	TAG_52:0	42.207	±	2.467	17.131	±	2.580	11.777	±	1.969
888.74	TAG_54:10	1460.000	±	114.089	132.358	±	15.435	95.879	±	12.899
890.74	TAG_54:9	4214.624	±	204.860	366.012	±	36.677	291.698	±	40.985
892.74	TAG_54:8	3528.911	±	153.431	303.838	±	30.669	241.339	±	26.296
894.74	TAG_54:7	6962.459	±	377.529	682.192	±	85.393	537.197	±	66.844
896.75	TAG_54:6	7733.498	±	131.990	797.857	±	83.838	610.803	±	75.079
898.75	TAG_54:5	8918.203	±	775.512	1218.004	±	104.306	969.848	±	121.089
900.75	TAG_54:4	7230.784	±	259.759	866.068	±	90.580	642.883	±	82.990
902.75	TAG_54:3	2344.707	±	121.601	358.237	±	35.590	265.891	±	38.673
904.75	TAG_54:2	506.591	±	22.639	98.683	±	10.293	75.581	±	10.983
906.76	TAG_54:1	114.215	±	13.457	30.284	±	4.391	29.864	±	2.507
908.76	TAG_54:0	18.236	±	1.912	8.154	±	1.142	6.697	±	1.276
912.76	TAG_56:12	5.162	±	0.811	4.127	±	0.536	1.270	±	0.376
914.76	TAG_56:11	325.841	±	33.409	37.431	±	4.218	31.293	±	2.540
916.77	TAG_56:10	890.812	±	39.937	78.458	±	6.516	69.841	±	7.236
918.77	TAG_56:9	858.261	±	36.856	123.594	±	14.026	96.557	±	13.439
920.77	TAG_56:8	1051.630	±	53.260	104.811	±	9.794	83.662	±	7.275
922.77	TAG_56:7	1390.029	±	144.321	152.326	±	15.792	113.413	±	15.980
924.77	TAG_56:6	477.105	±	31.406	53.411	±	7.099	50.039	±	6.159
926.78	TAG_56:5	571.953	±	35.916	67.288	±	7.718	54.249	±	8.449
928.78	TAG_56:4	372.982	±	13.540	56.277	±	6.550	45.446	±	6.770
930.78	TAG_56:3	147.794	±	13.160	25.467	±	2.439	18.625	±	3.562
932.78	TAG_56:2	91.613	±	6.606	24.535	±	2.075	20.820	±	2.866
934.78	TAG_56:1	46.628	±	3.704	13.585	±	2.262	10.869	±	1.312
936.79	TAG_56:0	3.387	±	0.658	2.124	±	0.361	1.628	±	0.623
938.79	TAG_58:13	33.901	±	3.253	10.790	±	2.262	4.889	±	1.003
940.79	TAG_58:12	81.521	±	5.402	15.340	±	1.802	10.516	±	2.634
942.79	TAG_58:11	76.574	±	4.337	9.404	±	1.633	6.715	±	1.810
944.79	TAG_58:10	144.008	±	10.534	17.525	±	3.442	14.549	±	2.421
946.80	TAG_58:9	94.210	±	9.063	18.144	±	2.186	12.119	±	1.862
948.80	TAG_58:8	66.211	±	4.348	15.535	±	1.892	12.524	±	1.621
950.80	TAG_58:7	53.594	±	2.897	15.760	±	1.121	13.641	±	2.973
952.80	TAG_58:6	59.941	±	5.547	8.461	±	1.448	5.136	±	1.637
954.80	TAG_58:5	143.332	±	11.020	14.801	±	1.510	7.103	±	1.579
956.81	TAG_58:4	98.195	±	5.572	14.094	±	1.518	9.923	±	1.681
958.81	TAG_58:3	37.608	±	5.773	8.708	±	1.183	5.301	±	1.148
960.81	TAG_58:2	27.519	±	2.648	10.467	±	1.245	5.655	±	1.393
962.81	TAG_58:1	2.229	±	0.457	0.994	±	0.336	0.330	±	0.169
964.81	TAG_58:0	0.683	±	0.414	0.832	±	0.264	0.308	±	0.178
964.81	TAG_60:14	9.067	±	1.068	6.751	±	0.906	3.793	±	1.233
966.82	TAG_60:13	15.941	±	1.894	9.357	±	1.003	4.121	±	0.606
968.82	TAG_60:12	16.851	±	1.924	13.836	±	2.114	7.948	±	1.194

970.82	TAG_60:11	15.468	±	0.707	3.980	±	1.453	2.908	±	0.896
972.82	TAG_60:10	8.918	±	1.414	4.147	±	0.816	3.277	±	1.039
974.82	TAG_60:9	11.597	±	1.496	5.107	±	0.937	2.366	±	0.632
976.83	TAG_60:8	7.192	±	0.932	2.064	±	0.382	1.727	±	0.248
978.83	TAG_60:7	18.299	±	1.705	2.570	±	0.891	2.359	±	0.846
980.83	TAG_60:6	7.347	±	1.246	2.039	±	0.391	0.938	±	0.350
982.83	TAG_60:5	16.478	±	1.791	2.543	±	0.886	1.306	±	0.731
984.83	TAG_60:4	10.780	±	1.340	0.816	±	0.574	0.799	±	0.300
986.84	TAG_60:3	5.899	±	1.539	1.791	±	0.580	0.971	±	0.337
988.84	TAG_60:2	3.173	±	0.490	1.714	±	0.540	0.570	±	0.250
990.84	TAG_60:1	0.444	±	0.237	0.339	±	0.180	0.276	±	0.154
992.84	TAG 60:0	N.D.	±	N.D.	0.331	±	0.154	0.202	±	0.202
990.84	TAG 62:15	6.363	±	0.735	4.684	±	1.562	3.743	±	0.679
992.84	TAG 62:14	4.863	±	0.463	4.403	±	0.787	2.617	±	0.615
994.84	TAG 62:13	6.607	±	0.471	2.973	±	0.874	2.981	±	0.818
996.85	TAG_62:12	3.966	±	0.837	0.823	±	0.499	0.593	±	0.410
998.85	TAG_62:11	1.291	±	0.452	0.663	±	0.324	0.387	±	0.316
1000.85	TAG_62:10	1.497	±	0.395	0.296	±	0.197	0.655	±	0.307
1002.85	TAG_62:9	1.647	±	0.470	1.351	±	0.568	0.687	±	0.270
1004.85	TAG_62:8	2.615	±	0.646	0.427	±	0.192	0.535	±	0.308
1006.86	TAG_62:7	2.254	±	0.819	0.510	±	0.267	0.554	±	0.267
1008.86	TAG_62:6	0.910	±	0.388	N.D.	±	N.D.	0.065	±	0.065
1010.86	TAG_62:5	2.951	±	0.739	0.158	±	0.158	0.152	±	0.152

Supplementary Table 17: Criteria for lipid identification for each lipid class include MS mode, molecular ion, scan mode, and fragment (m/z).

Class	MS Mode	Molecular Ion	Scan Mode	Fragment (m/z)
AC	pos	M+H	Precursor Ion Scan	85.0284
CE	pos	$M+NH_4$	Precursor Ion Scan	369.3516
Cer	pos	M+H	Precursor Ion Scan	264.2686
CoQ10	pos	$M+NH_4$	Precursor Ion Scan	197.0797
DAG	pos	$M+NH_4$	Neutral Loss Scan	-FA
Glycolipid	pos	M+H	Precursor Ion Scan	264.2686
LPC	pos	M+H	Precursor Ion Scan	184.0733
PC	pos	M+H	Precursor Ion Scan	184.0733
LPE	pos	M+H	Neutral Loss Scan	-141.0109
PE	pos	M+H	Neutral Loss Scan	-141.0109
SM	pos	M+H	Precursor Ion Scan	264.2686
TAG	pos	$M+NH_4$	Neutral Loss Scan	-FA
LPA	neg	M-H	Product Ion Scan	FA
PA	neg	M-H	Product Ion Scan	FA
FFA	neg	M-H	Neutral Loss Scan	-44.00
LPG	neg	M-H	Product Ion Scan	FA
PG	neg	M-H	Product Ion Scan	FA
LPS	neg	M-H	Product Ion Scan	FA
PS	neg	M-H	Product Ion Scan	FA
CL	neg	M-2H	Isotope Peak [M-2H+0.5]	

Supplementary Table 18: Internal standards used for quantification of lipid molecular species for each lipid class and their concentration (nmol/mg protein) in the internal standard cocktail spiked into every *Artemia* cyst, mitochondria, and mitoplast sample.

Internal Standards	**Concentration (nmol/ mg protein)**
^{13}C4-Carnitine_16:0	0.05
Ceramide_17:0	0.05
DAG_17:1/17:1	1.5
d4-FFA_16:0	2.0
N-15:0_Cerebroside	1.0
PA_12:0/12:0	0.5
LPC_17:0	1.5
PC_14:1/14:1	15.0
LPE_14:0	1.5
PE_16:1/16:1	19.0
PG_15:0/15:0	2.0
PS_14:0/14:0	4.0
SM_12:0	2.0
TAG_17:1/17:1/17:1	7.5
CL_14:0/14:0/14:0	4.0

***Conflict of Interest**

Click here to download Conflict of Interest: Conflict of Interest.doc